R80-35

OSP 85052

WATER BALANCE ESTIMATES OF THE MACHAR MARSHES

by
Ismail Ibrahim El-Hemry
and
Peter S. Eagleson

RALPH M. PARSONS LABORATORY
FOR
WATER RESOURCES AND HYDRODYNAMICS
Department of Civil Engineering
Massachusetts Institute of Technology

Report No. 260

Prepared under the support of
The Agency for International Development
The United States Department of State

August 1980

MIT

DEPARTMENT
OF
CIVIL
ENGINEERING

SCHOOL OF ENGINEERING
MASSACHUSETTS INSTITUTE OF TECHNOLOGY
Cambridge, Massachusetts 02139

R80-35 OSP 85052

WATER BALANCE ESTIMATES OF THE MACHAR MARSHES

by

Ismail Ibrahim El-Hemry

and

Peter S. Eagleson

RALPH M. PARSONS LABORATORY

FOR

WATER RESOURCES AND HYDRODYNAMICS

Department of Civil Engineering

Massachusetts Institute of Technology

Report No. 260

Prepared under the support of

The Agency for International Development

The United States Department of State

August 1980

WATER BALANCE ESTIMATES OF THE MACHAR MARSHES

ABSTRACT

Further increases of the River Nile discharge may come from reducing the water losses in the upstream swampy areas in the Nile basin. The Machar region is one of the main losers of water in this basin.

In this work, the general water balance of the Machar region is studied using new models which incorporate the dynamic interaction of climate, soil and vegetation. Also, the random variability of the different hydrologic components are investigated. Probabilistic estimates of annual water yield of the Machar catchments are presented. These estimates show the amount of water that may be saved and they provide a guide to the Egyptian and Sudanese water resource planners in their design of a channelization system in the region.

ACKNOWLEDGEMENTS

This work was sponsored by the M.I.T. Technology Adaptation Program which is funded through a grant from the Agency for International Development, United States Department of State.

Particular thanks are given to Professor Ismail E. Mobarek, Professor Mohamed H. Salem and Dr. Hassan H. Dorrah from Cairo University for their great help and valuable discussions.

Acknowledgement should also be given to Dr. Hassan Ibrahim, Director of the Water Resources Development Institute, Ministry of Irrigation, Egypt, for making the data available.

Thanks also to Mr. Siu-on Chan, Mohamed N.E.I. Allam and Tarek Habashy, research assistants at M.I.T.

A grateful word goes to Mrs. Anne Clee, who patiently typed this report.

TABLE OF CONTENTS

List of Symbols

A	short wave albedo of surface
A_i	area of catchment i
A_o	gravitational infiltration rate as modified by capillary rise from water table
a_i	shape parameter of Gamma distribution of the annual discharge at section i
B	ratio of the evapotranspiration to the water surface potential evaporation
$\overline{B}$	index relating soil properties
b_i	scale param of Gamma distribution of the annual discharge at section i
c	pore connectivity index
c_1	coefficient related to the two-variable model, coefficient related to the ratio B
c_2	coefficient related to the ratio B
c_3	coefficient related to the ratio B
D	soil moisture diffusivity
d	diffusivity index
d_1	coefficient related to the two-variable model
E	bare soil evaporation effectiveness (exfiltration parameter), integral variable of the annual (seasonal) water surface potential evaporation
E_n	upper limit of water surface potential evaporation
E_{P_A}	annual (seasonal) total potential evapotranspiration
E_{r_A}	annual (seasonal) surface retention
E_{rs_j}	interstorm bare soil surface retention

E_{rv_j}	interstorm vegetated surface retention
E_{T_A}	annual (seasonal) total evapotranspiration
$E_{T_{ca}}$	average seasonal evapotranspiration of catchments
$E_{T_{pl}}$	average seasonal evapotranspiration of plains
E_{T_o}	average annual evapotranspiration of swamps
E_o	lower limit of water surface potential evaporation
E_{T_j}	interstorm evapotranspiration
e_p	rate of bare soil potential evaporation
$\bar{e}_p$	long-term time average rate of bare soil potential evaporation
$\bar{e}_{p_v}$	long-term time average rate of vegetated surface transpiration
$\bar{e}_{piche}$	average rate of seasonal piche observations
$e_{p_{w_j}}$	rate of interstorm water surface potential evaporation
$\bar{\bar{e}}_{p_w}$	mean rate of seasonal water surface potential evaporation
e_v	rate of vegetated surface transpiration
f_e^*	exfiltration capacity
f_i^*	infiltration capacity
G	gravitational infiltration parameter
H	average sensible heat residual
h	storm depth

h_o	surface retention capacity
I	integral in the two-variable model
I_A	annual (seasonal) total infiltration
I_ν	integral in the two-variable model
i	precipitation rate (storm intensity), counting variable
J	evaporation efficiency (evapotranspiration function)
j	counting variable
K	constant related to the distribution of the water surface potential evaporation
K(1)	saturated hydraulic conductivity
k(1)	saturated intrinsic permeability
k_v	plant coefficient of the species
$\bar{k}_v$	average plant coefficient of mixed vegetation
L_e	latent heat of vaporization
L_o	closure error of the long-term average water balance
M	vegetation canopy density
$\bar{M}$	average vegetation canopy density of the catchment
m	pore size distribution index
m_e	mean value of annual (seasonal) water surface potential evaporation
m_H	mean storm depth
m_I	mean storm intensity
m_{P_A}	average annual precipitation

m_{p_s}	average seasonal precipitation
m_{t_b}	mean time between storms
m_{t_r}	mean storm duration
m_τ	mean length of rainy season
m_ν	mean annual (seasonal) number of storms
$m_\nu^\wedge$	mean annual (seasonal) number of rainy days of rainfall $\geq$ 1 mm
m_ν^*	mean annual (seasonal) number of rainy days of rainfall $\geq$ 10 mm
N	counting variable, number of years of record
$\bar{N}$	average fraction of the sky covered by clouds
n	effective medium porosity, counting variable in the numerical solution
n_a	sample porosity
P	precipitation, Pearson's incomplete Gamma function
P_A	annual (seasonal) total precipitation
P_{c_a}	long-term average seasonal precipitation of catchments
P_{pl}	long-term average seasonal precipitation of the plains
P_o	long-term average annual precipitation of swamps
Q_{A_i}	annual discharge of section i
q	integral variable of the annual discharge probability distribution
$\bar{q}_b$	average rate of longwave back radiation

$\bar{q}_i$	average rate receipt of shortwave radiation
$\bar{q}_{i_c}$	average rate of clear sky solar radiation
R_{g_A}	annual (seasonal) groundwater runoff
R_{s_A}	annual (seasonal) surface runoff
$R^*_{s_A}$	annual (seasonal) rainfall excess
R_{s_j}	storm surface runoff
R_1	integration region of the cumulative distribution function of annual yield
$\bar{R}_1$	reduction factor of the seasonal piche observations
R_2	integration region of the complementary probability distribution of annual yield
$\bar{R}_2$	ratio of seasonal potential evaporation of bare soil to that of water surface
$\bar{r}$	average relative humidity
S_i	infiltration sorptivity
S_p	net spilling from Baro River to the Macher region
s	effective medium saturation (i.e. soil moisture concentration)
s_a	sample degree of saturation
s_r	residual medium saturation
s_o	annual (seasonal) soil moisture concentration
$\bar{s}_o$	average annual (seasonal) soil moisture concentration
s_1	degree of saturation at surface of medium

$\bar{s}_1$	effective degree of saturation at 1/3 atm pressure (suction)
$\bar{s}_2$	effective degree of saturation at 15 atm pressure (suction)
T	full water year, coefficient related to the two-variable model
$\bar{T}_{a_C}$	average atmospheric temperature in °C
$\bar{T}_{a_F}$	average atmospheric temperature in °F
$\bar{T}_s$	average seasonal atmospheric temperature
t	time, dummy variable of integration
t_a	storm interarrival time
t_b	time between storms
t_r	storm duration
t_o	time at which time surface reaches saturation during precipitation
U_{c_a}	ungaged flow from catchments
v	apparent percolation velocity
v_e	coefficient of variation of the water surface (annual) seasonal potential evaporation
w	upward apparent pore fluid velocity
x	transformed variable of the annual yield
Y_A	annual (seasonal) yield
Y_{ca}	annual yield from catchments
Y_{pl}	annual yield from plains
y	integral variable of the annual yield

Z	depth to water table
α	reciprocal of average rainstorm intensity
β	reciprocal of average time between storms
γ	sensible heat transfer coefficient
γ_w	specific weight of water
Δ	slope of vapor pressure-temperature curve
ΔE	arbitrary small interval of water surface potential evaporation
δ	reciprocal of average storm duration
η	reciprocal of mean storm depth
θ	effective soil moisture
$\bar{\theta}_{a_1}$	soil moisture at 1/3 atm pressure (suction)
$\bar{\theta}_{a_2}$	soil moisture at 15 atm pressure (suction)
κ	shape parameter of Gamma distribution of storm depth
λ	scale parameter of Gamma distribution of storm depth
μ_w	dynamic viscosity of water
ν	counting variable of number of storms
ρ_e	mass density of evaporating water
σ	capillary infiltration parameter
σ_e	standard deviation of water surface potential evaporation
σ_{P_A}	standard deviation of annual precipitation
σ_{P_s}	standard deviation of seasonal precipitation
σ_w	surface retention of water

τ	length of rainy season
Φ	pore shape parameter
ϕ_e	exfiltration diffusivity function
ϕ_i	infiltration diffusivity function
$\Psi(1)$	saturated soil matrix potential
ω	average arrival rate of storms
$E[\ ]$	expected value of
erf( )	error function
$F_X(\ )$	cumulative distribution function, cdf, of X
$f_X(\ )$	probability density function, pdf, of X
$G_X(\ )$	complementary of cumulative distribution function of X
J( )	evapotranspiration function
$P[\ ,\ ]$	Pearson's incomplete Gamma function
$P^c[\ ,\ ]$	complementary of Pearson's incomplete Gamma function
$\delta(\ )$	Delta function (zero or one)
!	vectorial
$\Gamma(\ )$	Gamma function
$\gamma[\ ,\ ]$	incomplete Gamma function

LIST OF TABLES

LIST OF FIGURES

Chapter 1

INTRODUCTION

1.1 Background and General Description

The Machar region is one of the largest potential resources of water in the Upper Nile. More than 35 milliards (thousand million cubic meters) are lost there annually by evaporation and seepage. Reducing the water losses of this region by channelizing and reclaiming its swamps is a promising means of increasing the current annual Nile flow and thus of augmenting this vital water resource.

In the present work, new methods of water balance estimation are applied in the Machar region, incorporating the dynamic interaction of climate, soil and vegetation.

The Machar region is located at the southeastern borders of the Sudan between latitudes 8° and 11° North, and longitudes 31° and 35° East. The region is surrounded by the White Nile in the west, the Sobat and Baro rivers in the south, and the Ethiopian mountains in the east.

The swampy area of this region lies north of the Baro River. The main sources of water to this area are the direct rainfall, the drainage of the eastern catchments and the spillage from the Baro River.

1.2 Objectives

The main objective of this work is to calibrate and apply conceptual models for studying the hydrologic behavior of the Machar catchments and of estimating the uncertainty in the increased annual water yield from these catchments due to proposed channelization and

reclamation projects.

Improving these models to represent the physical properties of the Machar region is another objective of this work. This is by considering the annual variability of the potential evaporation and vegetation growth along with that of precipitation in the above models.

The results of this work can be utilized by the Egyptian and Sudanese water resource planners to economically design the proposed channel system in this region.

1.3 Method of Approach and Scope of Investigation

In these models, the water balance components will be estimated by considering the climate, the soil and vegetation as a coupled dynamic system in which energy and water mass are exchanged across the land surface.

The probability distribution function of the annual (seasonal) precipitation will be estimated from Poisson arrivals fitted by the method-of-moments. Transforming this function by the general water balance equation gives the probability distributions of the yield and other relevant components.

These investigations will make use of existing hydrometeorological data including the information which has been obtained from completed remote sensing studies.

Where available, discharge observations of the eastern catchments will be compared with the derived yields and will be used to calibrate the model with respect to certain of its soil and vegetation

parameters.

The calibrated model will be used to generate the discharge-frequency relation at critical sections along a proposed drainage channel in order to assist the planners in designing this system.

Chapter 2

REVIEW OF PREVIOUS WORK

Several attempts have been made to describe the Machar Marshes and their eastern catchments. Some investigators have roughly estimated the water losses of the swamps, while others have merely described the region.

Hurst and Phillips (1931) give a general description of the Sobat basin including the Machar area. They mention that information about the hydrology of the Sobat system is scanty and that the topography of the upper part of its basin is less well-known than that of any other part of the Nile Basin. Southwestern Abyssinia (now Ethiopia), which comprises the southeastern portion of the Machar region, is largely mountainous with large areas that are forest-covered. They classify these forests in three types: 1) bush and low trees, 2) large isolated trees surrounded by long grass, and, 3) thick tropical forests, sunless under the trees and with no undergrowth. They also describe the plains at the foot of the mountains as often being thickly wooded. Further west, trees occur in patches but the area is mainly open grass-covered plain, that is, swampy in the rainy season and nearly waterless in the dry season.

Hurst (1950) describes the hydrology of the eastern catchments, the plains, and the spilling from the Baro River into the permanent swamps. He attempts to estimate the amount of water flowing into the

Machar marshes and the water losses through evapotranspiration in these swamps.

Specifically, the main points of Hurst's description that may relate to the present work are:

a) The Khor* Yabus is a perennial stream, although a small one, with a discharge of perhaps 3 cubic meters per second in the dry season, while the Khors Daga and Lau cease to flow from January to April below where they enter the plains.

b) There is some spillage from the River Sobat between the Baro tail and Nassir, and a return flow of twice this amount back to the Sobat between September and December.

c) The Khor Adar is a small channel whose discharge has been measured occasionally and is in general negligible. Engineer Nasir, one of the principal investigators of the P.J.T.C. (Permanent Joint Technical Commission), mentioned, in January 1980, that the Khor Adar is almost blocked by vegetation and doesn't deliver a significant amount of water to the White Nile.

d) Hurst estimated the spilling from the Baro River to the swamps to be 2.5-3 milliards by computing the difference between the mean values of the streamflow at the head and tail of the Adura, including the inflow of Khor Jokau and the outflow of Khor Machar.

e) From rainfall and runoff data of Khor Jokau that delivers its water to the Baro River, Hurst finds that the runoff is about 14 percent of the total rainfall. He applied this ratio on the other

*The term "Khor" means small river.

eastern catchments to estimate annual runoff from these catchments as shown in Table (2-1).

Khor	Area of Effective Catchment	Annual Rainfall	Percentage Runoff	Annual Runoff
	(km^2)	(mm)		(10^3 m^3)
Daga	2200	1200	14	370
Yabus	5400	1200	14	910
Others	4680	1200	14	790
			TOTAL	2070

Table 2-1

AREAS, RAINFALLS AND ESTIMATED RUNOFF FOR THE EASTERN CATCHMENTS

(after Hurst, 1950)

According to Hurst's water balance, the permanent swamps, with an area of about 6500 km^2, and with annual rainfall of 0.9 meter, have water losses through evaporation of about 4 millimeters per day (10 mlds* per year).

In the Equatorial Nile Project report (1955), the investigators represent, in some detail, the general description and hydrology of the Machar Marshes, including the Eastern catchments and the spilling from the Baro River. They also attempt to configure these catchments from the maps available at that time. They conclude with another, roughly-estimated water balance for the plains (at the foot of the Eastern

*1 milliard (mld) $\equiv 10^9$ (one thousand million) cubic meters.

mountains) and the permanent swamps, which together have an area of about 20,000 km^2. This inclusion of the plains areas is the main difference between this report and that of Hurst (1950) who applied the water balance only to the permanent swamps.

Additional comcepts from this report that may be effective for the present work are:

a) The spilling into the swamps comes from four sources:

i) The discharge of the Jokau

ii) The discharge of the Machar,

iii) Three-fourths of the difference between the Baro discharges at Adura Head and Adura Tail after deducting the discharge of the Machar, and

iv) Two-thirds of the difference between the discharges at the Adura Tail and Baro mouth. The investigators estimate an average annual spilling of 2.82 milliards, which agrees closely with the 2.5 to 3 milliards estimated by Hurst (1950).

b) The runoff-rainfall percentage for the Eastern catchments is estimated at 15% whereas Hurst (1950) uses a percentage runoff of 14%.

c) The average annual rainfall falling over the area that lies between the other sources of water is estimated in the report as 15 milliards with a "variation" of the order of $\pm$ 1.5 milliards. This estimate of annual rainfall is the average of seven gauging stations situated around the plains and permanent swamps.

d) The reversal of flow downstream of the Baro-Pipor junction is estimated. The investigators mention that the measurements show that on a rising flood water travels from the Sobat to the Machar (0.15 milliard), but that on a falling flood, even more water returns to the Sobat (0.400 milliards).

e) The investigators include in their study the plains north of the Sobat River where there are some khors, called the Wol system, that extend parallel to the Sobat. These khors drain the water from the plains north of the Sobat to the White Nile. The investigators mention that the water drained by this system is less than 0.5 milliard. In the present work, this portion of the plains will be omitted from study, because its waters have no effect on the water budget of the Machar Marshes.

f) The investigators also mention that the drainage of the Marshes to the Sobat River and to the White Nile through the Khors Wakau and Adar, respectively, is probably negligible. This makes their total estimated inflow 19.6 milliards per year with a maximum variation from normal of $\pm$ 3.7 milliards.

g) The investigators also estimate a movement of water through the swamps from the Khors Daga and Yabus to the White Nile at a mean velocity of 1 km/day. This movement is called "creeping flow".

Bhalotra (1963) describes the climate and the other hydrological features of the Sudan, including the Machar region, as follows:

a) The rainfall is mainly convective in origin coming from instability showers and thunderstorms, and is localized in character.

b) He defines a rainy day as a day on which the rainfall is equal to or greater than 1 mm. From this definition, he concludes that the daily intensities of the rainfall are about the same magnitude throughout the Sudan and the wide variations in the seasonal total rainfall are mainly due to variations in the number of storms occurring and not to any significant differences in the average amounts of rainfall yielded by individual storms.

c) The evaporation from an open water surface is estimated by multiplying the Piche measurements by 0.5. It is observed that the normal evaporation follows closely the normal temperature and that the coefficient of correlation of the mean annual evaporation and the mean annual temperature for stations in the Sudan is about 0.69. The other factors that control the evaporation are the wind speed and the humidity.

d) He defines the evapotranspiration as the loss through evaporation from water and soil surfaces, including evaporation of intercepted precipitation and transpiration from vegetation.

e) Referring to Thornthwaite (1948) and Satakopan (1961), he classifies the climate in the Sudan into four zones. According to this classification, the plains of the Machar Marshes, including the permanent swamps, lie in the semi-arid zone and the eastern watersheds of the Machar region are in the dry sub-humid soil.

Oliver (1969) describes the climate, soil and vegetation all over the Sudan. The following properties and characteristics of the Machar region may be concluded from this work:

a) The rainy season period extends from April to November and there is a water deficit in the dry season, when the rainfall is less than the potential evapotranspiration. This deficit is sufficient to produce a definite water stress in the vegetation.

b) There are a considerable number of dry days (i.e., time between storms), even in the wet season, and many stations with an annual rainfall total of 1,000 mm or more have less than 100 days on which rain falls. Slight showers (less than 1.0 mm) are evaporated before soil moisture (and thus plants) can benefit.

c) The distributions of annual rainfall (after Thornthwaite, 1955) and potential evapotranspiration (after Satakopan, 1961) vary almost with the longitude in the Machar region rather than latitude, as might be expected. This is apparent in the shaded areas in Figures 2.1 and 2.2 and is apparently due to the orographic effects of the Eastern mountains. Also, Figure 2.1 shows that the eastern part of the Machar Marshes (the Eastern catchments) and the plains containing the permanent swamps lie in the dry sub-humid and semi-arid zones, respectively, as mentioned before.

d) Over eastern Sudan, a large proportion of the rain is received during the hours of darkness.

e) The number of hours in which rain is recorded (not the total duration of rainfall which would be less), in the central and northern Sudan is found to be between 60 and 120 in sites where the mean rainfall is 150-400 mms. Although the number of rainy hours increases southward, it does not do so at the same rate as the increase in total rainfall. Individual rain storms rarely continue for many hours, and frequently

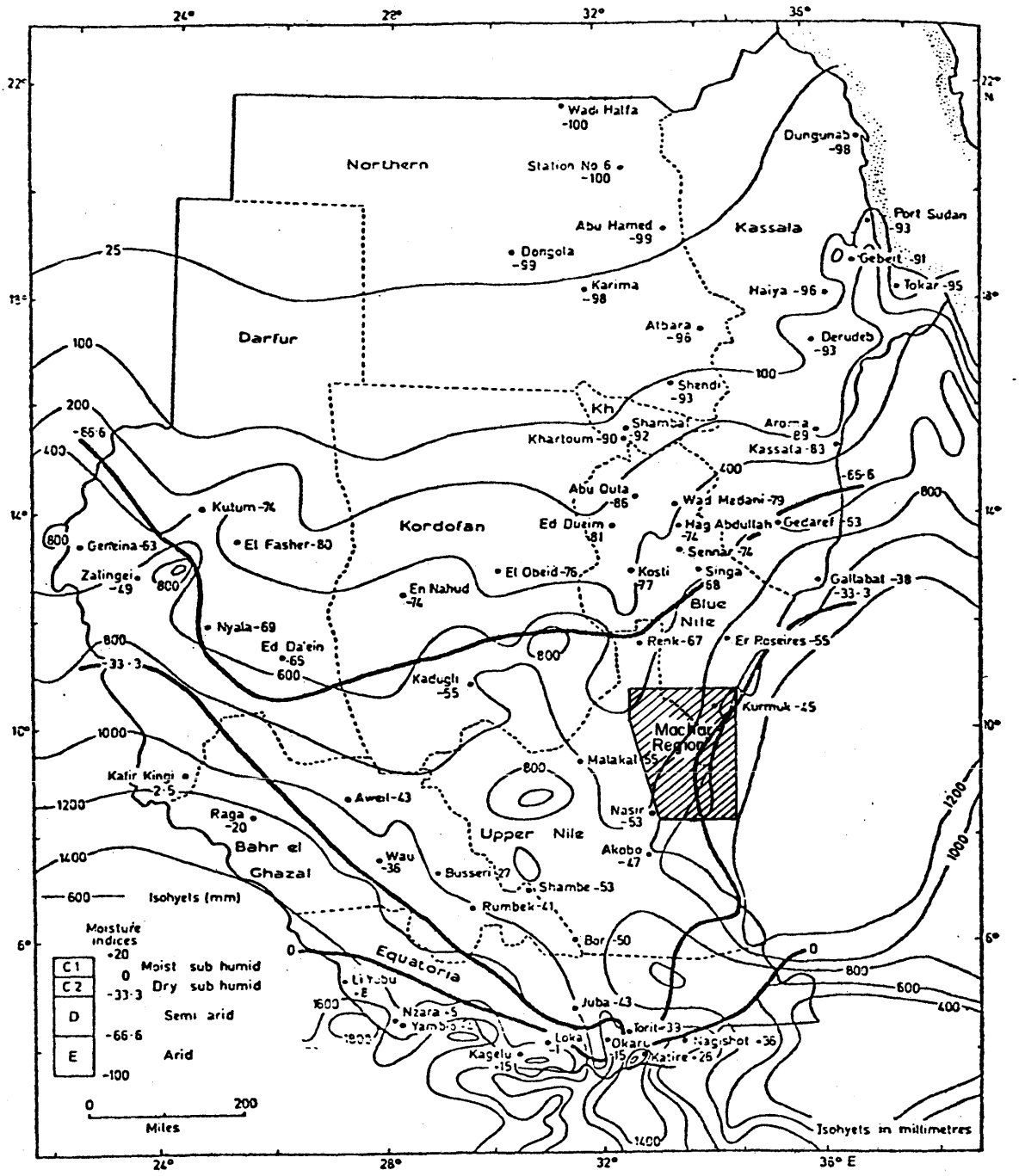

Figure 2.1

RAINFALL DISTRIBUTION AND MOISTURE REGIONS IN THE SUDAN
(after Oliver, 1969)

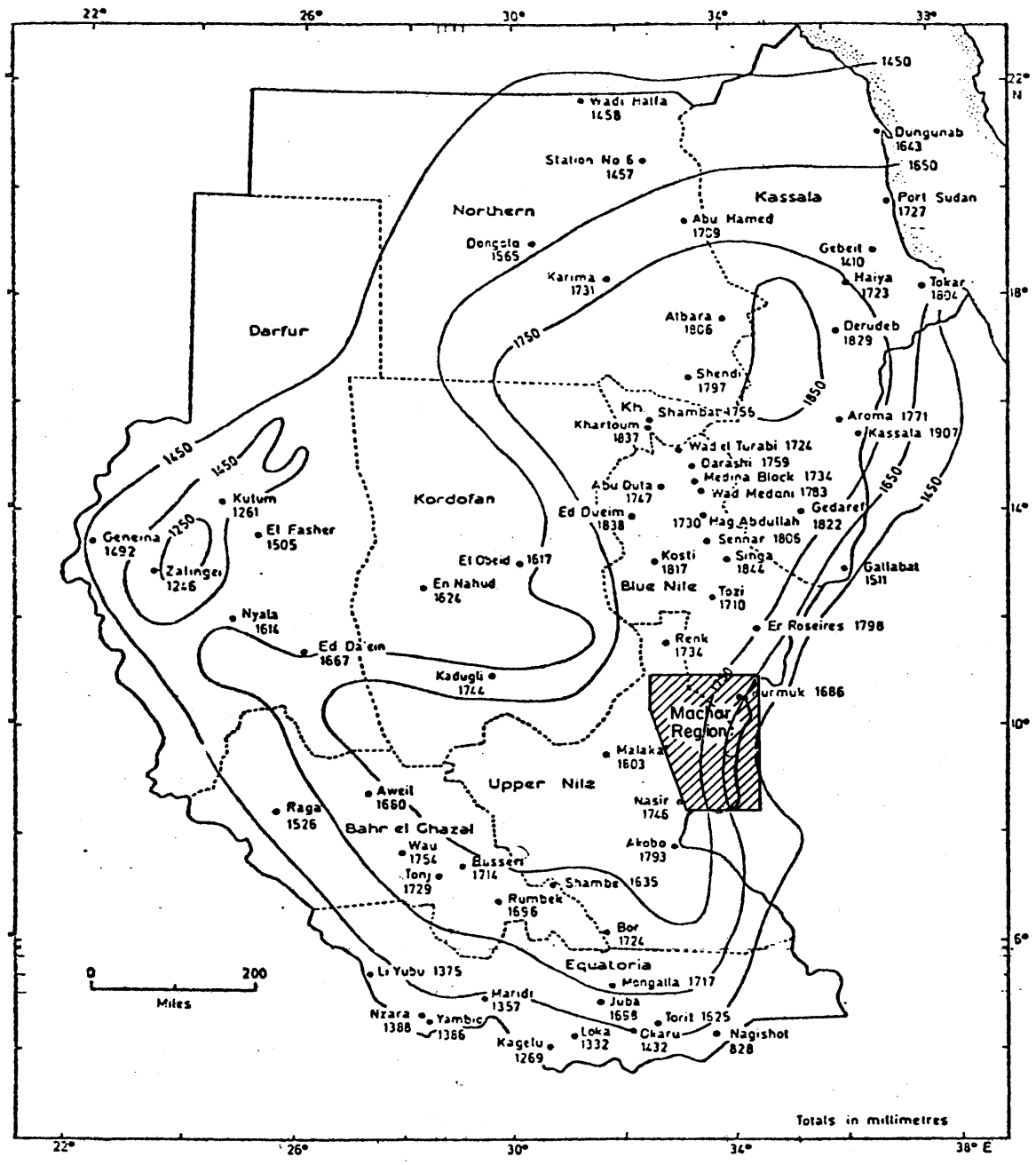

Figure 2.2

ANNUAL POTENTIAL EVAPOTRANSPIRATION IN THE SUDAN
ACCORDING TO THORNTHWAITE'S 1948 METHOD
(after Oliver, 1969)

their duration is merely a few minutes.

f) The soils in the eastern and southeastern part of the Sudan (the Machar region) are extensively-cracking montmorillonitic clays. Once the cracks close after the first wetting, water is held near the surface, and a large proportion of it is evaporated or transpired at the potential rate.

g) In the central Sudan, the soils are quite permeable and the prevalent annual grasses live only for a few weeks. They exhaust the shallow soil moisture in this time while trees flourish by extracting the plentiful deeper soil moisture. In the regions with clays, shallow rooting grasses make use of the plentiful shallow water, while the deeper rooting trees are starved.

Rzoska (1976) represents the vegetation and soil types in the Sudan, through a general map, referring to Wickens (1975). The types are classified, particularly in the Machar regions, as shown in Table (2-2).

Area	Soils and Vegetation
Swamps	Wetland savanna and swamps, including the Cyperus papyrus, Acacia seyal and Balanites aegyptiaca among tree species.
Plains	Thorn savanna and scrub on clay soils, including Acacia seyal and Balanites aegyptiaca.
Eastern Catchments	Deciduous savanna woodland on clay soils. The major tree constituents are Conbretum hartmannianum and Anogeisses leiocarpus, and the dominant grasses are Hydarrhenia spp.

Table 2-2

THE VEGETATION DISTRIBUTION IN THE MACHAR REGION

Berry and Whiteman (1968) represent the land elevations of the Sudan through a physiographic map. In this map, the topography of the Machar region is evaluated, as in Table (2-3).

Area	Elevation (m) (a.s.l.)
Swamps	less than 400
Plains	400-500
Eastern Catchments	more than 500

Table 2-3

THE LAND ELEVATION OF THE MACHAR REGION

Chapter 3

MODEL FORMULATION

The present work is based on a dimensionless, analytical model of the one-dimensional annual (seasonal) water balance. This model is presented by Eagleson (1978a, b, c, d, e, f, g) and incorporates certain simplifications and assumptions that allow analytical derivation of the probability distributions of the different hydrologic components.

The components of the general water balance model operate in the vertical direction at the upper surface of the control volume shown in Figure 3.1. Assuming the system is stationary, the expected values of these components are connected by the general water balance equation

$$E[P_A] - E[E_{T_A}] = E[R_{s_A}] + E[R_{g_A}] = E[Y_A] \qquad (3.1)$$

where

P_A = annual (seasonal) total precipitation

E_{T_A} = annual (seasonal) total evapotranspiration

R_{s_A} = annual (seasonal) total surface runoff

R_{g_A} = annual (seasonal) total groundwater runoff

Y_A = annual (seasonal) total yield

and

$E[\ ]$ = expected values of $[\ ]$

Equation (3.1) may take another form for the soil moisture,

$$E[I_A] = E[P_A] - E[R^*_{s_A}] = E[E_{T_A}] - E[E_{r_A}] + E[R_{g_A}] \qquad (3.2)$$

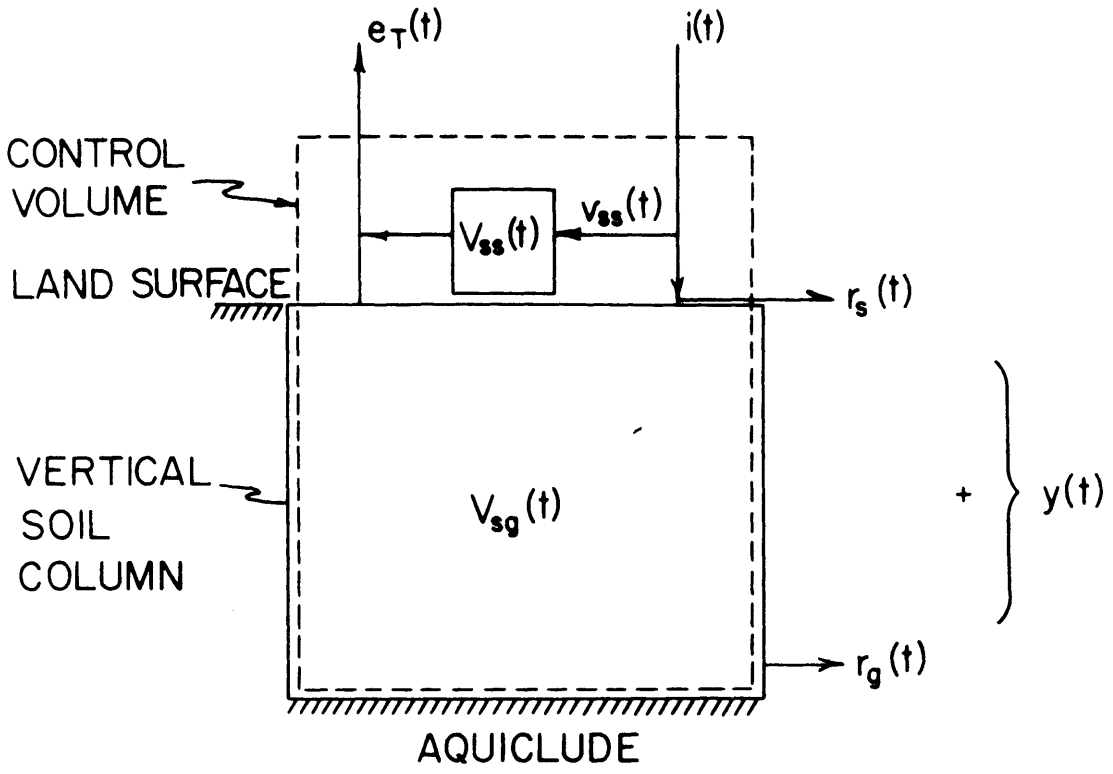

a. CONTROL VOLUME FOR WATER BALANCE

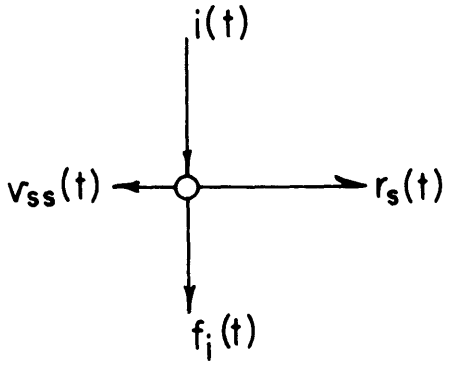

b. PARTITION OF PRECIPITATION AT SURFACE

Figure 3.1

INSTANTANEOUS WATER BALANCE
(from Eagleson, 1978a)

where

I_A = annual (seasonal) infiltration

$R^*_{s_A}$ = annual (seasonal) rainfall excess

and

E_{r_A} = annual (seasonal) surface retention

To the first order, the average annual (seasonal) water balance equation (3.2) gives the annual water balance which is used to compute the cumulative distribution functions of all components in terms of parameters estimated from the physical system.

3.1 Principal Assumptions and Simplifications

Some assumptions and simplifications have been used [Eagleson, 1978a] to define the analytical framework for the first order water balance.

A. General Assumptions

1. One-dimensional behavior (vertical direction)
2. Ice or snow processes are negligible.
3. All processes are stationary in long-term average.

B. Precipitation

1. Storm series is represented by Poisson arrivals of independent and identically-distributed, rectangular pulses of rainfall intensity.
2. Average interstorm period is much greater than average storm duration.

3. Interstorm period and storm duration are statistically independent.

C. Soil

1. Soils are homogeneous.
2. Movement of water vapor is not considered.
3. Soil column is effectively semi-infinite as far as surface processes are considered.
4. Infiltration, exfiltration, percolation and capillary rise from water table are formulated separately and their fluxes are linearly superimposed.
5. Carryover moisture storage (or deficit) from storm to interstorm period (and vice versa) is neglected with moisture at the start of every period being $\bar{s}_o$, the space-time average in the surface boundary layer.

D. Vegetation (natural systems only)

1. Transpiration occurs at the potential rate.
2. Rate of soil moisture extraction by the root system is constant throughout the entire soil volume above the maximum root depth regardless of the canopy density.
3. Canopy density seeks an equilibrium state at which soil moisture is a maximum.

E. Infiltration and surface runoff

1. No surface inflows from outside the region.
2. Storm intensity and duration and statistically independent.

F. Evapotranspiration

1. Vegetation transpires at the potential rate.
2. Potential rate of evapotranspiration averaged over the inter-storm period has a negligible coefficient of variation during the rainy season.

G. Percolation to water table

1. Steady throughout rainy season at rate determined by the average soil moisture, $\bar{s}_o$.
2. Percolation is zero during dry season.

H. Capillary rise from water table

1. Potential rate of evapotranspiration is much greater than rate of capillary rise from water table.
2. Dry surface matrix potential is much greater than saturated matrix potential.

I. Water table

1. Water table is constant (no carryover groundwater storage from year-to-year).

J. Yield and other water balance components

1. Relation among annual (seasonal) quantities is given, to the first order, by the relation among the average annual (seasonal) quantities.

In the present work, two modifications of this model are explored. The first one is to take the canopy density as a function of the soil moisture, depending on the amount of precipitation. This

function will be presented in Chapter 5. The second treats the potential evaporation of the bare soil as a random variable when deriving the cumulative distribution function of the annual (seasonal) yield.

In application of the model to an entire catchment, the physical parameters are lumped avoiding the spatial variation of climate, soil and vegetation inside this catchment.

A technical summary of the model upon which this research is based will be presented in the next sections.

3.2 The Annual Water Balance

3.2.1 Distribution of Annual (Seasonal) Precipitation

In this section, the point precipitation is represented by Poisson arrivals of rectangular intensity-pulses having random depth, h, and duration, t_r (Eagleson, 1978b). The chosen distribution for the storm depth is the Gamma distribution, represented by shape and scale parameters, κ and λ, respectively. This distribution is mathematically simple, provides a good fit with observations, and facilitates the summation of many storms.

For the same reasons, exponential distributions are selected for the storm duration, t_r, the interstorm period, t_b, and the storm intensity, i. They have parameters δ, β and α, respectively.

The interarrival time, t_a, is assumed to be exponentially distributed, as is consistent with Poisson arrivals. The parameter, ω, is the storm arrival rate.

The coefficient of variation of the rainy season length, τ, is assumed small and thus τ is replaced by its mean value, m_τ. In this case, the mean number of storms per season, m_ν, can be expressed as

$$m_\nu = \omega \cdot m_\tau \tag{3.3}$$

Considering the above assumptions and distribution, the cumulative distribution function, cdf, of the total annual (seasonal) distribution, P_A, is derived analytically, using Eq. (3.3) as

$$F_{P_A}(p) \equiv \text{prob}[P_A < p] = e^{-m_\nu} \left\{1 + \sum_{\nu=1}^{\infty} \frac{(m_\nu)^\nu}{\nu!} P[\nu\kappa, \eta\kappa p]\right\} \tag{3.4}$$

where

ν = counting variable for number of storms

η = reciprocal of mean storm depth, m_H^{-1}, $= \frac{\lambda}{\kappa}$ (3.5)

and

$P[\nu\kappa,\eta\kappa p]$ = Pearson's incomplete Gamma function, that is

$$P[a, x] = \gamma[a, x]/\Gamma(a) \tag{3.6}$$

The mean and variance of the annual (seasonal) precipitation are, respectively

$$E[P_A] \equiv m_{P_A} = m_\nu \cdot m_H \tag{3.7}$$

and

$$\sigma^2_{P_A} = \frac{m^2_{P_A}}{m_\nu}\left[1 + \frac{1}{\kappa}\right] \tag{3.8}$$

Substituting Eq. (3.7) in Eq. (3.4) gives the dimensionless form of the cumulative distribution function of the total annual (seasonal) precipitation

$$\text{Prob}\left[\frac{P_A}{m_{P_A}} < z\right] = e^{-m_\nu}\left\{1 + \sum_{\nu=1}^{\infty} \frac{(m_\nu)^\nu}{\nu!} P[\nu K,\ m_\nu K z]\right\} \qquad (3.9)$$

When annual (seasonal) observations are few, but storm observations are available, Eq. (3.9) tends to improve the estimate of the variance over that estimated using only the observations of the annual (seasonal) totals.

3.2.2 Soil Moisture and Groundwater Runoff

Eagleson (1978c) formulates a one-dimensional, physical model representing the movements of soil moisture in the vertical direction. These movements, as shown in Fig. 3.2, are storm infiltration, inter-storm exfiltration, percolation to the water table, and capillary rise from the water table to the surface.

The modes of soil moisture movement are analyzed separately in terms of the physical parameters. Then, linear superposition is utilized to approximate the actual movements during the rainy and dry seasons.

The soil is assumed to be homogeneous and is defined in terms of the following parameters:

$$k(s) = \frac{\mu_w}{\gamma_w} K(s) \equiv \text{effective intrinsic permeability} \qquad (3.10)$$

$$K(s) = K(1)\ s^c \equiv \text{effective hydraulic conductivity} \qquad (3.11)$$

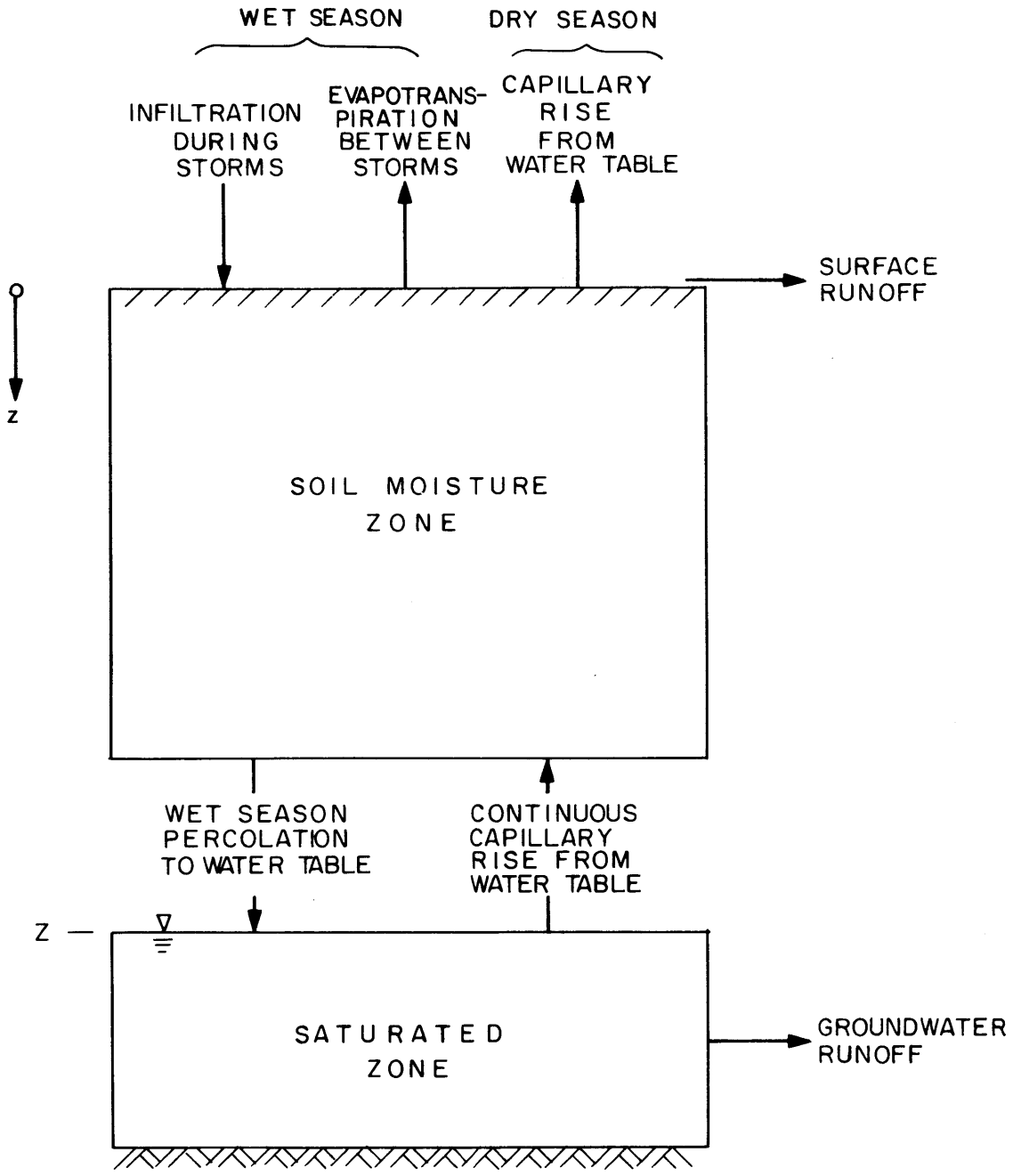

SCHEMATIC REPRESENTATION OF SOIL COLUMN

Figure 3.2

SCHEMATIC REPRESENTATION OF SOIL COLUMN
(from Eagleson, 1978c)

$$\Psi(s) = \Psi(1)\, s^{-\frac{1}{m}} \equiv \text{soil matrix potential} \tag{3.12}$$

$$\Phi = \left(\frac{\sigma_w}{\gamma_w}\right) \frac{n}{k(1)\ \Psi(1)} \equiv \text{pore shape parameter} \tag{3.13}$$

and

$$D(\theta) = \frac{\Psi(1)\ K(1)\ s^{d}}{m\ n} \equiv \text{soil moisture diffusivity} \tag{3.14}$$

where

$$s = \text{effective degree of saturation} = \frac{s_a - s_r}{1 - s_r} \tag{3.15}$$

s_a = sample degree of saturation

s_r = residual degree of saturation due to immovable water

μ_w = dynamic viscosity of water at the mean temperature

γ_w = specific weight of water at the mean temperature

σ_w = surface retention of water at the mean temperature

$K(1)$ = saturated effective hydraulic conductivity

$\Psi(1)$ = saturated soil matrix potential

$$n = \text{effective porosity} = (1 - s_r)n_a \tag{3.16}$$

n_a = sample porosity

m = pore size-distribution index

$$c = \text{pore connectivity index} = \frac{2 + 3m}{m} \tag{3.17}$$

$$d = \text{diffusivity index} = c - \frac{1}{m} - 1 \tag{3.18}$$

One of two empirical relationships is used to reduce the number of independent soil parameters. These are

$$\Phi = 10^{0.66+0.55/m+0.14/m^2} \tag{3.19}$$

and

$$K(1) = 3.4\text{x}10^{-3}(m)^{2.75} \qquad (3.20)$$

The separate soil moisture movements are summarized as follows:

A. Infiltration and exfiltration

The one-dimensional, concentration-dependent diffusion equation is solved (Eagleson, 1978c) under simple initial and boundary conditions. The boundary conditions are shown in Fig. 3.3.

In the application of these conditions, some simplifications have been made:

1. The medium is assumed semi-infinite. This means that the groundwater table depth, Z, is much greater than the surface boundary layer thickness where the infiltration and exfiltration take place.
2. The soil moisture concentration, $\bar{s}_o$, throughout the surface boundary layer is spatially uniform at the start of each storm or interstorm period.
3. The vegetation is distributed uniformly over a part of the land surface, M, while its roots extend through the entire boundary layer and extract moisture during the interstorm period only.

The storm infiltration capacity, f_i^*, (when $s_1 = 1$) is expressed as

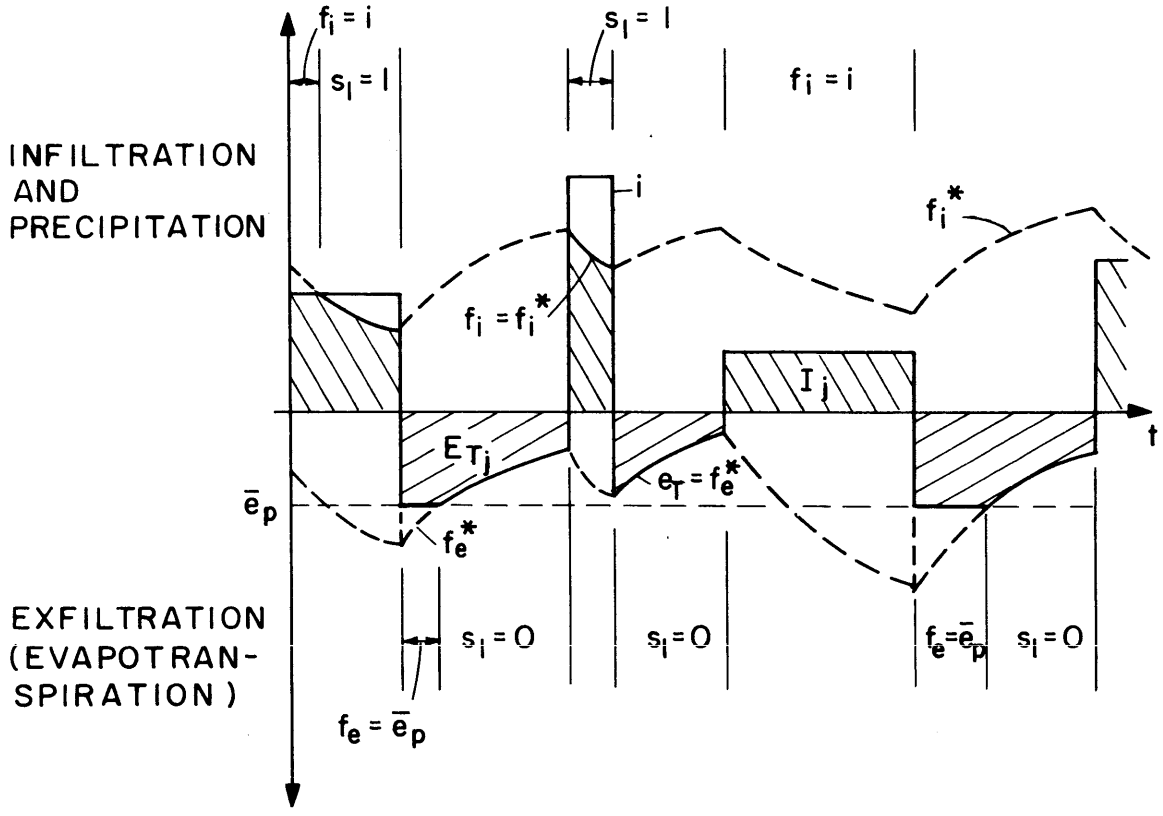

SURFACE BOUNDARY CONDITIONS FOR IDEALIZED STORM AND INTER-STORM PERIODS

Figure 3.3

(from Eagleson, 1978c)

$$f_i^*(t, \bar{s}_o) = (1 - \bar{s}_o) \left[\frac{5n\ K(1)\ \Psi(1)\ \phi_i(d, \bar{s}_o)}{3\ \pi\ m\ t}\right]^{1/2} + \frac{K(1)}{2}\ [1 + \bar{s}_o^c] \tag{3.21}$$

and the interstorm exfiltration capacity, f_i^*, (when $\bar{s}_1 = 0$) is

$$f_e^*(t, \bar{s}_o) = \bar{s}_o^{1+d/2} \left[\frac{n\ K(1)\ \Psi(1)\ \phi_e(d)}{\pi\ m\ t}\right]^{1/2} - M \cdot e_v \tag{3.22}$$

where

$\phi_i(d, \bar{s}_o)$ = dimensionless infiltration diffusivity

$\phi_e(d)$ = dimensionless exfiltration diffusivity

M = vegetation capacity density

e_v = rate of transpiration by vegetation

The dimensionless infiltration and exfiltration diffusivities are evaluated (Eagleson, 1978c) and are presented here in Figs. 3.4 and 3.5.

B. Capillary rise

Considering the capillary rise to be steady through the whole year, the solution of the one-dimensional, steady-state diffusion equation gives the capillary rise, w, to a dry surface as

$$w = \bar{B}\ K(1) \left[\frac{\Psi(1)}{Z}\right]^{mc} \quad , \qquad w < \bar{e}_p \tag{3.23}$$

where

$$\bar{B} = 1 + \frac{3/2}{mc - 1} \tag{3.24}$$

and

$\bar{e}_p$ = average rate of bare soil potential evaporation

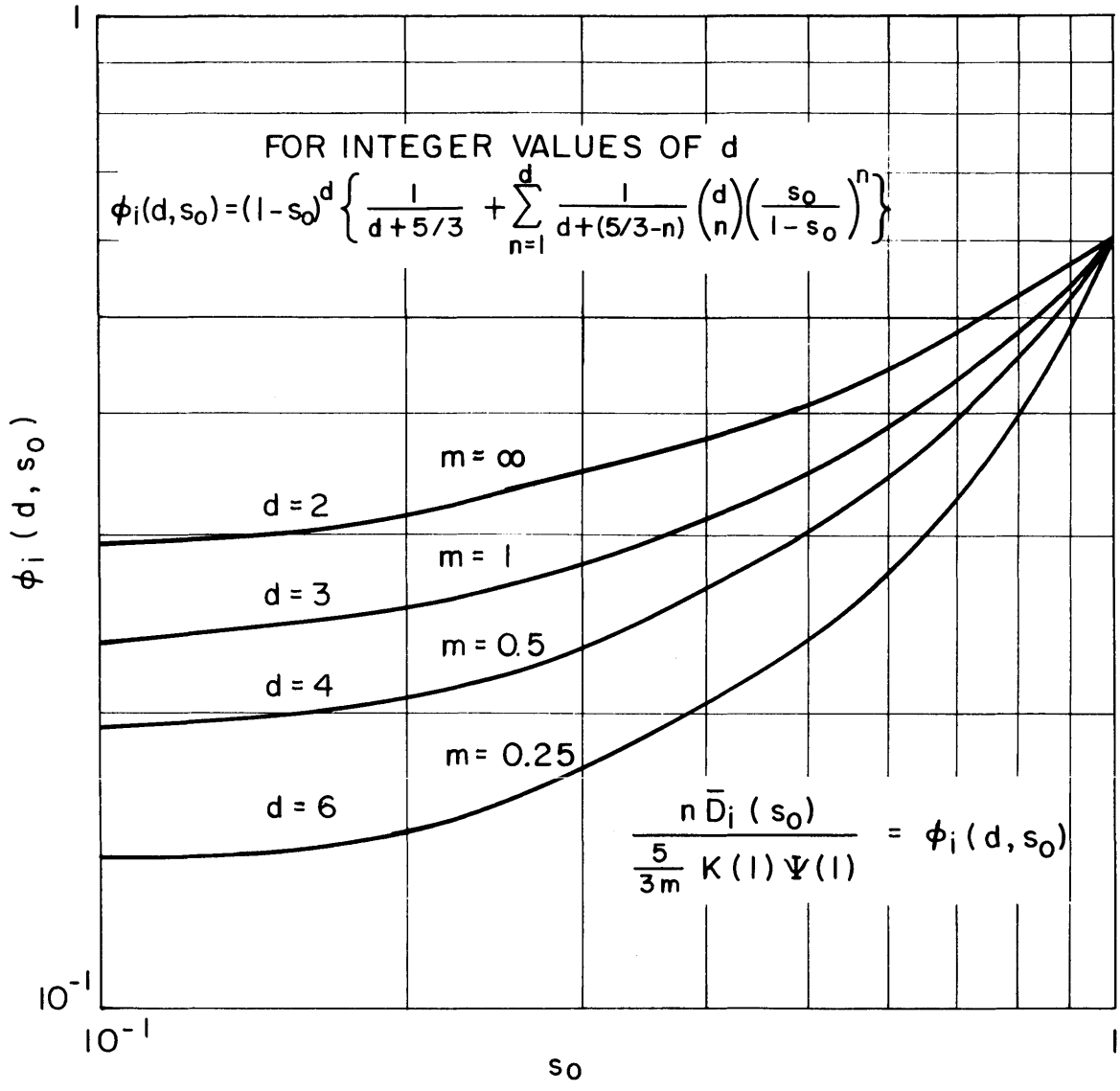

WEIGHTED MEAN DIFFUSION COEFFICIENT-SORPTION

Figure 3.4

(from Eagleson, 1978c)

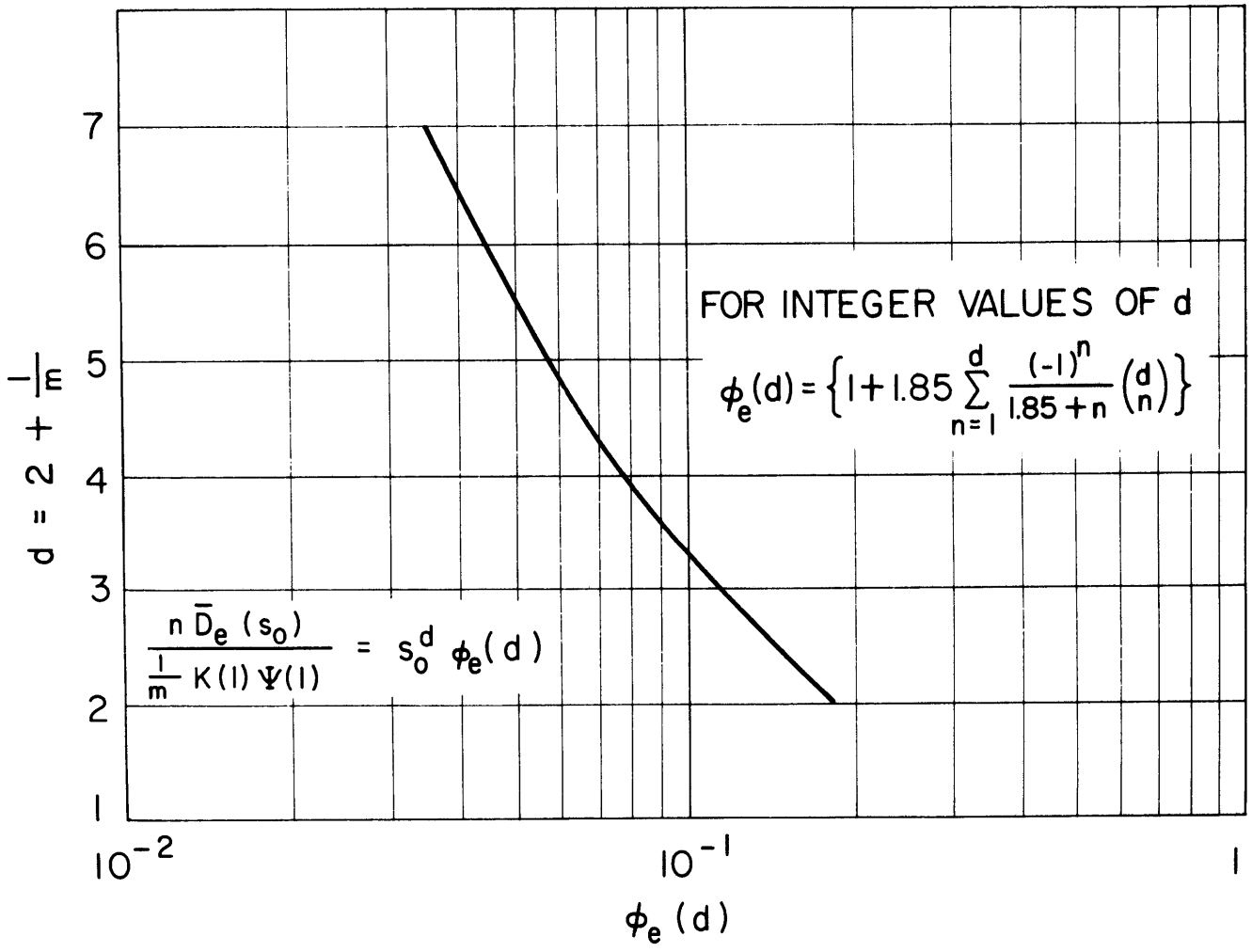

WEIGHTED MEAN DIFFUSION COEFFICIENT-DESORPTION

Figure 3.5

(from Eagleson, 1978c)

C. Percolation

The soil moisture concentration outside the boundary layer is assumed to be constant during the wet season at its average value, $\bar{s}_o$. With this assumption, the apparent percolation velocity, $v(s_o)$, is considered as a steady, gravitational seepage,

$$v(\bar{s}_o) = K(\bar{s}_o) \tag{3.25}$$

During the dry season, the soil moisture is assumed to go to zero, hence the percolation is also neglected in this period of the year.

Applying linear superposition to the above apparent velocities gives estimates of the total soil moisture fluxes (the plant growing season is assumed to be coincident with the rainy season).

In the rainy season: the infiltration during storms is obtained from Eqs. (3.21) and (3.23) as

$$\frac{f_i^*(t,\bar{s}_o)}{K(1)} = (1-\bar{s}_o)\left|\frac{5n\,\Psi(1)\,\phi_i(d,\bar{s}_o)}{3\,\pi\,m\,t\,K(1)}\right|^{1/2} + \frac{1}{2}(1+\bar{s}_o^c) - \frac{w}{K(1)} \tag{3.26}$$

The exfiltration between storms can be expressed, using Eqs. (3.22) and (3.23) as

$$\frac{f_e^*(t,\bar{s}_o)}{K(1)} = \bar{s}_o^{1+d/2}\left[\frac{n\,\Psi(1)\,\phi_e(d)}{\pi\,m\,t\,K(1)}\right]^{1/2} - \frac{Me_v}{K(1)} + \frac{w}{K(1)} \tag{3.27}$$

The net percolation to the water table is represented, using Eqs. (3.23) and (3.25), as

$$\frac{v(\bar{s}_o)}{K(1)} = \bar{s}_o^c - \frac{w}{K(1)} \qquad (3.28)$$

where the capillary rise, in the rainy season, is as in Eq. (3.23), or

$$\frac{w}{K(1)} = \left[1 + \frac{3/2}{mc - 1}\right]\left[\frac{\bar{\Psi}(1)}{Z}\right]^{mc} \quad , \quad w/\bar{e}_p < 1 \qquad (3.29)$$

In the dry season: the capillary rise is the same as in the rainy season.

The groundwater runoff is derived from the conservation of mass equation (Eagleson, 1977), assuming no change in groundwater storage.

The expected value of the annual groundwater runoff is then expressed as

$$E[R_{g_A}] = m_T\, K(1)\, \bar{s}_o^c - Tw \qquad (3.30)$$

where

T = full water year

3.2.3 Evapotranspiration and Surface Retention

Eagleson (1978d) derives separately the expected value of interstorm evaporation from the bare soil fraction, $E[E_{s_j}]$, and transpiration from the vegetated fraction of the surface, $E[E_{v_j}]$, using the exfiltration capacity, Eq. (3.27), with some assumptions, as mentioned in Section 3.1. The surface retention is included in these expected values.

The total interstorm evapotranspiration can be obtained by weighting these two components according to the canopy density, M, as

$$E[E_{T_j}] = (1 - M)\, E[E_{s_j}] + M\, E[E_{v_j}] \tag{3.31}$$

The total annual (seasonal) evapotranspiration is obtained by

$$E[E_{T_A}] = \sum_{j=1}^{\nu} E[E_{T_j}] = m_{\nu}\, E[E_{T_j}] \tag{3.32}$$

The potential rates of bare soil evaporation, e_p, and vegetated surface transpiration, e_{p_v}, are replaced by their mean values, $\bar{e}_p$ and $\bar{e}_{p_v}$. Then the plant coefficient is defined as

$$k_v = \bar{e}_{p_v} / \bar{e}_p \tag{3.33}$$

The value of this coefficient depends upon the coefficient species in the region.

The total annual (seasonal) potential evapotranspiration is then

$$E[E_{p_A}] = m_{\nu}\, m_{t_b} [(1 - M)\, \bar{e}_p + M k_v\, \bar{e}_p] \tag{3.34}$$

Dividing Eq. (3.32) by Eq. (3.34) gives the so-called evapotranspiration function or evaporation efficiency

$$J(E, M, k_v, \lambda h_o, \beta h_o/\bar{e}_p)^1 = \frac{E[E_{T_A}]}{E[E_{p_A}]} = \frac{(1-M)\, E[E_{s_j}] + M E[E_{v_j}]}{m_{t_b}\, \bar{e}_p\, [1 - M(1 - k_v)]} \tag{3.35}$$

where

h_o = surface retention capacity

and

$$E = [2\beta n\, K(1)\, \Psi(1)/\pi\, m\, \bar{e}_p^2]\, \phi_e(d)\, \bar{s}_o^{d+2} \tag{3.36}$$

---

[1] $J(E, M, k_v, \lambda h_o, \beta h_o/\bar{e}_p) = J(E, M, k_v, h_o) = J$

E is called the bare soil evaporation effectiveness.

The expected values of interstorm bare soil surface retention, $E[E_{rs_j}]$, and vegetated surface retention, $E[E_{rv_j}]$, are derived separately in a manner analogous to the bare soil evaporation.

Following the same procedures as in the evapotranspiration yields the expected value of annual (seasonal) surface retention as

$$E[E_{r_A}] = m_v\{(1 - M)\ E[E_{rs_j}] + ME[E_{rv_j}]\} \qquad (3.37)$$

3.2.4 Surface Runoff and Total Infiltration

The probability distribution of the surface runoff is derived, (Eagleson, 1978e), employing the infiltration capacity, Eq. (3.26).

It is assumed that the rainfall intensity, i, is constant during the storm and has an exponential distribution. Also, independence is assumed between i and the exponentially-distributed t_r.

In the present work, the surface runoff derivation has been modified (see Tellers and Eagleson, 1980), considering that the whole surface retention occurs at the beginning of the storm, Fig. 3.6, as

$$R_{s_j} = \int_{t_o+ho/i}^{t_r} (i - f_i^*)\ dt \quad , \quad t_r > h_o/i \qquad (3.38)$$

in which (Eagleson, 1978e)

$$t_o = \frac{S_i^2}{2(i - A_o)^2} \quad , \quad i >> A_o \qquad (3.39)$$

where

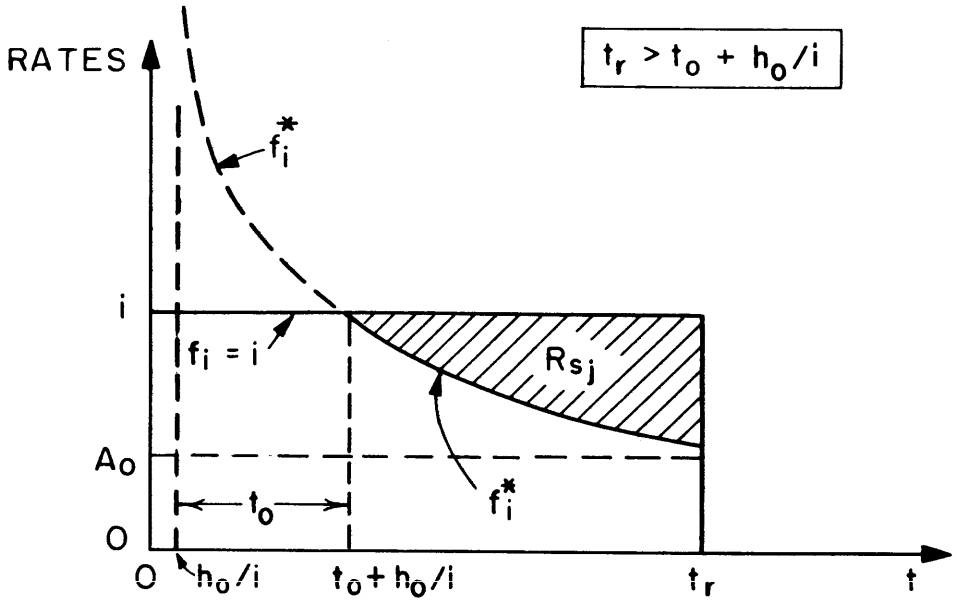

SURFACE RUNOFF GENERATION DURING TYPICAL STORM ($t_r > t_o$)

Figure 3.6

(after Eagleson, 1978e)

$$S_i = \text{infiltration sorptivity} = 2(1 - \bar{s}_o) \left[\frac{5n\ K(1)\ \Psi(1)\ \phi_i(d, \bar{s}_o)}{3\ \pi\ m}\right]^{1/2} \tag{3.40}$$

and

$$A_o = \frac{1}{2} K(1)[1 + \bar{s}_o^c] - w \tag{3.41}$$

In the manner of Eagleson (1978e),

$$R_{s_j}(i, t_r, h_o, \bar{s}_o) = (i - A_o)t_r - S_i(t_r/2)^{1/2} \tag{3.42}$$

and the expected value of the annual (seasonal) surface runoff becomes

$$\frac{E[R_{s_A}]}{E[P_A]} = e^{-G-2\sigma}\ \Gamma(\sigma + 1) \cdot (\sigma)^{-\sigma} \tag{3.43}$$

where

$G \equiv$ gravitational infiltration parameter

$$= \frac{\alpha K(1)}{2} [1 + \bar{s}_o^c] - \alpha w \tag{3.44}$$

and

$\sigma \equiv$ capillary infiltration parameter

$$= \left[\frac{5n\ \eta^2\ K(1)\ \Psi(1)(1 - \bar{s}_o^c)\ \phi_i(d, \bar{s}_o)}{6\ \pi\ \delta\ m}\right] \tag{3.45}$$

Now, the expected value of the annual (seasonal) rainfall excess, $E[R^*_{s_A}]$, takes the value

$$\frac{E[R^*_{s_A}]}{E[P_A]} = e^{-G-2\sigma}\ \Gamma(\sigma + 1) \cdot (\sigma)^{-\sigma} + \frac{E[E_{r_A}]}{E[P_A]} \tag{3.46}$$

where $E[E_{r_A}]$ is defined in Eq. (3.37).

Substituting Eq. (3.46) in Eq. (3.3) gives the infiltration,

$$\frac{E[I_A]}{E[P_A]} = 1 - e^{-G-2\sigma}\,\Gamma(\sigma+1)\cdot(\sigma)^{-\sigma} - \frac{E[E_{r_A}]}{E[P_A]} \qquad (3.47)$$

and the dimensionless water balance equation will be

$$1-e^{-G-2\sigma}\,\Gamma(\sigma+1)\cdot(\sigma)^{-\sigma} = \frac{E[E_{p_A}]}{E[P_A]}\,J(E,M,k_v,h_o) + \frac{m_\tau\,K(1)}{E[P_A]}\,\bar{s}_o^{c} - \frac{Tw}{E[P_A]} \qquad (3.48)$$

3.3 First Order Analysis of Annual (Seasonal) Water Balance

For a given climate and soil, the water balance equation, Eq. (3.48), has a unique solution for $\bar{s}_o$. This solution may be obtained by iteration.

Eliminating the soil moisture concentration, $\bar{s}_o$, Eagleson (1978g) gives

$$E[Y_A] = g_2(m_{P_A},\ E[E_{p_A}],\ m_\tau;\ \text{parameters}) \qquad (3.49)$$

He assumes that all Y_A variability comes from P_A and none from E_{p_A} and/or τ. Dropping the expectation notations in the average annual (seasonal) water balance equation, Eq. (3.48), to obtain a first order approximation of the annual (seasonal) water balance, gives the monotonic function

$$Y_A = g_2(P_A;\ \text{parameters}) \qquad (3.50)$$

The cumulative distribution function of the annual (seasonal) yield now can be obtained from that of the precipitation, Eq. (3.9), using Eq. (3.50) (see Benjamin and Cornell, 1970). That is

$$F_{Y_A}(y) = F_{P_A}(g_2^{-1}(y)) \tag{3.51}$$

or

$$\text{Prob}[\frac{Y_A}{m_{P_A}} < z] = e^{-m_\nu}\{1 + \sum_{\nu=1}^{\infty} \frac{(m_\nu)^\nu}{\nu!} P[\nu\kappa, m_\nu\kappa\, g_2^{-1}(z)] \tag{3.52}$$

where

$$g_2^{-1}(z) = P_A/m_{P_A} \tag{3.53}$$

3.4 Potential Evapotranspiration as a Random Variable

In this section, we will consider variability of the annual (seasonal) potential evapotranspiration in order to omit the simplification of fixing this variable at its long-term mean value, $E[E_{p_A}]$, in the original model (Eagleson, 1978d).

Analyzing the observed data of water surface potential evaporation, E_{p_w}, during the rainy season in the Machar region, as shown in Table 3.1. We find that it has a coefficient of variation, v_e,

$$v_e \equiv \frac{\sigma_e}{m_e} = O(10^{-1}) \tag{3.54}$$

where

m_e = mean value of water surface-seasonal potential evaporation

and

σ_e = standard deviation of water surface-seasonal potential evaporation

More importantly, perhaps, the coefficients of variation of the water surface potential evaporation and seasonal precipitation are of the same order as shown in Table 3.1. Both are, therefore, important as contributors to variance in the annual yield.

One can write a simple relationship between the seasonal potential evaporation of water surface, E_{p_w} and the seasonal evapotranspiration, E_{T_s}, as

$$E_{T_s} = B \cdot E_{p_w} \tag{3.55}$$

in which

$$B = J \cdot [1 - M(1 - k_v)] \cdot \bar{R}_2 \tag{3.56}$$

where

$$J \equiv J(E, M, k_v, h_o) \quad [\text{Eq. (3.35)}]$$

and

$$\bar{R}_2 = \frac{\text{bare soil seasonal potential evaporation, } E_{p_s}}{\text{water surface seasonal potential evaporation, } E_{p_w}} \tag{3.57}$$

The ratio $\bar{R}_2$ depends on the values of albedo of both bare soil and water surfaces according to the energy transfer equation. This ratio is always less than unity. In our region of research, it is about 0.94 (Chapter 4).

Table 3.1

STATISTICAL PARAMETERS OF SEASONAL PRECIPITATION AND WATER SURFACE POTENTIAL EVAPORATION IN MACHAR REGION*

Station / Parameter	Kurmuk		Gambela	
	P_s	E_{p_w}	P_s	E_{p_w}
Mean Value (cm)	96.25	65.05	130.64	64.16
Standard Deviation (cm)	18.28	16.46	23.71	10.84
Coeff. of Variation	0.19	0.25	0.18	0.17
Coeff. of Correlation	0.26		0.12	

*Complete Data Analysis is in Chapter 4.

The water surface seasonal potential evaporation, E_{p_w}, can be determined, following Eagleson (1978d), as

$$E_{p_w} = \sum_{j=1}^{\nu} e_{p_{w_j}} (t_{a_j} - t_{r_j}) \tag{3.58}$$

where

$e_{p_{w_j}}$ = interstorm water surface potential evaporation rate

t_{a_j} = storm interarrival period

and

t_{r_j} = storm duration

The storm duration, t_{r_j}, in the Machar region is very short in comparison to the storm interarrival period, t_{a_j}, because the storms are convective (Chapter 2). Therefore, we may neglect the storm duration, t_{r_j}, in Eq. (3.58).

Neglecting the variability of the interstorm potential evaporation rate during the rainy season and replacing this rate by its mean value, $\bar{e}_{p_w}$, Eq. (3.58) yields

$$E_{p_w} = \bar{e}_{p_w} \sum_{j=1}^{\nu} t_{a_j} \tag{3.59a}$$

or

$$E_{p_w} = \tau \cdot \bar{e}_{p_w} \tag{3.59b}$$

3.4.1 Fitted Distribution of Seasonal Water Surface Potential Evaporation

The seasonal values of water surface potential evaporation, E_{p_w}, will be calculated in Chapter 4 through Piche observations. Plotting

these values gives an essentially normal probability density function, as shown in Figs. 3.7 and 3.8 for Kurmuk and Gambela meteorological stations, respectively.

Since there is no possibility of negative events, the truncated normal probability density function is chosen for the seasonal water surface potential evaporation, as shown in Fig. 3.9a. This is

$$f_{E_{p_w}}(E) = K \cdot e^{-\frac{1}{2}\left(\frac{E - m_e}{\sigma_e}\right)^2}, \quad E \geq 0 \tag{3.60}$$

where

K = constant

The value of K can be obtained as

$$K \int_0^\infty e^{-\frac{1}{2}\left(\frac{E - m_e}{\sigma_e}\right)^2} \cdot dE = 1 \tag{3.61}$$

then

$$K = \frac{2}{\sqrt{2\pi}\,\sigma_e\left[1 + \operatorname{erf}\left(\frac{m_e}{\sqrt{2}\,\sigma_e}\right)\right]} \tag{3.62}$$

where

erf( ) = error function of ( )

The probability density function of the seasonal water surface potential evaporation, Eq. (3.60), using Eq. (3.62), is

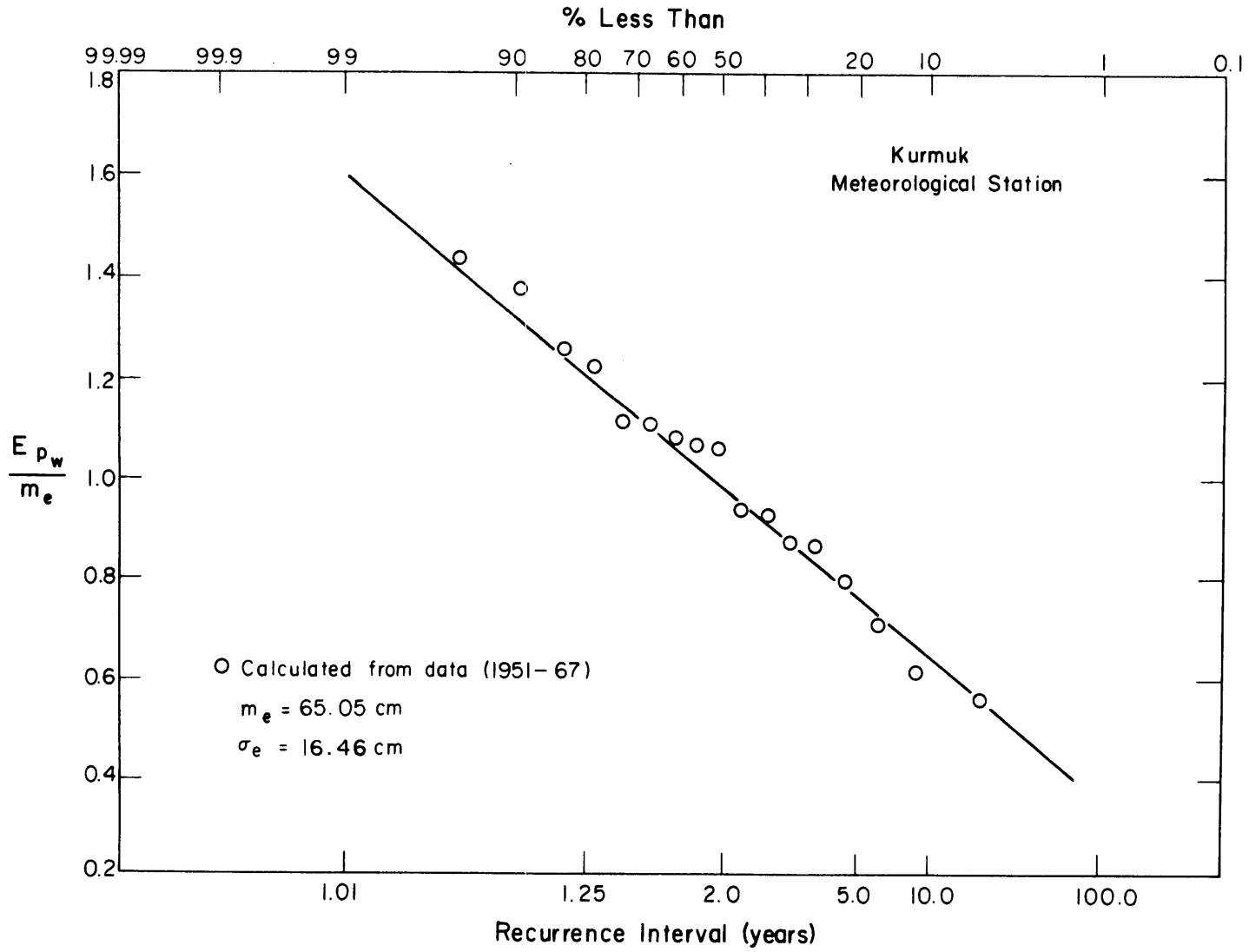

Figure 3.7

FITTED NORMAL DISTRIBUTION OF WATER SURFACE SEASONAL POTENTIAL EVAPORATION AT KURMUK

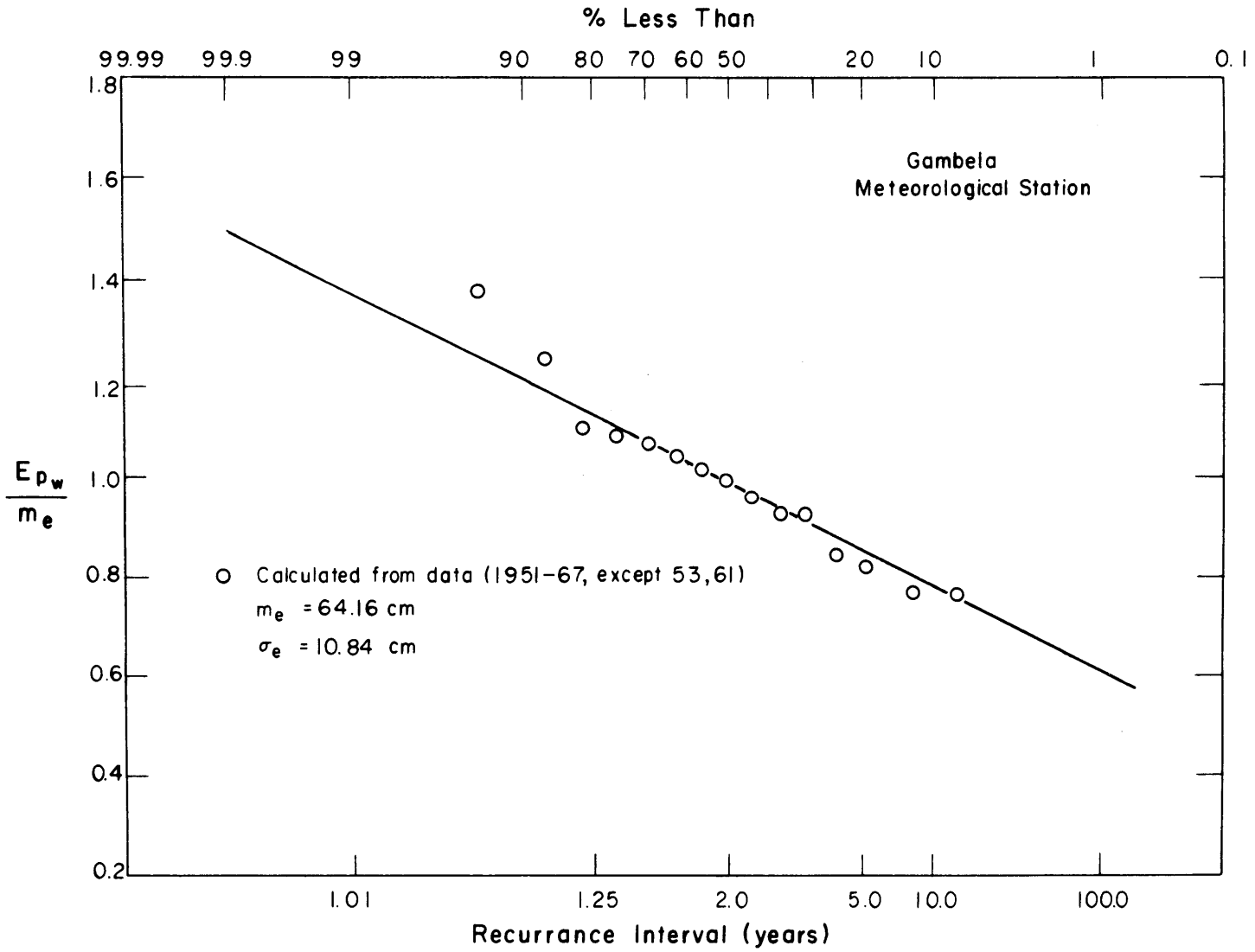

Figure 3.8

FITTED NORMAL DISTRIBUTION OF WATER SURFACE SEASONAL POTENTIAL EVAPORATION AT GAMBELA

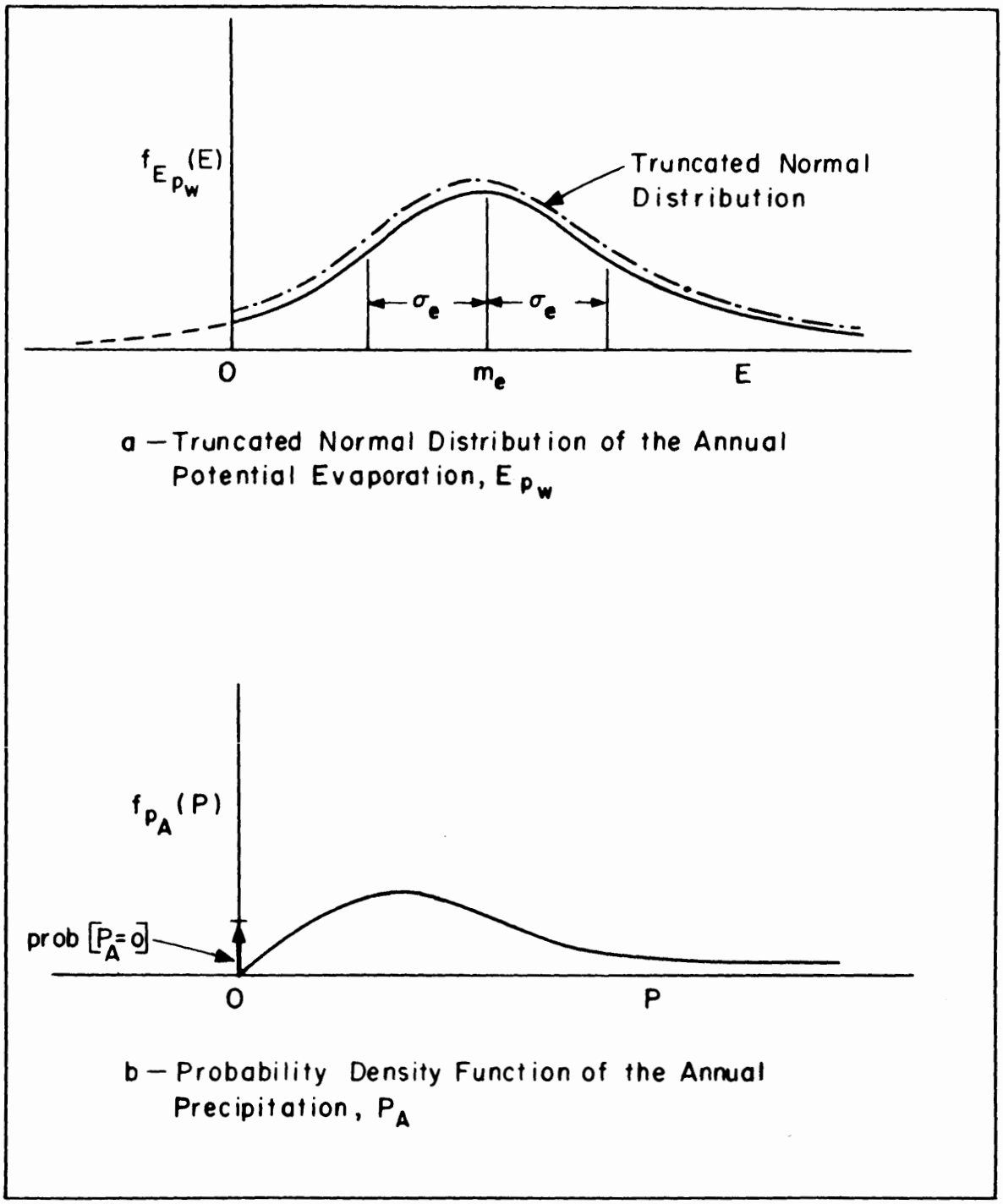

Figure 3.9

PROBABILITY DENSITY FUNCTIONS OF THE ANNUAL (SEASONAL) POTENTIAL EVAPORATION AND PRECIPITATION

$$F_{E_{p_w}}(E) = \frac{1}{\sqrt{\frac{\pi}{2}}\,\sigma_e\,T}\, e^{-\frac{1}{2}\left(\frac{E - m_e}{\sigma_e}\right)^2}, \qquad E \geq 0 \tag{3.63}$$

where

$$T = 1 + \operatorname{erf}\left(\frac{m_e}{\sqrt{2}\,\sigma_e}\right) \tag{3.64}$$

After dropping the expected value notations from the average annual (seasonal) water balance equation, this equation shows that there is a non-linear relationship between the evapotranspiration efficiency, J, and the annual (seasonal) yield, Y_A, through the annual (seasonal) soil moisture concentration, s_o. To continue the mathematical derivation of the cumulative distribution function of the yield, we will assume that the evapotranspiration efficiency, J, is constant.

3.4.2 Derived Distribution of Annual (Seasonal) Yield

The water balance equation now has the form

$$Y_A = P_A - B\,E_{p_w} \tag{3.65}$$

in which B is constant.

The coefficient of correlation between P_A and E_{p_w} is so small (Table 3.1) that we can assume that these two variables are statistically independent.

The cumulative distribution function of the annual (seasonal) yield is given by either (Benjamin and Cornell, 1970),

$$F_{Y_A}(y) = \iint_{R_1} f_{P_A,E_{p_w}}(P, E)\, dP \cdot dE \tag{3.66}$$

or

$$F_{Y_A}(y) = 1 - G_{Y_A}(y) = 1 - \iint_{R_2} f_{P_A,E_{p_w}}(P, E)\, dP \cdot dE \tag{3.67}$$

where

$f_{P_A,E_{p_w}}(P, E) \equiv$ joint probability density function of P_A and E_{p_w}

and

R_1, R_2 = integration regions, as shown in Fig. 3.10

Due to the assumption of independence of P_A and E_{p_w}, the joint probability density function is

$$f_{P_A,E_{p_w}}(P, E) = f_{P_A}(P) \cdot f_{E_{p_w}}(E) \tag{3.68}$$

The probability density function of the annual (seasonal) precipitation $f_{P_A}(P)$, is derived by Eagleson (1978b):

$$f_{P_A}(P) = e^{-m_\nu}\left\{\delta(P) + \sum_{\nu=1}^{\infty} \frac{\eta\kappa(\eta\kappa p)^{\nu\kappa-1}\, e^{-\eta\kappa p}(m_\nu)^\nu}{\nu!\ \Gamma(\nu\kappa)}\right\} \tag{3.69}$$

where

$$\delta(P = 0) = 1 \tag{3.70}$$

and

$$\delta(P > 0) = 0 \tag{3.71}$$

It takes the form sketched in Fig. 3.9b.

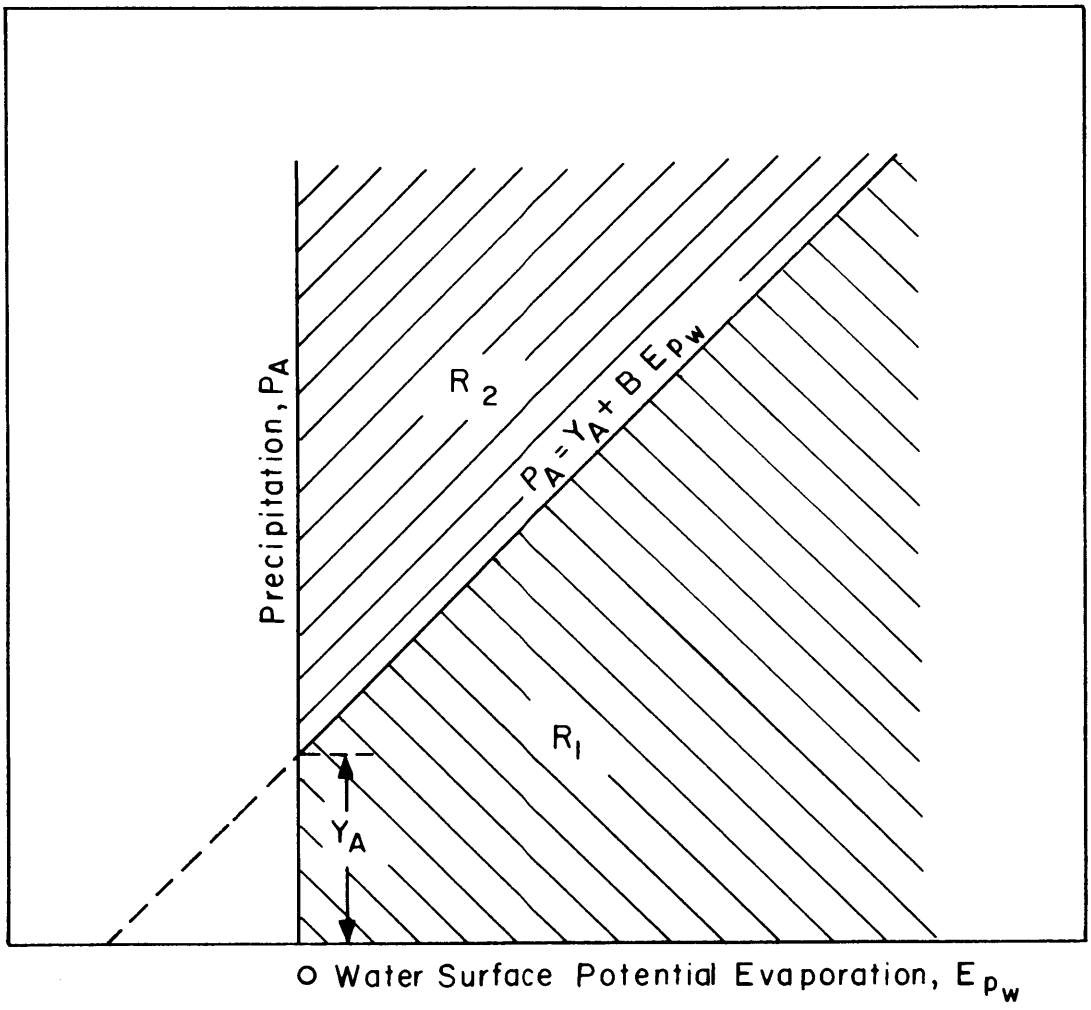

Figure 3.10

REGIONS OF INTEGRATION, R_1 AND R_2

Substituting Eqs. (3.63) and (3.69) in Eq. (3.68) and using Eq. (3.7), Eq. (3.66) gives

$$F_{Y_A}(y) = \frac{e^{-m_\nu}}{\sqrt{\frac{\pi}{2}}\,\sigma_e\,T} \int_0^\infty e^{-\left(\frac{E-m_e}{\sqrt{2}\,\sigma_e}\right)^2} \cdot dE \int_0^{y+BE} \left\{\delta(P) + \sum_{\nu=1}^{\infty} \frac{\eta\kappa(\eta\kappa P)^{\nu k-1} \cdot e^{-\eta\kappa P}(m_\nu)^\nu}{\nu!\,\Gamma(\nu\kappa)}\right\} dP \qquad (3.72)$$

or

$$F_{Y_A}(y) = e^{-m_\nu}\left\{1 + \frac{1}{\sqrt{\frac{\pi}{2}}\,\sigma_e\,T} \sum_{\nu=1}^{\infty} \frac{(m_\nu)^\nu}{\nu!} \int_0^\infty e^{-\left(\frac{E-m_e}{\sqrt{2}\,\sigma_e}\right)^2} \cdot P\left[\nu\kappa,\ m_\nu\kappa\left(\frac{y+BE}{m_{P_A}}\right)\right] dE\right\} \qquad (3.73)$$

The integration in Eq. (3.73) cannot be carried out analytically. However, it can be performed numerically. The numerical solution is shown in Appendix (A). The sensitivity analysis of this solution will be presented in Chapter 5.

To derive an approximate solution for the cumulative distribution function of the total annual (seasonal) yield, we use Eq. (3.67) in which

$$G_{Y_A}(y) = \int_y^\infty f_{P_A}(p)\,dp \int_0^{\frac{p-y}{B}} f_{E_{P_w}}(E)\,dE \qquad (3.74)$$

Using Eqs. (3.63) and (3.69) gives

$$G_{Y_A}(y) = \frac{e^{-m_\nu}}{\sqrt{\frac{\pi}{2}}\,\sigma_e\,T} \int_y^\infty \left[\delta(p) + \sum_{\nu=1}^{\infty} \frac{\eta\kappa(\eta\kappa p)^{\nu\kappa-1} e^{-\eta\kappa p}}{\Gamma(\nu\kappa)\,\nu!}\right] dp \cdot I \tag{3.75}$$

where

$$I = \int_0^{\frac{p-y}{B}} e^{-\left(\frac{E-m_e}{\sqrt{2}\,\sigma_e}\right)^2} \cdot dE \tag{3.76}$$

Changing the variables in Eq. (3.76), $x = \frac{E-m_e}{\sqrt{2}\,\sigma_e}$, and integrating gives,

$$I = \sqrt{\frac{\pi}{2}}\,\sigma_e \left\{ \operatorname{erf}\left(\frac{p-y-Bm_e}{\sqrt{2}\,B\,\sigma_e}\right) + \operatorname{erf}\left(\frac{m_e}{\sqrt{2}\,\sigma_e}\right)\right\} \tag{3.77}$$

Substituting Eq. (3.77) in Eq. (3.75), we obtain

$$\begin{aligned} G_{Y_A}(y) = \frac{e^{-m_\nu}}{\sqrt{\frac{\pi}{2}}\,\sigma_e\,T} \Bigg\{ & \operatorname{erf}\left(\frac{m_e}{\sqrt{2}\,\sigma_e}\right) \int_y^\infty \delta(p)\,dp + \operatorname{erf}\left(\frac{m_e}{\sqrt{2}\,\sigma_e}\right) \sum_{\nu=1}^{\infty} \frac{(m_\nu)^\nu}{\Gamma(\nu\kappa)\nu!} \\ & \int_y^\infty (\eta\kappa p)^{\nu\kappa-1}\, e^{-\eta\kappa p}\, \eta\kappa\, dp + \int_y^\infty \delta(p)\, \operatorname{erf}\left(\frac{p-y-Bm_e}{\sqrt{2}\,B\,\sigma_e}\right) dp \\ & + \sum_{\nu=1}^{\infty} \frac{(m_\nu)^\nu}{\Gamma(\nu\kappa)\,\nu!} \int_y^\infty (\eta\kappa p)^{\nu\kappa-1}\, e^{-\eta\kappa p}\, \operatorname{erf}\left(\frac{p-y-Bm_e}{\sqrt{2}\,B\,\sigma_e}\right) \cdot \eta\kappa\, dp \Bigg\} \end{aligned} \tag{3.78}$$

in which

$$\operatorname{erf}\left(\frac{m_e}{\sqrt{2}\,\sigma_e}\right) \int_y^\infty \delta(p)\,dp = \begin{vmatrix} \operatorname{erf}\left(\frac{m_e}{\sqrt{2}\,\sigma_e}\right), & y = p = 0 \\ 0, & \text{otherwise} \end{vmatrix} \tag{3.79}$$

and

$$\int_{y}^{\infty} \delta(p)\ \mathrm{erf}\left(\frac{p-y-Bm_e}{\sqrt{2}\ B\ \sigma_e}\right) dp = \begin{vmatrix} -\mathrm{erf}\left(\frac{m_e}{\sqrt{2}\ \sigma_e}\right) & , \quad y = p = 0 \\ 0 & , \quad \text{otherwise} \end{vmatrix} \tag{3.80}$$

From Eqs. (3.79) and (3.80), the sum of these two terms in Eq. (3.78) is always zero, even if y = p = 0.

Changing the variables in the other terms of Eq. (3.78) and integrating gives

$$\text{in which} \quad G_{Y_A}(y) = \frac{e^{-m_\nu}}{T}\left\{\mathrm{erf}\left(\frac{m_e}{\sqrt{2}\ \sigma_e}\right) \sum_{\nu=1}^{\infty} \frac{(m_\nu)^\nu}{\Gamma(\nu\kappa)\ \nu!}\ I_1 + \sum_{\nu=1}^{\infty} \frac{(m_\nu)^\nu}{\Gamma(\nu\kappa)\ \nu!}\ I_\nu\right\} \tag{3.81}$$

and

$$I_1 = \Gamma(\nu\kappa)(1 - P[\nu\kappa,\ \eta\kappa y]) \tag{3.82}$$

are

$$I_\nu = \int_{\eta\kappa y}^{\infty} (z)^{\nu\kappa-1} \cdot e^{-z}\ \mathrm{erf}(c_1 z - d_1)\ dz \tag{3.83}$$

where

$$c_1 = 1/[\sqrt{2}\ B\ \sigma_e \eta\kappa] \tag{3.84}$$

and

$$d_1 = \frac{y + Bm_e}{\sqrt{2}\ B\ \sigma_e} \tag{3.85}$$

There is not an analytical solution for I_ν. Since the range of integration begins from $\eta\kappa y$, the approximate solution of I_ν is

For $\nu\kappa-1 \geq \eta\kappa y$ or $\nu \geq N$

$$I_\nu = \mathrm{erf}(c_1(\nu\kappa-1) - d_1)\ \Gamma(\nu\kappa)(1 - P[\nu\kappa,\ \eta\kappa y]) \tag{3.86}$$

For $\nu\kappa-1 < \eta\kappa y$ or $\nu < N$

$$I_\nu = \text{erf}(c_1\eta\kappa y - d_1)\ \Gamma(\nu\kappa)(1 - P[\nu\kappa,\ \eta\kappa y]) \tag{3.87}$$

in which

$$\text{erf}(c_1\eta\kappa y - d_1) = \text{erf}(-\frac{m_e}{\sqrt{2}\ \sigma_e}) = -\ \text{erf}(\frac{m_e}{\sqrt{2}\ \sigma_e}) \tag{3.88}$$

and

$$N = \text{integer of } (\eta y + 1/\kappa) \tag{3.89}$$

Using Eqs. (3.82), (3.86) and (3.87), besides Eqs. (3.84), (3.85), (3.88) and (3.89), Eq. (3.81) takes the form

$$G_{Y_A}(y) = \frac{e^{-m_\nu}}{T}\left\{\text{erf}(\frac{m_e}{\sqrt{2}\ \sigma_e})\ \sum_{\nu=1}^{\infty}\frac{(m_\nu)^\nu}{\nu!}\ P^c[\nu\kappa,\ \eta\kappa y]\right.$$

$$- \text{erf}(\frac{m_e}{\sqrt{2}\ \sigma_e})\ \sum_{\nu=1}^{N-1}\frac{(m_\nu)^\nu}{\nu!}\ P^c[\nu\kappa,\eta\kappa y] + \sum_{\nu=N}^{\infty}\frac{(m_\nu)^\nu}{\nu!}\ P^c(\nu\kappa,\ \eta\kappa y)$$

$$\left.\cdot\ \text{erf}(c_1(\nu\kappa-1) - d_1)\right\} \tag{3.90}$$

Then

$$F_{Y_A}(y) = 1 - G_{Y_A}(y) = 1 - \frac{e^{-m_\nu}}{T}\left\{\sum_{\nu=N}^{\infty}\frac{(m_\nu)^\nu}{\nu!}\ P^c[\nu\kappa,\ \frac{m_\nu\kappa y}{m_{P_A}}](\text{erf}(x)\right.$$

$$\left. + \text{erf}(\frac{m_e}{\sqrt{2}\ \sigma_e}))\right\} \tag{3.91}$$

where

$$P^c[\nu\kappa,\ \frac{m_\nu\kappa y}{m_{P_A}}] = 1 - P[\nu\kappa,\ \frac{m_\nu\kappa y}{m_{P_A}}] \tag{3.92}$$

$$x = \frac{m_{P_A}(\nu\kappa-1) - m_\nu \kappa(y + Bm_e)}{\sqrt{2}\,\sigma_e\, B\, m_\nu\, \kappa} \tag{3.93}$$

and

$$T = 1 + \mathrm{erf}\left(\frac{m_e}{\sqrt{2}\,\sigma_e}\right) \tag{3.94}$$

As far as approximate solutions are concerned, Eq. (3.91) is inferior to Eagleson's approximation of constant potential evaporation as will be presented in Chapter 5. Therefore, we may conclude that the latter is the best approximate solution for this region.

Chapter 4

DATA ANALYSIS AND PRELIMINARY WATER BALANCE

4.1 Remote Sensing Maps and Catchments Identification

Landsat satellite images, scanned in February 1973, have been analyzed by the Remote Sensing Center of the Egyptian Academy of Sciences. These images cover the whole Machar area in the dry season and their analysis concentrates only on the drainage system and on the spatial distribution of vegetation.

From these maps, the drainage system can be described as follows:

a. There are four zones, having the same characteristics, 1) the eastern watersheds (catchments), 2) the toich* plains, 3) the permanent swamps within these plains, and 4) the plains lying between the Sobat and the White Nile (Wol-system plains).

b. The eastern watersheds drain to the permanent swamps through the khors (small streams), Ahmar, Tombak, Yabus, Daga and Lau (arranged from north to south).

c. The toich plains, including the permanent swamps, receive the spilled water from the Baro River through Khor Machar and some other small khors, in addition to the yields from the eastern catchments.

d. The toich plains drain through Khor Adar to the White Nile

*"Toich", i.e., flood plains of the rivers and water courses inundated and exposed by the fluctuations in water-levels.

south of Melut station.

e. The predominant vegetation in the eastern watersheds is light forest, while that in the toich plains is grass with scattered trees.

f. The permanent swamps contain various regional types of vegetation in addition to open water surfaces.

The spatial boundaries should be defined to determine the water balance and the different parameters that are used in the application of the models presented in Chapter 3. In these, it is assumed that there is no surface inflow from outside the catchment. The boundaries of the all zones have been identified to satisfy this assumption. Figure 4.1 shows the drainage system and eastern catchments in the Machar region, according to the Remote Sensing maps.

The divides and sub-divides have been plotted on the vegetation map to determine the vegetation densities and species distributions all over the region zones, as shown in Fig. 4.2.

Now, we can describe the eastern catchments separately as follows:

a. Ahmar catchment is the smallest (1750 km^2). It has vast areas of marshlands and river meanders. Its khor connects with Khor Wadudu after passing by the permanent swamps.

b. Tombak catchment is well-defined. The main vegetation is grass with scattered trees. Its meteorological parameters can be estimated accurately by three stations, Doro, Chali and Kurmuk. Its area is about 2600 km^2.

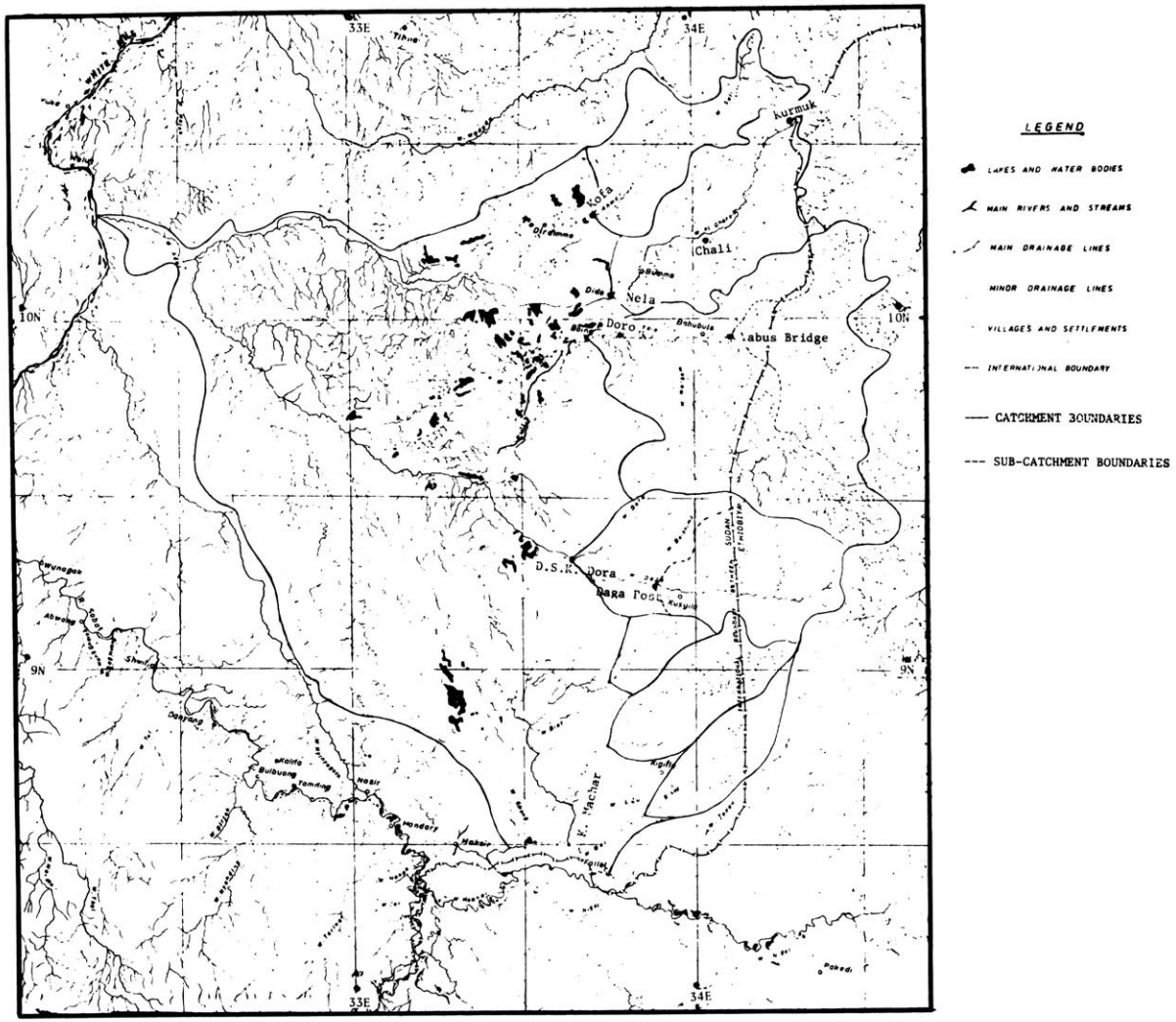

Figure 4.1

GENERAL DRAINAGE MAP OF MACHAR REGION

(after Remote Sensing Center, Cairo, 1979)

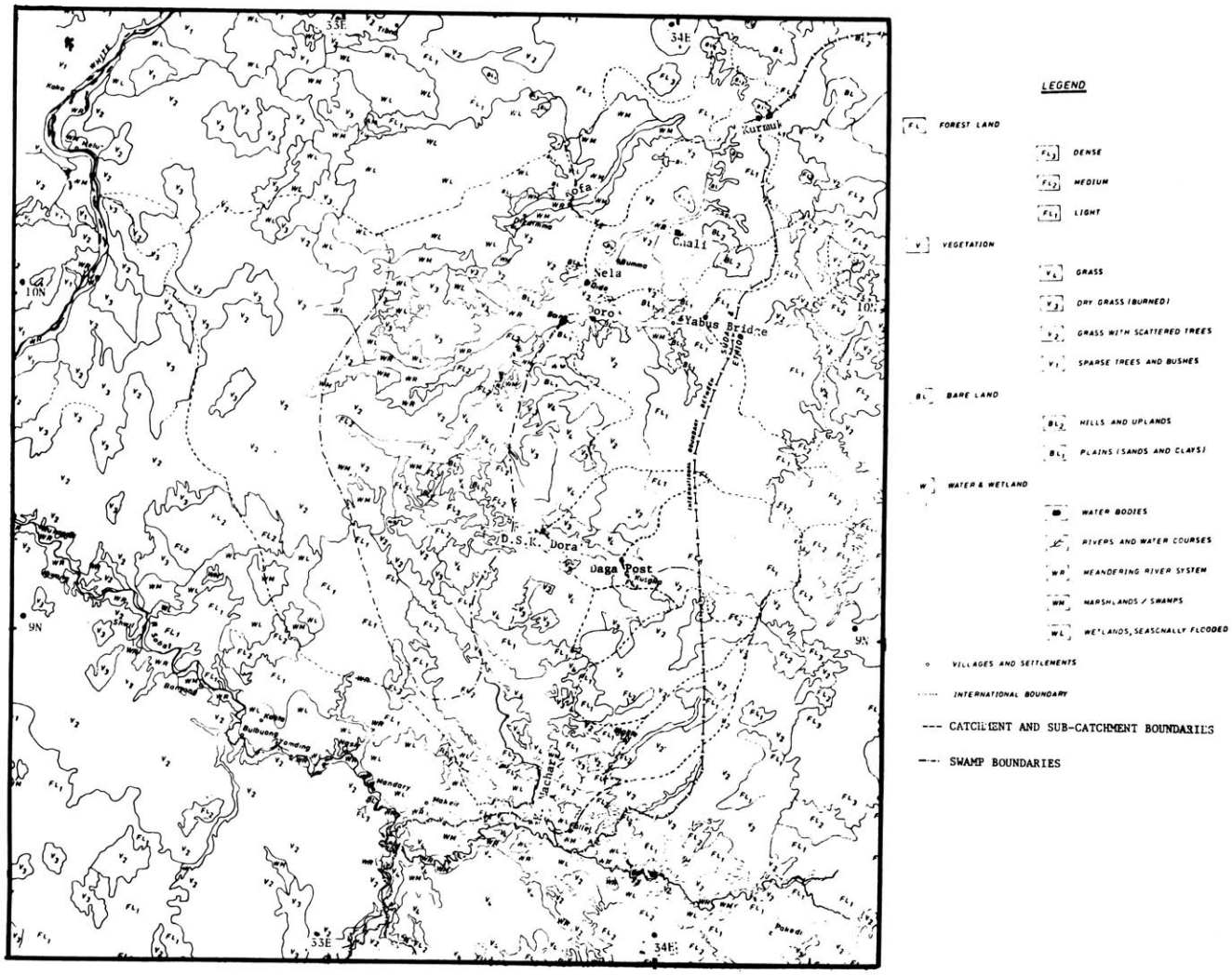

Figure 4.2

GENERAL LAND COVER MAP OF MACHAR REGION

(after Remote Sensing Center, Cairo, 1979)

c. Yabus catchment is the largest (6050 km^3). About 73% of its area is covered by forests. Its sub-catchment that ends at Yabus Bridge gaging station will be employed in Chapter 5 to verify the present model and to estimate some required parameters.

d. Daga catchment has an area of 3200 km^2. Two thirds of this area are almost covered by forests. Its khor connects with Khor Adar through the plains and swamps. The present model will be verified using its sub-catchment above Daga Post.

e. Lau catchment contains three sub-catchments, Lau (1), Lau (2) and Lau (3). Only one sub-catchment has a gaging station, Kigille. About 74% of its total area (2700 km^2) is covered by grasses and scattered trees. One of its branches connects with Khor Machar.

The measured areas of all zones are shown in Table 4.1. The whole area of the Machar region is about 39,100 km^2, excluding plains surrounded by the Sobat and White Nile rivers. Table 4.2 also shows the ratios of different vegetation species in each catchment. These ratios will be used in estimating the average canopy density of each catchment in the rainy season. We assume that these ratios are slightly time-varying in both the dry and rainy seasons.

Table (4-1)

The Areas of Machar Catchments,

Plains and Swamps

Catchment	Area* (Km^2)	sub-catchment	Area* (Km^2)
Ahmar (to Kofa)	1,750		
Tombak (to Nela)	2,600		
Yabus (to Boing)	6,050	Yabus Bridge	2,200
Daga (to D.S. Dora Junction)	3,200	Daga Post	1,900
Lau	2,700	Lau (1)	470
		Lau (2)	1,290
		Lau (3)	940
Sub-total	16,300		
Plains**	22,800	Permanent Swamps	8,700
Total Area	39,100		

*These areas are estimated from the drainage map, Fig. (4-1)

**Including the permanent swamps

Table (4-2)

The Species Ratios in the Catchments

(Estimated from Figure 4-2)

Classification / Catchment	Dense Forest	Medium Forest	Light Forest	Grasses	Grasses With Scattered Trees and Bushes	Bare Land	Marshes and Meanders
Ahmar	0.00	0.00	0.34	0.00	0.20	0.07	0.39
Tombak	0.00	0.00	0.27	0.00	0.42	0.25	0.06
Yabus	0.00	0.13	0.57	0.00	0.21	0.06	0.03
Daga	0.00	0.10	0.57	0.12	0.21	0.00	0.00
Lau	0.00	0.12	0.14	0.00	0.74	0.00	0.00
M†	1.00	0.90	0.85	0.70	0.80	0.00	0.70*
k_v††	1.25	1.25	1.25	0.88	0.88	-	1.55*

† M = The average canopy density of each species

†† k_v = The plant coefficient estimated in Section (4-4)

* Assuming that 70% of the Marshes and Meanders is covered by 2/3 papyrus and 1/3 grasses

4.2 Rainfall Characteristics

The annual rainfall data have been collected from the Nile Basin (Volume VI and its supplements) from 1906 to 1972, and from the Sudan Meteorological Department from 1973 to 1975. These data are analyzed for various stations which are used to calculate the preliminary water balance for the whole study area. Table 4.3 summarizes the analysis of these data.

The averages of annual areal rainfall over each catchment, plains and swamps are estimated using Table 4.3 and Thiessen's meteorology which can be illustrated as

$$P_j = \sum_{i=1}^{N} a_{ij} P_i \qquad (4.1)$$

in which

$$\sum_{i=1}^{N} a_{ij} = 1 \qquad (4.2)$$

where

P_j = estimated areal average values of catchment j

P_i = average value of station i

a_{ij} = weight applied to the average value P_i for catchment j

and

N = number of stations affect the catchment j

The weights, a_{ij}, have been evaluated from Fig. 4.3 for all catchments and other zones (plains and swamps). These weights represent how much the zones are influenced by the different stations and are

Table (4-3)

Station Rainfall Analysis

(Data of 1973, 74, 75 are estimated from [30])

Rainfall Station	Latitude N	Longitude E	Altitude (m)	Average Annual Rainfall (mm)	Coeff. of Variation	Periods of Records
	0 '	0 '				
Renk	11 - 45	32 - 47	382	532.10	0.238	1906-1975
Kurmuk	10 - 33	34 - 17	702	960.85	0.177	1912-69, 71-75
Melut	10 - 27	32 - 12	383	636.06	0.221	1906-1975
Kodok	9 - 53	32 - 07	384	779.62	0.216	1906-14, 1916, 1918-64, 1967-75
Malakal (H.)	9 - 32	31 - 39	389	805.79	0.187	1915-1975
Abwong	9 - 07	32 - 12	389	766.50	0.195	1919-56, 1958-61
Nassir	8 - 37	33 - 04	397	803.46	0.184	1919-61, 1963-75
Gambela	8 - 15	34 - 35	450	1295.29	0.213	1907-1975
Chali**	10 - 13†	34 - 02†	-	860.50	0.291	1950-1967, 1973,74
Doro**	9 - 58†	33 - 42†	-	815.43	0.201	1950-1963
Yabus Br.**	9 - 55†	34 - 10†	-	943.85	0.125	1951-1963
Daga P.**	9 - 12†	33 - 55†	-	939.44	0.202	1952-54, 56, 1958-1961, 64

** Calculated from [30]

† Estimated from the navigation maps

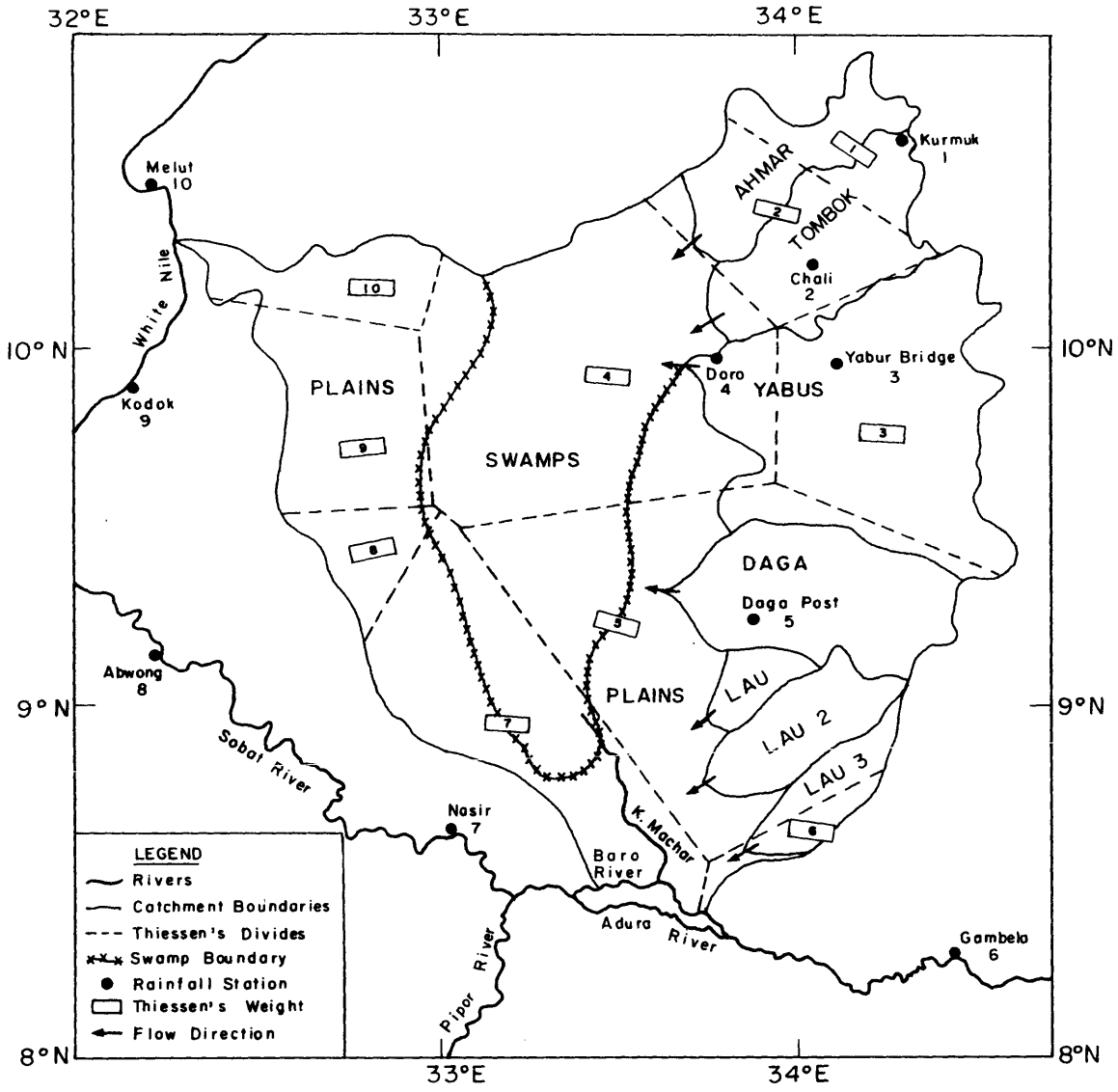

Figure 4.3

THIESSEN'S WEIGHTS OF THE RAINFALL STATIONS IN MACHAR REGION

shown in Table 4.4. This table shows the effect of the stations on the combined catchment,useful for study of the cumulative distribution of flow in the interceptor channel that is proposed to collect the yield of these catchments.

We notice, from Table 4.4 and Fig. 4.3, that Tombak catchment is affected by four stations, Kurmuk, Chali, Doro, and Yabus Bridge, while Daga catchment is affected only by Daga Post station, $\rho = 1$.

Table 4.4 is used not only for areal rainfall, but also for other rainfall characteristics, such as the rainy season length and the number of seasonal storms of the different catchments.

Finally, Table 4.4 gives the stations whose data are required for estimating the model parameters of the eastern watersheds (catchments). These stations are Kurmuk, Gambela, Chali, Dora, Yabus Bridge and Daga Post (arranged according to the available data records).

For various reasons, only twenty years of monthly rainfall records have been analyzed (1950-1967, 1973 and 1974), to estimate the model parameters:

1) The model needs only short records (one of its advantages)
2) Three of the six stations have few records within this period.
3) The meteorological data, temperature, relative humidity, cloud cover, ... etc., are available only during this period. These data will be used to calculate the rate of potential evaporation for both bare soil and water surfaces.

Table (4-4)

Station Thiessen Weights for the Different Zones of Machar Region

Zone \ Station	Kurmuk	Chali	Doro	Yabus Br.	Daga P.	Gambela	Nassir	Abowing	Kodok	Melut	Area (Km^2)
(1)Catchments:											
Ahmar	0.48	0.52	-	-	-	-	-	-	-	-	1,750
Tombak	0.23	0.61	0.11	0.05	-	-	-	-	-	-	2,600
Yabus	-	-	0.09	0.82	0.09	-	-	-	-	-	6,050
Daga	-	-	-	-	1.00	-	-	-	-	-	3,200
Lau	-	-	-	-	0.85	0.15	-	-	-	-	2,700
(2)Plains	-	-	0.13	-	0.24	-	0.24	0.07	0.21	0.11	14,100
(3)Swamps	-	-	0.63	-	0.19	-	0.18	-	-	-	8,700
(4)Combined Catchments Ahmar and Tombak	0.33	0.57	0.07	0.03	0.0	-	-	-	-	-	4,350
Ah.,Tom, and Yabus	0.14	0.24	0.08	0.49	0.05	-	-	-	-	-	10,400
Ah.,Tom, Yab., and Daga	0.11	0.18	0.06	0.37	0.28	-	-	-	-	-	13,600

Most of the total annual precipitation falls in a few months (rainy season). Therefore, the model parameters are seasonally-based, assuming that the system dynamics stop in the dry season (except the capillary rise which occurs around the year). The rainy season length, τ, has been determined at all stations for each year in the short period of record.

During the rainy season, the monthly values of rainfall and the number of rainy days that have a storm depth equal to or greater than one millimeter are used to get the seasonal rainfall, P_s, and the seasonal number of rainy days, ν', respectively.

The seasonal rainfall, rainy season length and number of rainy days ($\geq$ 1 mm) in the rainy season are listed in Appendix B. These values have been analyzed statistically. The mean values of all measured (P_A) and estimated (P_s, τ and ν') variables are evaluated and shown in Table 4.5. The standard deviations of both annual and seasonal rainfall are also given and will be used later for estimating the shape parameter, κ, of the precipitation distributions using the method-of-moments.

The ratio of the mean seasonal precipitation to the mean annual value is almost constant all over the eastern catchments. This ratio is about 0.95.

We also notice from Table 4.5 that the rainfalls are rapidly decreasing from the east (Gambela and Kurmuk stations) to the west (Doro station).

Table (4-5)

Statistical Analysis for The Available Rainfall Data*

Parameter / Station	m_{P_A} (mm)	σ_{P_A} (mm)	m_{P_s} (mm)	σ_{P_s} (mm)	m_T (months)	m_ν (days)	No. of Records (years)	$\frac{m_{P_s}}{m_{P_A}}$	Periods
Kurmuk	1012.55	178.16	962.45	182.84	6.35	70.55	20	0.95	1950-67, 1973,74
Gambela	1368.25	237.39	1306.35	237.05	7.85	104.30	20	0.96	1950-67, 1973,74
Chali	860.50	250.61	817.15	267.14	6.15	61.45	20	0.95	1950-67, 1973,74
Doro	815.43	163.63	773.21	162.05	6.00	64.00	14	0.95	1950-63
Yabus Br.	943.85	118.15	904.08	122.38	6.85	87.77	13	0.96	1951-63
Daga Post	939.44	189.83	894.33	181.75	6.67	77.00	9	0.95	1952-54,56 1958-61,64

*Data are from Sudan Meteorological Department and Appendix (B)

Since the storms are convective and usually occur at the same time of day (Chapter 2), there is little likelihood of any storm having a duration exceeding one day, or for there to be more than one independent storm. Therefore, we assume in the present work that the average number of storms, m_v, is the same as the average number of rainy days, m'_v (both determined in the rainy season).

4.3 Spilling and Drainage

In this section, the spilling of the Baro River along with the drainage of the eastern catchments are studied. These represent a significant part of the water supplies of the permanent swamps.

4.3.1 Spilling Out of the Baro River

The normal (long-term average) discharges of the khors that carry water between the Baro River and the Machar plains and swamps are estimated from the Nile Basin, Vol. IV, until year 1967. Table 4.6 shows these normal discharges and their directions. Khor Machar is the most significant one, having the highest discharge into the area of study.

These discharges don't represent the entire inflow from the Baro River, however, because, in the flood period, water spills over the banks of the Baro and flows overland to the marshes.

To estimate the total inflow from the Baro (spillage), some investigations are made along the Baro River. Figure 4.4 shows a schematic representation of the spilling system along the Baro River. The monthly normals (long-term average until 1967) records of the

Table (4-6)

Discharges of Khors Along Baro River

and Out of Machar Marshes

Khor	Average* Discharge mld/year	Direction
Jakaw	0.244	to Baro
18.5km U.S.K.[1] Machar	0.120	to Macher Marshes
4.8 km U.S.K. Machar	0.060	to Machar Marshes
K Machar	0.861	to Machar Marshes
4.3 km D.S.K.[2] Machar	0.085	to Machar Marshes
K. Makier (net)	0.030	to Machar Marshes
K. Wakaw(net)	0.080	to Sobat
K. Adar	0.040	to White Nile

[1] U.S.K. = up stream of Khor

[2] D.S.K. = down stream of Khor

* Normals (long-term averages) until 1967 (Nile Basin Vol. IV)

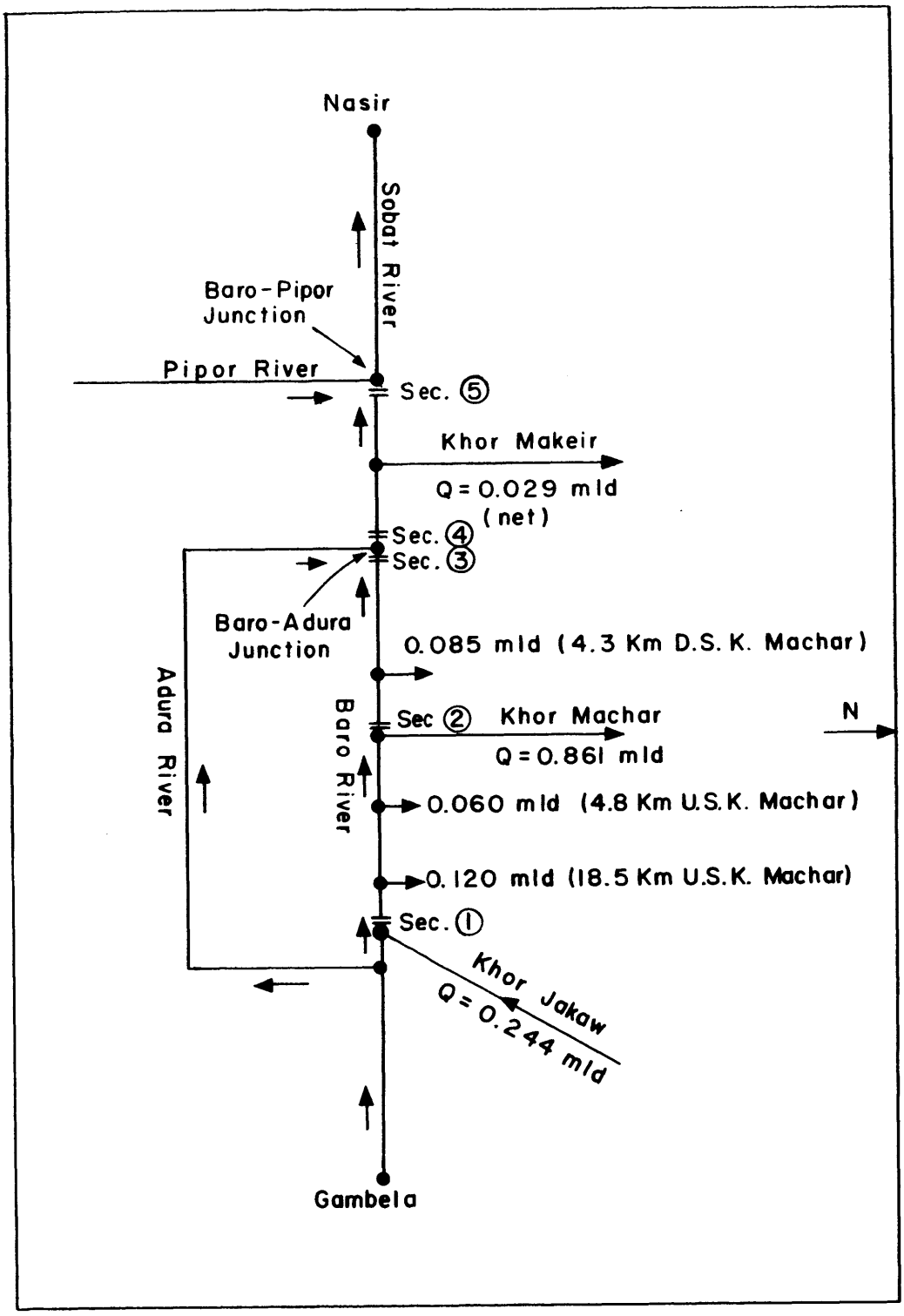

Figure 4.4

SCHEMATIC REPRESENTATION OF SPILLING SYSTEM ALONG BARO RIVER

sections shown in Fig. 4.4 have been analyzed to get the total losses (spilling) between section 1 and 5, along the Baro River.

According to the Nile Basin records, there are some missing data (monthly normals) at sections 1, 2, 3 and 4. These missing data are in the drought (non-flood) season when the Baro is low and without significant losses. Section 5 is used to estimate these missing data at the other sections using the empirical relationships for the flood season presented in Fig. 4.5. Extrapolating these curves into the drought season provides the missing data. The spilling appears, clearly, in Fig. 4.5, where section 5 has a limited capacity in the flood season.

Table 4.7 shows the completed average annual discharges (normals) at the different sections. The differences between sections are summed to give the total flow spilled along both banks of the Baro River. This flow is about 4.6 mld.

As mentioned in Chapter 2, the Equatorial Nile Project (1955) found that 3/4 and 2/3 of the Baro losses, U.S. and D.S. of the Baro-Adura junction, respectively, are the total spilling out of the Baro River to the Machar marshes (deducting the discharges of Khor Machar). Following this estimation, the average total spilling is about 3.54 mld/year. The remainder is spilling to the south of the Baro River.

Drainage from the Machar region occurs through Khors Wakaw and Adar to the Sobat and the White Nile, respectively, as shown in Table 4.6. Their combined total average discharge is about 0.12 mld. Subtracting this outflow from the total spilling that is estimated above gives the net spilling to the Machar swamps of about 3.42 mld which will

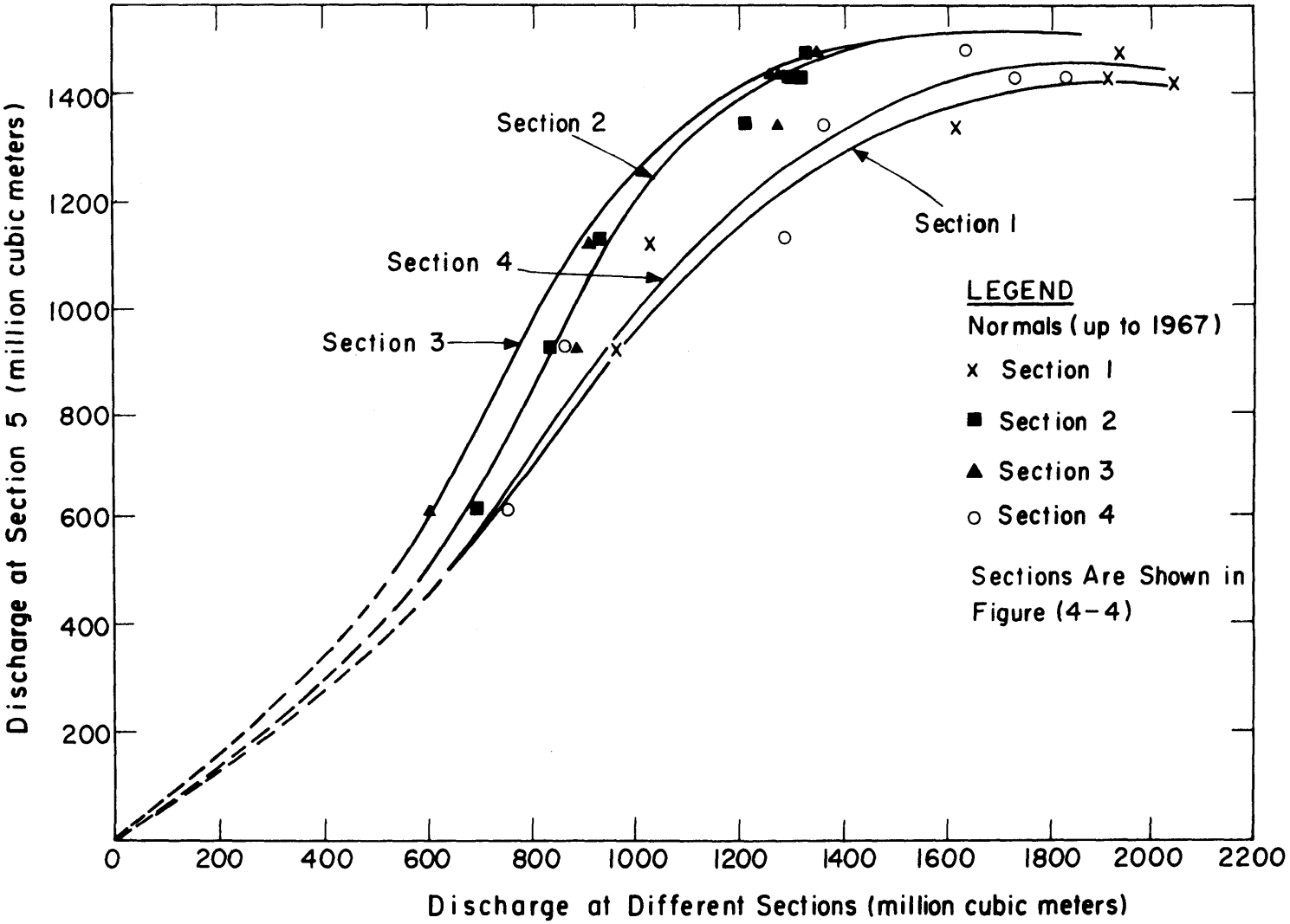

Figure 4.5

STREAMFLOW RELATIONSHIPS AT DIFFERENT STATIONS ALONG BARO RIVER

Table (4-7)

Average Monthly and Annual Discharges** at Different Sections

Along Baro River ($m\text{-}m^3$)†

Section††	Jan.	Feb.	March	April	May	June	July	Aug.	Sept.	Oct.	Nov.	Dec.	Total	Spilling
1	440*	240*	200*	270*	580*	964	1630	1940	2050	1910	1020	755	12000	1814+
2	420*	240*	200*	270*	540*	860	1210	1330	1320	1310	927	698	9325	257
3	357	200*	180*	230*	480*	889	1280	1340	1280	1280	933	619	9068	-
4	442	240*	200*	270*	580*	860	1350	1640	1760	1860	1280	750	11232	1695
5	297	162	129	179	429	925	1340	1480	1430	1430	1120	616	9537	
K.Machar	0.9	0.2	0.0	3.3	37.0	118	145	157	156	147	75.7	20.7	861	861

** Normals up to 1967 [Nile Basin Vol. (IV)]

* Estimated from Fig. (4-5)

† $m.m^3$ = Million Cubic Meters

†† Sections are Shown in Fig. (4-4)

+ After deducting 861 $m.m^3$ (The average discharge of Khor Machar)

be used in the preliminary water balance of the region.

4.3.2 Drainage Out of the Eastern Catchments

Few monthly data have been collected at Yabus Bridge and Daga Post gaging stations from the Egyptian General Inspectorate of Irrigation in Sudan. These data are in Appendix C. In addition, records for the 4 months in the rainy season of 1974 at Kofa, Nela and Kigille were collected. These data will be considered as the measured yields of catchments or sub-catchments upstream of the gaging stations, and will be used to verify the water balance model presented in this work.

The summary of average monthly and total discharges (sub-catchment yields) at Yabus Bridge and Daga Post is shown in Table 4.8. A graphical comparison of these values for the two sub-catchments is presented in Fig. 4.6.

From Fig. 4.6, we find some significant characteristics:

1. A considerable baseflow around the year for both sub-catchments. This is clear in the dry season when the rainfall almost stops. The baseflow of Yabus Bridge is greater than that of Daga Post.
2. The peak of average monthly discharges at Yabus Bridge gaging station lags that of Daga Post gaging station by one month. This lag-time is due to the differences in rainfall and drainage characteristics of the two sub-catchments.
3. At the beginning of the dry season, when the rainfall stops, the two sub-catchments are still draining. This

Table (4-8)

Summary of Monthly Discharges (Yield)
at Yabus Bridge and Daga Post

Gaging Station	Month	Jan.	Feb.	March	April	May	June	July	Aug.	Sept.	Oct.	Nov.	Dec.	Total
Yabus Bridge	Average 1950-55 ($m.m^3$)†	9.88	4.70	3.39	3.15	8.59	17.68	30.11	88.70	118.50	108.23	42.78	19.64	445.35
	Average* 1950-55 (Cm)	0.449	0.214	0.154	0.143	0.390	0.804	1.369	4.032	5.386	4.920	1.945	0.893	20.70
Daga Post	Average 1950-54 ($m.m^3$)†	1.78	1.24	0.31	1.04	5.85	16.38	48.14	112.70	93.80	91.50	36.32	10.92	420.00
	Average** 1950-54 (Cm)	0.094	0.065	0.016	0.055	0.308	0.862	2.534	5.932	4.937	4.816	1.912	0.575	22.10

† $m.m^3$ = million cubic meter

* Area of Yabus Sub-Catchment = 2,200 Km^2

** Area of Daga Sub-Catchment = 1,900 Km^2

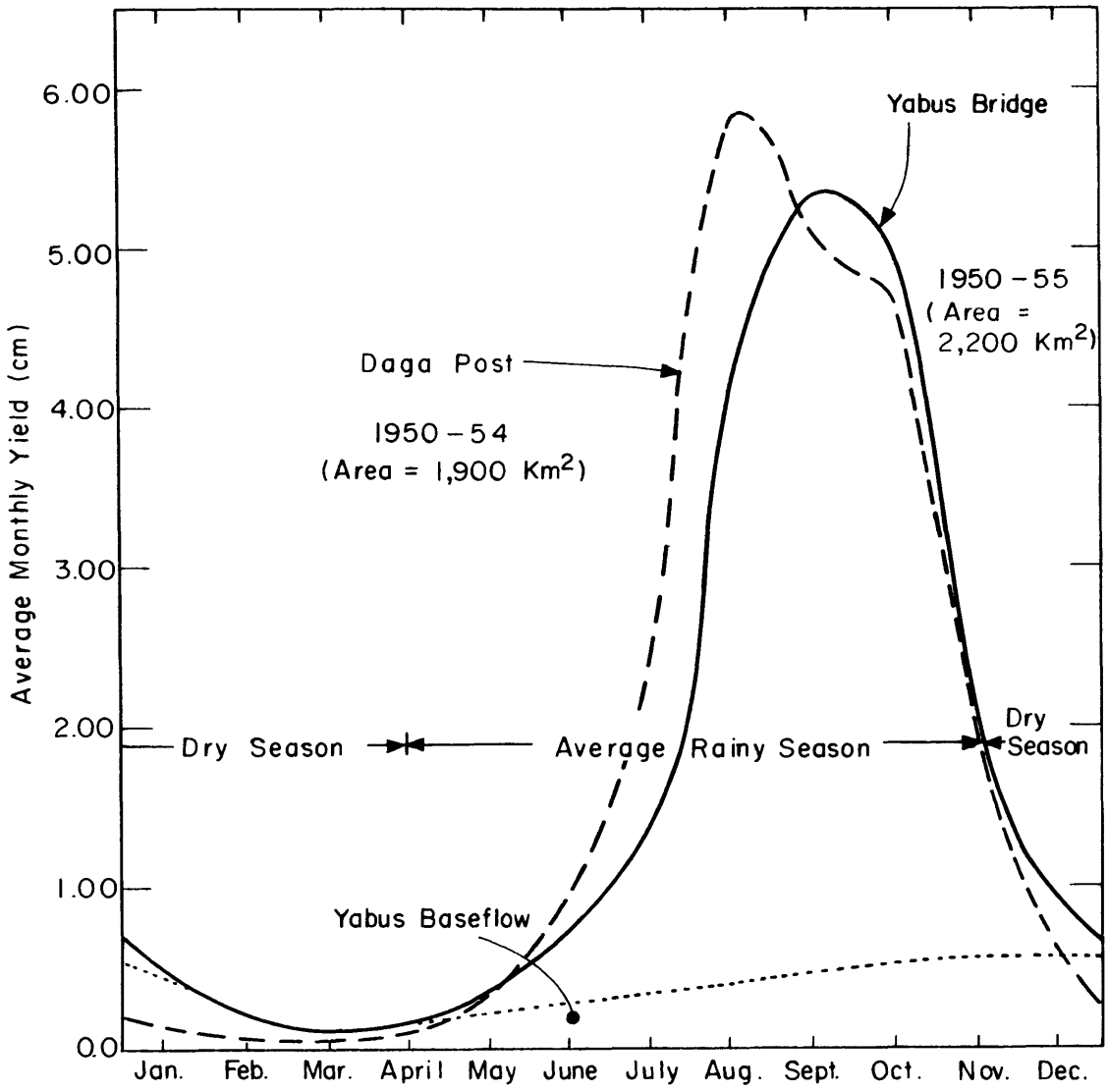

Figure 4.6

COMPARISON OF AVERAGE MONTHLY YIELDS AT YABUS BRIDGE
AND DAGA POST GAGING STATIONS

suggests that a part of surface runoff is stored through the rainy season and then released. We will treat this stored surface runoff, in a later hydrograph separation, as if it occurs during the rainy season because it is created in this period.

4. The average annual yield of Daga Post, in centimeters, is less than that of Yabus Bridge, as shown also in Table 4.8.

The monthly discharge (yield) and rainfall in 1952 at Yabus Bridge are plotted in Fig. 4.7 and an approximate hydrograph separation is indicated. From this, we conclude:

1. About 98% of the total rainfall occurs during the rainy season.
2. The rainy season length is 7 months.
3. The total yield is only about 20% of the normal rainfall.
4. About 10% of the total yield is stored during June and July, then drained in November and December.
5. The baseflow occurs throughout the year and is about 25% of the total yield.

The above analysis for one year at the Yabus Bridge sub-catchment gives us a general idea about the behavior of all the eastern catchments.

The annual discharges (yields) of the other catchments are mentioned in Table 4.9. The total yield of all the catchments is about

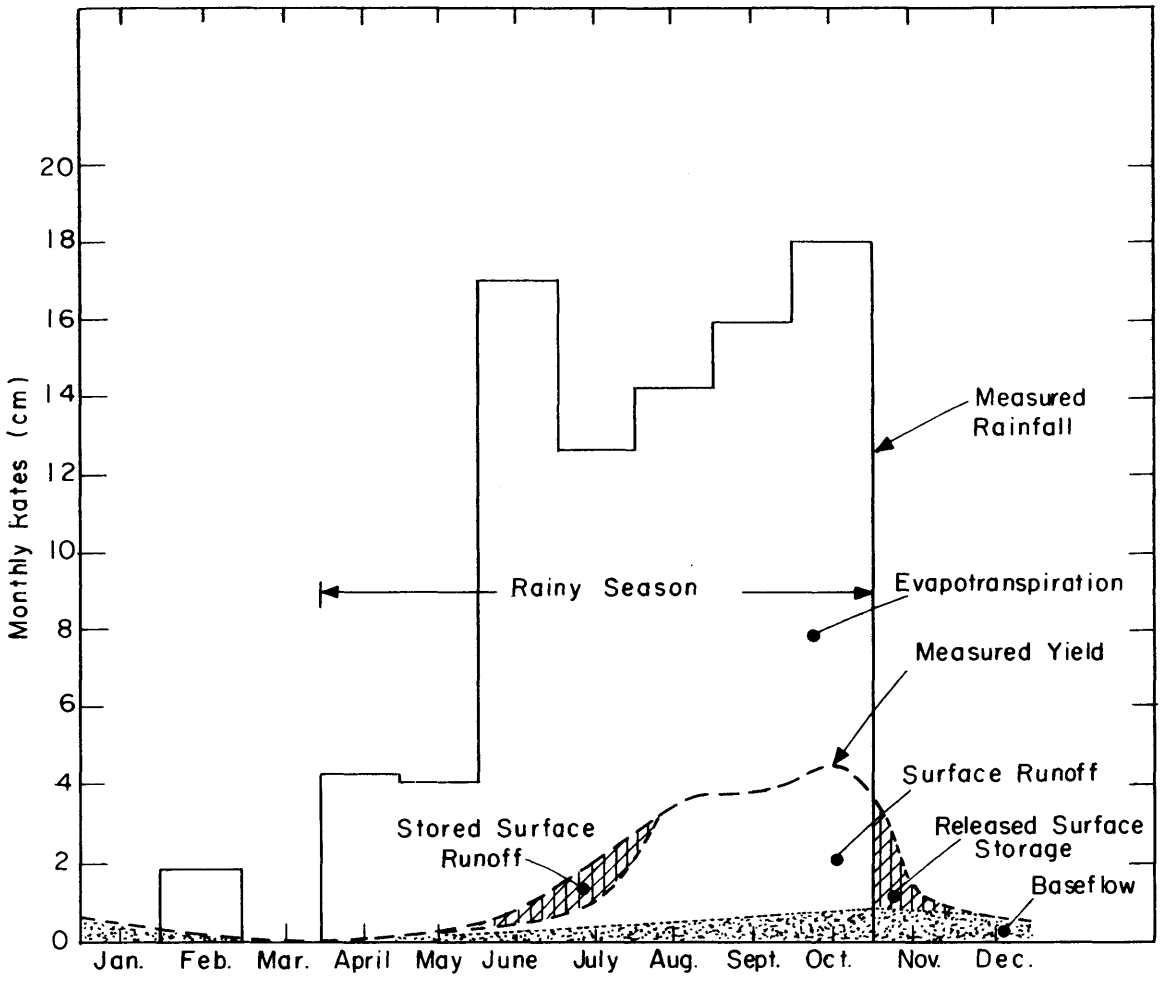

Figure 4.7

APPROXIMATE HYDROGRAPH SEPARATION AT YABUS BRIDGE IN 1952

Table (4-9)

Annual Discharges at Different Gaging Stations

in the Eastern Catchments

Catchment	Streamflow Gaging Station	Latitude† N	Longitude† E	Average Discharge* (mld)	Period
		0 '	0 '		
Ahmar	Kofa	10 - 23	33 - 40	0.075	July - October (1974)
Tombak	Nela	10 - 05	33 - 47	0.715	July - October (1974)
Yabus	Yabus Bridge	9 - 55	34 - 10	0.455	1950 - 55
Daga	Daga Post	9 - 12	33 - 55	0.420	1950 - 54
Lau	Kigille	8 - 40	34 - 02	0.300	July - October (1974)
Total Discharge				= 1.965 mld	

† Estimated from maps.

* Data are from Egyptian General Inspectorate of Irrigation in Sudan

2 milliards. This does not represent the total average yield of the eastern catchments for several reasons:

1. Yabus Bridge and Daga Post are upstream of the catchment mouths.
2. Kigille measures only one of three branches draining the Lau catchment, as shown in Fig. 4.1.
3. Some of the records are very short (less than 1 year).
4. There are some ungaged flows, either surface or sub-surface, which are difficult to measure, specially the flood period.

4.4 Potential Evaporation and Plant Coefficient

Monthly meteorological data are available for only three stations in the Machar region. These stations are Kurmuk, Gambela and Nasir. The total period of records is almost the same as that for rainfall.

As shown in Fig. 2.2, the annual potential evapotranspiration varies with longitude, according to Thornthwaite's method (1948). It is clear from the same figure that Kurmuk represents the eastern watersheds while Nasir represents the plains and swamps, according to their longitudes. Therefore, we will use the seasonal meteorological data of Kurmuk in the preliminary water balance and model application on the eastern watersheds and the annual meteorological data of Nasir in the preliminary water balance of the plains and swamps.

Gambela meteorological records, seasonally-based, will be used, along with Kurmuk, to calibrate their Piche observations, and then to estimate the probability distributions of water surface seasonal potential evaporation, E_{p_w}.

Using the rainy season length, τ, of Kurmuk and Gambela, as estimated in Appendix B, the seasonal meteorological data have been estimated, from the Sudan Meteorological Service records for 1950-1975. These data are seasonal temperature, relative humidity, cloud amount and Piche evaporation. The data are shown in Appendix D.

The annual records of Nasir are collected from the same source of data and are also shown in Appendix D.

From the records, we notice the long-term average Piche evaporation and cloud cover of the three stations are quite different. For cloudy conditions, as in Gambela (about 76%), the Piche evaporation is relatively small (3.21 millimeters/day). This is because the short-wave (solar) radiation, main supply of the atmospheric energy, is reflected and/or absorbed by the clouds before reaching the ground.

Eagleson (1977) estimates the average annual (seasonal) rate of potential evaporation (evapotranspiration) from the energy balance equation. This is,

$$\bar{e}_p = \frac{\bar{q}_i(1 - A) - q_b + H}{\rho_e L_e(1 + \gamma/\Delta)} \quad , \qquad \text{(cm/min)} \qquad (4.3)$$

in which

$\bar{q}_i$ = average rate of receipt of short-wave radiation from the sun, ly/min

A = surface albedo

$\bar{q}_b$ = average net rate of long-wave back radiation, ly/min

H = average sensible heat residual, ly/min

ρ_e = mass density of evaporating water = 1 gm/cm^3

L_e = latent heat of vaporization = 597 cal/gm

and

$$\frac{1}{1 + \gamma/\Delta} = 0.42 + 0.013\bar{T}_{a_C} \qquad \text{(empirically)} \qquad (4.4)$$

where

$\bar{T}_{a_C}$ = average atmospheric temperature, °C

He formulates empirically two other relationships, besides Eq. (4.4),

$$\bar{q}_b = (1 - 0.8\bar{N})[0.245 - 0.145 \times 10^{-10\bar{T}_{a_F}^4}], \quad \text{ly.min} \qquad (4.5)$$

and

$$H = \bar{q}_b\left[\frac{1}{0.25 + \left(\frac{1}{1-\bar{r}}\right)}\right], \quad \text{ly/min} \qquad (4.6)$$

where

$\bar{N}$ = average fraction of the sky covered by clouds

$\bar{T}_{a_F}$ = average atmospheric temperature, °F

and

$\bar{r}$ = average relative humidity

The clear sky solar radiation, $\bar{q}_{i_c}$, is presented in World Maps of Climatology (Landsberg, et al., 1966). The insolation at the soil surface, $\bar{q}_i$, in Eq. (4.3) can be obtained empirically (T.V.A., 1972) as

$$\bar{q}_i = \bar{q}_{i_c} (1 - 0.65 \bar{N}^2) \tag{4.7}$$

The albedo, A, is equal to 0.05 for water surface and 0.10 for moist soil (Eagleson, 1977).

The average climatic parameters, energy fluxes and potential rates of evaporation, calculated by Eqs. (4.3) through (4.7), seasonally for Kurmuk and Gambela, and annually for Nasir, are shown in Table 4.10.

The ratio of average rate of bare soil evaporation to that of water surface, $\bar{R}_2$, is about 0.94, as mentioned in Section 3.4.

Now, using Table 4.10, we can calibrate or reduce only the rainy season Piche observations of Kurmuk and Gambela. The reduction factor, $\bar{R}_1$, can be estimated as

$$\bar{R}_1 = \frac{\bar{e}_{p_w}}{\bar{e}_{piche}} \tag{4.8}$$

where

$\bar{e}_{p_w}$ = average rate of water surface potential evaporation

and

$\bar{e}_{piche}$ = average of the Piche observations

The reduction factors of Kurmuk and Gambela are 0.78 and 0.85, respectively.

Reducing the seasonal Piche evaporation records, and multiplying them by the corresponding rainy seasons gives the totals

Table (4-10)

Average Climatic Parameters, Energy Fluxes and

Potential Evaporation Rates in Machar Region

Station	$\bar{e}_{piche}$ mm/day Ap.(D)	$\bar{T}_{a_c}$ °C Ap.(D)	$\bar{r}$ Ap.(D)	$\bar{N}$ Ap.(D)	$\bar{q}_{ic}$ ly/min Ref.[20]	$\bar{q}_i$ ly/min Eq.(4-7)	$\bar{q}_b$ ly/min Eq.(4-5)	H ly/min Eq.(4-6)	$\frac{1}{1+\gamma/\Delta}$ Eq.(4-4)	Surface	A Ref.[8]	$\overline{e_p}$ mm/day Eq.(4-3)
Kurmuk (seasonal)	4.29	27.5	0.65	0.67	0.323	0.229	0.059	0.019	0.777	Bare Soil	0.10	3.11
										Water	0.05	3.33
Gambela (seasonal)	3.23	28.6	0.66	0.76	0.300	0.187	0.049	0.015	0.792	Bare Soil	0.10	2.57
										Water	0.05	2.74
Nasir (annual)	7.51	28.8	0.58	0.53	0.304	0.249	0.072	0.027	0.794	Bare Soil	0.10	3.43
										Water	0.05	3.67

of seasonal water surface potential evaporation, E_{p_w}, as shown in Appendix D (Table D.4) along with the seasonal precipitation of Kurmuk and Gambela meteorological stations. Table 3.1 gives the summary of their statistical analysis.

The totals of seasonal water surface potential evaporation have been plotted using the Thomas plotting position in Figs. 3.7 and 3.8. They essentially fit normal distributions. From these figures, the mean values of their distribution are the same as those calculated in Table 3.1.

The plant coefficients of forests (woodlands) and grasses are investigated separately.

Balek and Perry (1973) apply the monthly water balance equation to four Zambian regions covered by woodland (forests). Assuming that the species transpire potentially in the rainy season, the ratio of transpiration to <u>water surface</u> evaporation in the rainy season is averaged over three years and modified by $\overline{R}_2$ (Eq. 3.57) to give the plant coefficient, k_v, of the woodland. This coefficient is about 1.25.

The evapotranspiration of grasses is studied by Chapas and Rees (1963) near Benin City, Nigeria, using 4-week records over two years. The potential transpirations are measured by transpirometers in which the grasses are always watered. The watered bare soil potential evaporations are measured by similar experiments. Averaging the ratios of these two values only in the rainy season yields the plant coefficient, k_v, of the grasses, assuming the grasses cover the whole transpirometers. The coefficient, k_v, is about 0.88.

We find that the plant coefficient of forests is greater than that of grasses, a rather surprising result. In case of mixed species, this coefficient depends on the mixture.

The mean annual potential evapotranspiration of papyrus swamps is about 2.2 meters per year (Eagleson and Chan, 1979).

4.5 Soil

There are no soil data for the region. Rzoska (1976) describes through a map that the soil is clay (Chapter 2). He agrees with Oliver (1969) who describes also the southeastern part of the Sudan as "extensively-cracking montmorillonitic clays."

Soil samples, taken from the Jonglei project area in the southwestern Machar region, have been experimentally analyzed (Remote Sensing Center, 1978). The soil moistures are determined under two suction pressures, 1/3 and 15 atmospheres. The clay-texture profiles, including more than 50% clay, are selected and analyzed in Appendix E.

The soil parameters estimated in Appendix E will be used as primary parameters in the model application to the Yabus sub-catchment. The analysis gives us the range of the saturated hydraulic conductivity (coefficient of permeability), K(1). This range is about $(4 - 14) \times 10^{-5}$ cm/sec.

The empirical relationship between the permeability coefficient, K(1), and pore size-distribution index, m, Eq. (3.20) will be employed to reduce the number of independent soil parameters.

In the absence of data on water table depth, we will use $Z = \infty$ cm in the application of the model on the eastern catchments.

4.6 Preliminary Water Balance

Based on Thiessen's weighting, the average annual precipitation over the eastern catchments, plains and permanent swamps is estimated, as shown in Table 4.11. The total average annual precipitation over the Machar region is about 34 mlds.

The average canopy density and plant coefficient of each can be expressed as

$$\bar{M} = \sum M_i \, r_i \tag{4.9}$$

and

$$\bar{k}_v = \sum M_i \, r_i \, k_{v_i} / \sum M_i \, r_i \tag{4.10}$$

where

M_i = canopy density of species i

r_i = fraction of species i in the catchment

and

k_{v_i} = plant coefficient of species i

Using Eqs. (4.9) and (4.10) and Table 4.2), the averages of canopy density and plant coefficient are calculated for all catchments, as shown in Table 4.11.

In preliminary water balance calculations, we consider:

1. The evapotranspiration in the eastern catchments and plains occurs potentially during the rainy season.
2. The evapotranspiration in the swamps occurs potentially around the year.

Table (4-11)

The Average Annual Rainfall, Canopy Density and Plant Coefficient all over Machar Catchments

Catchment	m_{p_A} (mld)	$\bar{M}$	$\bar{k}_v$
Ahmar	1.591	0.72	1.28
Tombak	2.296	0.61	1.07
Yabus	5.639	0.79	1.18
Daga	3.005	0.83	1.14
Lau (1,2,3)	2.681	0.82	0.98
Sub-total	15.212	-	-
Plains	11.449	0.71†	0.97†
Swamps	7.282	0.81*	1.05*
Total	33.943	-	-

† From Appendix (F)

* The vegetated part only as in Appendix (F)

3. The average rate of bare soil potential evaporation estimated at Kurmuk is used to calculate the total average evapotranspiration in the eastern catchments while that estimated at Nasir is used in the plains and permanent swamps.
4. The average canopy densities, plant coefficients and rainy season lengths of the eastern catchments are lumped.
5. The swampy area (permanent swamps) is divided into vegetated land and water badies with marshes, covered by papyrus. These two parts are studied separately.
6. The mass conservation equation is used to estimate a) the yields from the eastern catchments and plains to the swamps, and b) the ungaged flow from the swamps to either the White Nile or the northern drainage system (Khor Wadudu) through small khors, as shown in Fig. 4.1.

The preliminary water balance calculations are presented in Appendix F and are summarized graphically in Fig. 4.8. The average seasonal total precipitation of the whole eastern catchments is about 14.45 mlds while the average seasonal evapotranspiration is estimated to be about 11.15 mlds. Assuming that there is no inflow from the adjacent catchments (outside the Machar region), then the average seasonal yield becomes about 3.30 mlds. The average measured discharges from the different catchments total about 1.97 mlds. Therefore, the ungaged (unmeasured) flow is about 1.33 mlds. The average total yield

of these catchments enters the plains around the permanent swamps through a very complicated net of small branches.

From the difference between precipitation and evapotranspiration, we find that the plains that surround the permanent swamps also contribute a yield of about 1.41 mlds in addition to that from the eastern catchments. The average total yield from both catchments and plains is thus about 4.71 mlds.

We assume as before that the seasonal yield of the eastern catchments and plains is the same as the annual value. This assumption allows us to complete the annual water balance of the swamps which evaporation water around the year.

From the annual mass conservation equation, taking the estimated spilling from the Baro River (3.42 mlds) into account, we find that about 1.95 mlds are leaving the swamps in one or more of the following forms:

1. Groundwater flow to the White Nile.
2. Ungaged flow to the Wadudu swamps that lie north of the Machar region.
3. Additional evaporation due to error in our estimate of the papyrus area within the swamps.

This "error" (i.e., lack of closure) represents about 5% of the total supply of water to the region. The estimated papyrus area is about 40% of the total swamp area. If we increase this fraction to 50%, we find that the above error (1.95 mlds) is reduced to 1.00 mld. The

percentage error will then be about 2.7%. This means that a 10% error in estimating the papyrus area reduces the closure error by 50%.

Considering the closure error to be unavailable water for whatever reason, a channelization system in the region will save the flow which now enters the permanent swamps, about 8.13 mlds, as shown in Fig. 4.8.

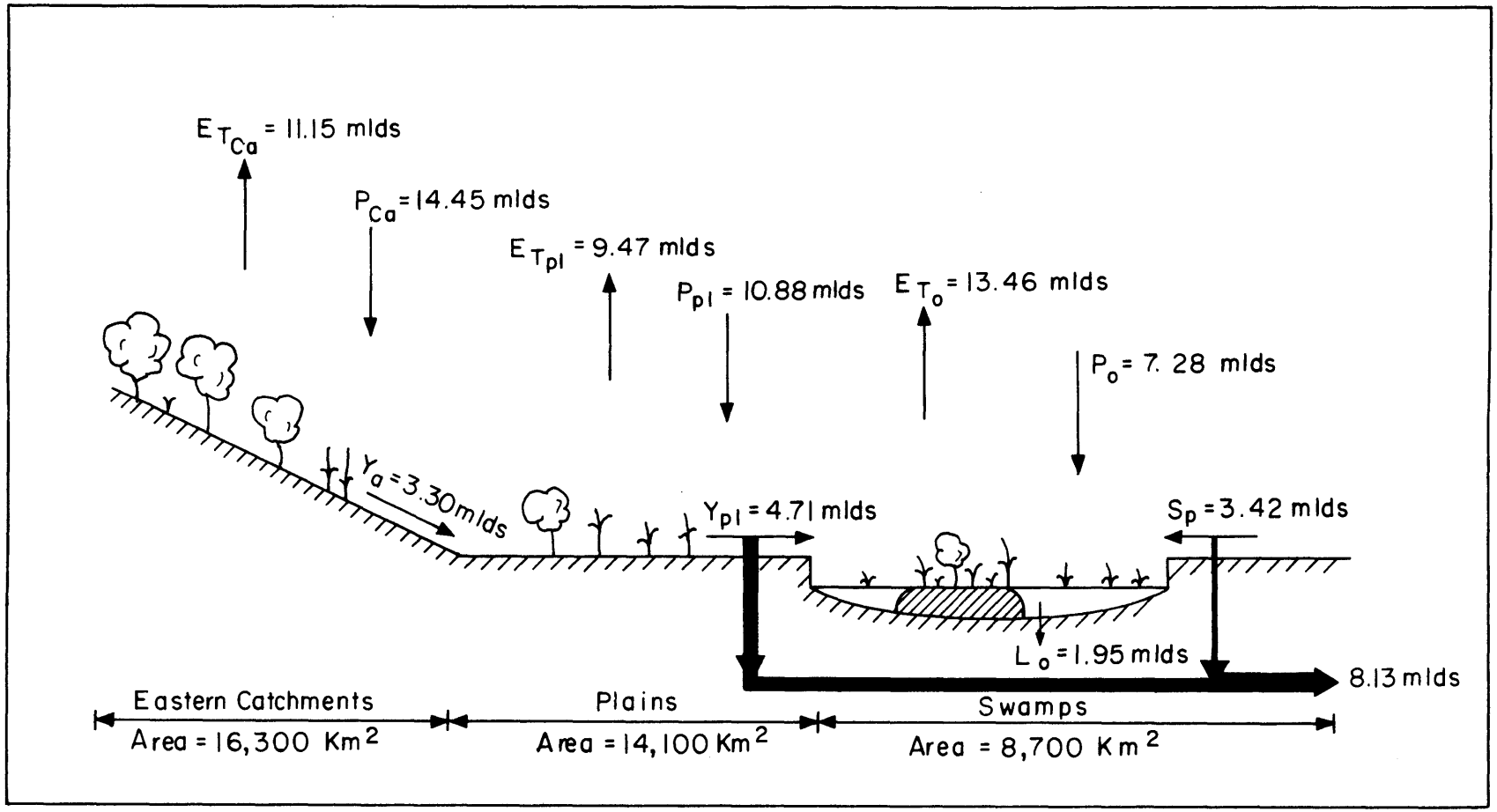

Figure 4.8

MEAN ANNUAL WATER BALANCE OF MACHAR REGION

Chapter 5

PARAMETER ESTIMATION AND MODEL VERIFICATION

5.1 Introduction

Various catchment parameters are required for application of the present models. These parameters can be classified as:

1. Climatic parameters (m_{p_s}, m, m_{t_r}, m, m_I, , $\bar{e}_p$ and $\bar{T}_s$)
2. Soil parameters (n, m and K(1))
3. Vegetal parameters ($\bar{M}$ and $\bar{k}_v$)
4. Groundwater table and surface retention parameters (Z and h_o)

Studying the effect of random variability of the water surface potential evaporation, E_{p_w}, introduces two more parameters, the mean and standard deviation of this variable.

Most of the above parameters (such as the climatic and groundwater table parameters) can be estimated from field data. The others must be obtained experimentally or from maps and the literature.

Other, dependent parameters are estimated by simple relationships presented in Chapter 3 or from hydrograph and sensitivity analysis. These studies will be presented in this chapter.

5.2 Climatic Parameters

The precipitation parameters of the meteorological stations are estimated and then areally-averaged to give estimates representative of each catchment. However, the seasonal averages of bare soil potential

evaporation rate and atmospheric temperature for all catchments are taken to be that of the Kurmuk meteorological station. This is because the other stations in the eastern catchments measure only precipitation. These two parameters are shown in Table 4.10.

Most of the seasonal precipitation parameters for the stations in the eastern catchments were estimated in Chapter 4, as shown in Table 4.5. The dependent climatic parameters can be estimated from these as follows:

$$m_H \equiv \kappa/\lambda = m_{p_s}/m_\nu \tag{5.1}$$

$$m_I \equiv \alpha^{-1} = m_H/m_{t_r} \tag{5.2}$$

$$m_{t_b} \equiv \beta^{-1} = m_\tau/m_\nu - m_{t_r} \tag{5.3}$$

As mentioned in Chapter 2, Oliver (1969) estimates the annual number of hours in which rain is recorded, describing it as "...not the total duration of rainfall which would be less." This number of hours is about 120 at sites where the mean is 400 mm. Eagleson and Chan (1979) estimate the average storm duration in the Bahr el Ghazal region to be about 1.2 hours which agrees with Oliver (1969). Therefore, m_{t_r} is taken to be 1.2 hours in the present work.

Observations of the storm depths are few. The Sudan Meteorological Service gives the monthly average number of rainy days with storm depth, h, greater than 0.1 mm (only at Kurmuk and Gambela), greater than 1.0 mm and greater than 10.0 mm. We assume that the

average number of rainy days ($\geq$ 1.0 mm) is the same as the number of storms during the rainy season. For uniformity of the analysis, we neglect the data for $h \leq 1.0$ mm. Thus, we have only one point on the probability distribution function of the storm depth. This point is

$$\text{Prob}[h \leq 10.0] = 1 - (m_{\nu}^{*}/m_{\nu}) \tag{5.4}$$

where

m_{ν}^{*} = average seasonal number of storms (rainy days with rainfall greater than 10.0 mm)

and

m_{ν} = average seasonal number of storms (rainy days with rainfall greater than 1.0 mm)

Integrating the Gamma probability density function of storm depth gives

$$\text{Prob}[h \leq z] = P[\kappa, \lambda z] \tag{5.5}$$

where

$P[a, x] \equiv$ Pearson's incomplete Gamma function

From Eqs. (5.1), (5.4) and (5.5), we find that

$$1 - (m_{\nu}^{*}/m_{\nu}) = P[\kappa, 10.0\ \kappa/m_{H}] \tag{5.6}$$

with m_{H} in millimeters.

Solving Eq. (5.6) by trial yields a unique value of the shape parameter, κ, for each meteorological station.

Where the record of annual observations is long, κ can perhaps be best estimated directly from the set of annual observations by the method-of-moments, using Eq. (3.8).

Table 5.1 shows a summary of the shape factors calculated by the above methods using the seasonal parameters presented earlier in Table 4.5. We find a significant difference between these parameters as estimated by the two methods.

In Appendix G, the total seasonal point precipitation at each station is presented in the form of the cumulative distribution function, Eq. (3.9), using the two different values of shape parameter. The observed probability distribution of the seasonal total precipitation is obtained from the actual observations using Thomas' plotting position (1948). That is

$$\text{Prob}[P_s/m_{p_s} < z] = m_z/(N + 1) \qquad (5.7)$$

where

m_z = ascending rank of observation magnitude z

and

N = number of years of record

This is plotted for each station in Appendix G.

We notice that κ determined by the second method gives a better-fitting cumulative distribution function, particularly for Daga Post and Chali.

Table (5-1)

Calculation of The Shape Parameter

Station	m_ν	m_ν^*	Prob[h≤10 mm]	m_H (mm)	κ (1)	κ (2)
Kurmuk	70.55	33.85	0.520	13.64	0.997	0.647
Gambela	104.30	41.10	0.606	12.53	0.607	0.411
Chali	61.45	27.50	0.553	13.30	0.818	0.180
Doro	64.00	25.07	0.608	12.08	0.651	0.552
Tabus Bridge	87.77	30.38	0.654	10.30	0.647	1.643
Daga Post	77.00	31.44	0.592	11.61	0.858	0.458

(1) Fitting the Gamma distribution of storm depth using one point on the cdf.

(2) Fitting the distribution of annual precipitation by the method-of-moments using the complete record of annual observations.

The first method would be perfectly accurate if the estimates of m_ν and m_ν^* were exact. The value obtained for κ by this method is very sensitive to the estimate of m_ν^* and this estimate involves assuming that the number of storms equals the number of rainy days.

The second method utilizes the "integrated" storm depths (i.e., annual totals) and does not utilize an estimate of m_ν^*. This method-of-moments fitting will thus be used here.

The average seasonal climatic records of m_{p_s}, m_ν and m_τ are lumped using Table 4.4 to give the areal average values for each catchment. The variance of areal (i.e., catchment) average seasonal precipitation, σ_j^2, on catchment j is given by (Benjamin and Cornell, 1970)

$$\sigma_j^2 = \sum_{i=1}^{N} a_{ij}^2 \sigma_i^2 + 2 \sum_{i=1}^{N} \sum_{k=i+1}^{N} \rho_{ik} a_{ij} a_{kj} \sigma_i \sigma_k \qquad (5.8)$$

where

a_{ij} = Thiessen's weight of station i to catchment j

σ_i^2 = variance of seasonal precipitation at station i

ρ_{ik} = correlation coefficient of seasonal precipitation at stations i and k

and

N = number of stations that affect the catchment j

The calculated correlation coefficients for seasonal precipitation among the stations are presented in Table 5.2.

Using Eqs. (5.8) and (3.8), we can estimate the areal shape parameter, κ, for each catchment. Table 5.3 shows this parameter along

Table (5-2)

Correlation Coefficients* of

Seasonal Precipitation

Among the Rainfall Stations

Station	Kurmuk	Chali	Doro	Tabus B.	Daga P.	Gambela
Kurmuk	1.000					
Chali	0.52	1.000				
Doro	0.75	0.01	1.000			
Yabus B.	0.51	0.31	0.49	1.000		
Daga P.	0.65	0.31	0.62	0.82	1.000	
Gambela	0.23	0.46	0.10	0.85	0.50	1.000

* Only 8 years are used, 1952-54, 56, 58-61, in Appendix (B).

Table (5-3)

The Estimated Parameters of Catchments

Parameter \ Catchment	Ahmar	Tombak	Yabus	Daga	Lau	Units
Area	1,750	2,600	6,060	3,200	2,700	Km^2
m_{p_s}	88.69	85.01	89.14	89.43	95.61	Cm/season
m_ν	65.82	65.14	84.66	77.00	81.10	storms/season
m_H	1.348	1.305	1.053	1.161	1.179	Cm/storm
m_{t_r}	0.05	0.05	0.05	0.05	0.05	days
m_{t_b}	2.81	2.82	2.39	2.55	2.48	days
m_T	187.88	187.08	206.4	200.0	205.4	days
m_I	1.123	1.088	0.878	0.968	0.983	Cm/hr
T	1.00	1.00	1.00	1.00	1.00	year
κ	0.432	0.413	1.677	0.458	0.582	-
k_v	1.28	1.07	1.18	1.14	0.98	-
$\bar{M}$	0.72	0.61	0.79	0.83	0.82	-
$\overline{ep}$	0.013	0.013	0.013	0.013	0.03	Cm/hr
h_o	0.10	0.10	0.10	0.10	0.10	Cm/storm
$\bar{T}_s$	27.5	27.5	27.5	27.5	27.5	^oC
Z	∞	∞	∞	∞	∞	Cm
n	0.35	0.35	0.35	0.35	0.35	-
m	0.28	0.28	0.28	0.28	0.28	-
K(1)	10.0×10^{-5}	10.0×10^{-5}	10.0×10^{-5}	10.0×10^{-5}	10.0×10^{-5}	Cm/sec
$\Psi(1)$	65.0	65.0	65.0	65.0	65.0	Cm(Suction)

with all the other areal parameters for each catchment.

5.3 Soil Parameter

Data for a clay soil at the Jonglei project (Remote Sensing Center, 1978) are analyzed in Appendix E. We find that the coefficient of permeability, K(1), varies from 4 x 10^{-5} cm/sec to 14 x 10^{-5} cm/sec. The other two independent parameters, n and m, are roughly estimated in order to have initial values for preliminary analysis. These values are shown in Table 5.4.

Yabus Bridge sub-catchment is chosen in this analysis to estimate more accurate values for the soil parameters of the eastern catchments. This choice is made because:

1. The rainfall and corresponding yield records are available in some years.
2. It is almost in the center of the eastern catchments.
3. Its gaging station is at a channel section where there should be little if any ungaged (i.e., overbank) flow, as shown in the rating curve presented by the Equatorial Nile Project (1955).

Covering the above range of the coefficient of permeability, K(1), a sensitivity analysis is made using the approximate hydrograph separation at Yabus Bridge (Chapter 4).

As shown in Fig. 4.3, the Yabus Bridge gaging station receives flow from the entire Yabus sub-catchment. Thus, its climatic parameters will be used in applying the long-term average water balance model, Eq.

Table (5-4)

Clay Soil Parameters for Different

Coefficients of Permeability

K(1) Cm/Sec	n	m	Ψ(1) Cm-Section
arbitrary	Eagleson(1977)†	Eq.(3-20)	(proportionally)
$x10^{-5}$			
3.0	0.46	0.180	100.0
4.0	0.45	0.200	95.0
5.0	0.44	0.215	90.0
6.0*	0.43	0.230	85.0
7.0	0.41	0.245	80.0
8.0	0.39	0.260	75.0
9.0	0.37	0.270	70.0
10.0	0.35	0.280	65.0
12.0	0.33	0.300	60.0
15.0	0.30	0.330	55.0

† Interpolating between clay and clay loam.

* The initial values as in Ap. (E).

(3.48), on this sub-catchment over the range of soil properties shown in Table 5.4.

The surface retention capacity and groundwater table depth are taken to be 0.1 cm and ∞ cm, respectively, as initial values.

The mean seasonal temperature and bare soil potential evaporation rate are taken to be the same as at Kurmuk meteorological station.

The average canopy density and plant coefficient of the Yabus sub-catchment are estimated in Chapter 4.

The monthly average values of yield at Yabus Bridge are calculated from the available records and are plotted in Fig. 4.6, as shown before. The baseflow is then separated linearly beginning at a minimum rate equal to the yield at the end of the dry season, and rising to a maximum at the end of the rainy season when release of surface storage begins. It maintains this maximum until it equals the total yield following which time baseflow and yield are identical, as shown in Figs. 4.6 and 4.7.

From this separation, the average total baseflow (groundwater runoff) is estimated to be about 0.20 of the average total annual (seasonal) yield, or 0.25 of the surface runoff. This average ratio is utilized to estimate the coefficient of permeability and other soil properties from the average annual (seasonal) water balance.

The long-term average water balance components are computed for different canopy densities at each set of soil parameters and are listed in Table 5.4. These calculations are presented in Appendix H.

Preserving constant values of $E[R_{g_A}]/E[R_{s_A}]$ (around the value estimated by the approximate average hydrograph separation) yields the canopy density-permeability relationships shown in Fig. 5.1.

Dropping the expected values from the long-term average water balance equation, Eq. (3.48), the above relationships indicate that

1. For constant climatic conditions and soil properties, the groundwater runoff decreases with increasing vegetation canopy density. This occurs because the soil moisture must increase to support increasing vegetation density. Increasing soil moisture increases the fraction of yield that occurs as surface runoff.
2. For constant climatic conditions and vegetation density, the catchment that has the same parameters as Yabus Bridge sub-catchment but a more permeable soil, percolates more water to the water table. In this case, the total yield is almost constant while the ratio R_{g_A}/R_{s_A} increases.

From Fig. 5.1, we can estimate the coefficient of permeability that satisfies the estimated values of $\bar{M}$ and $E[R_{g_A}]/E[R_{s_A}]$. This coefficient is about 1×10^{-4} cm/sec. The other corresponding soil parameters can be estimated from Table 5.4. Assuming that the soil is spatially homogeneous, these parameters will be used for all the eastern catchments of the Machar region.

The estimate coefficient of permeability is very close to the middle of the estimated range using the experimental data of the Jonglei

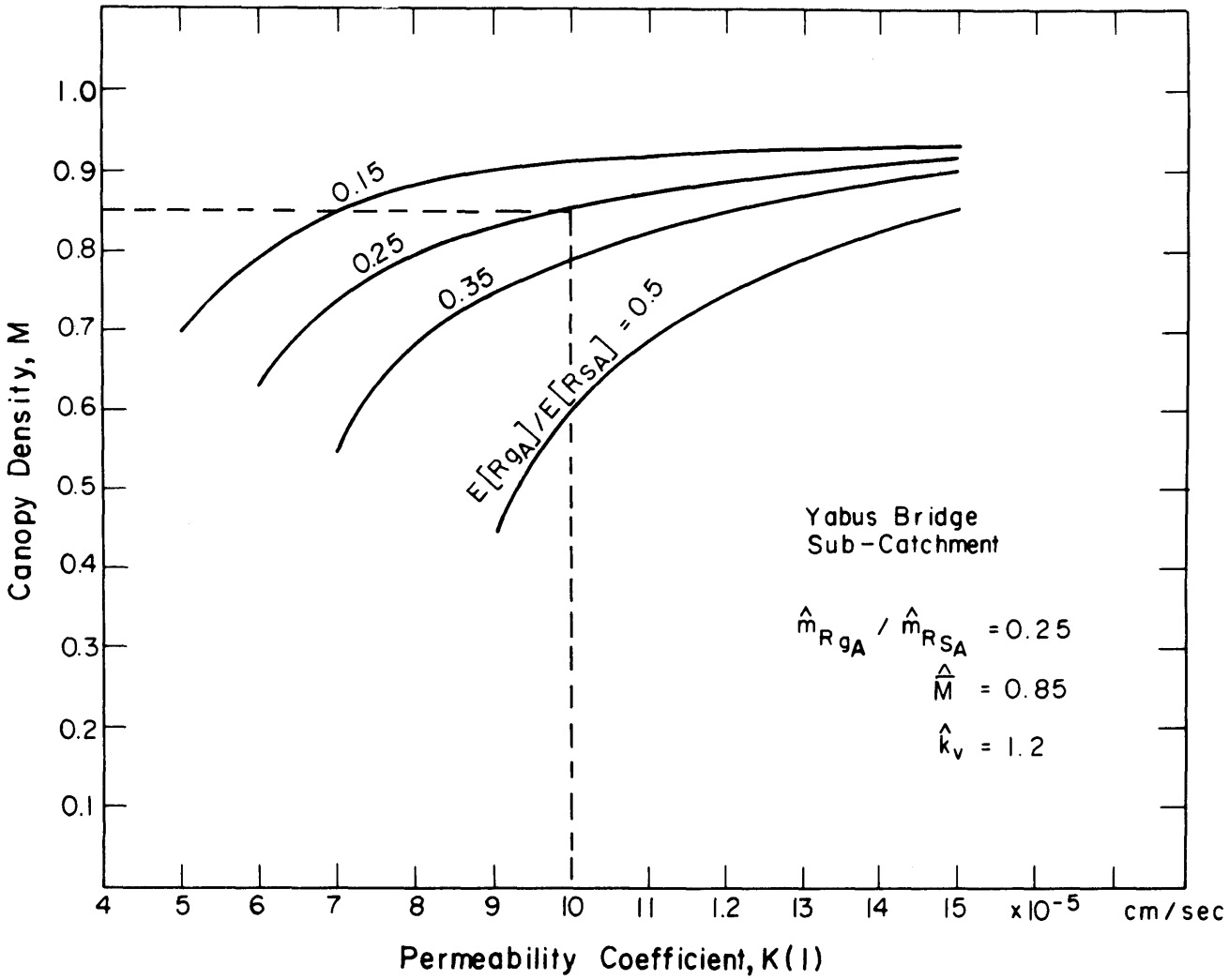

Figure 5.1

SENSITIVITY ANALYSIS OF THE SOIL PARAMETERS WITH VEGETATION CANOPY DENSITY AT DIFFERENT VALUES OF $E[R_{g_A}]/E[R_{s_A}]$ FOR YABUS BRIDGE SUB-CATCHMENT

project (Remote Sensing Center, 1978), indicating that the soil in Machar catchments is clay loam.

5.4 Sensitivity Analysis of the Single-Variable Model

We continue here to use the Yabus Bridge sub-catchment to check the parameters and to calibrate the single-variable (first order) water balance model, Eq. (3.52). The calibrated model will then be applied to Data Post sub-catchment to determine its ungaged flow.

The yield records of the two gaging stations, Yabus Bridge and Daga Post, are arranged in ascending order and Eq. (5.7) is applied. Table 5.5 shows the results. We assume that the whole annual yield is the same as the seasonal yield because the percolation (along with the stored surface runoff) occurs during the rainy season and then appears in the form of baseflow during the entire year, as shown in Fig. 4.7. In other words, we assume that the dry season rainfall is completely evaporated during the dry season and contributes nothing to the yield.

The cumulative distribution function of the annual (seasonal) yield, Eq. (3.52), is evaluated for the Yabus Bridge sub-catchment using its initially-estimated parameters. A few of these parameters are quite uncertain and for this reason, the model is reapplied changing one parameter at a time and fixing the others. The uncertain parameters are $\bar{M}$, k_v, h_o and Z. These trails are made using a modified program which calculates the cumulative distribution functions (i.e. cdf's) of all annual (seasonal) water balance components, as presented in Appendix I. The cumulative distribution functions of the annual (seasonal) yield resulting from these trials are plotted in Fig. 5.2. The reference of

Table (5-5)

The Observed Probability Distribution of Yabus Bridge

and Daga Post Water Yields by Thomas' Method

Yabus Bridge				Daga Post			
m	Y_A †	$\frac{m}{N+1}$	$\frac{Y_A}{mp_s}$	m	Y_A †	$\frac{m}{N+1}$	$\frac{Y_A}{mp_s}$
1	16.77	0.143	0.186	1	18.92	0.167	0.212
2	17.25	0.286	0.191	2	19.43	0.333	0.217
3	19.44	0.429	0.215	3	19.53	0.500	0.219
4	19.66	0.571	0.218	4	23.44	0.667	0.262
5	21.10	0.714	0.233	N=5	29.21	0.833	0.327
N=6	29.97	0.857	0.332	-	-	-	-

† $Y_A = Y_s$

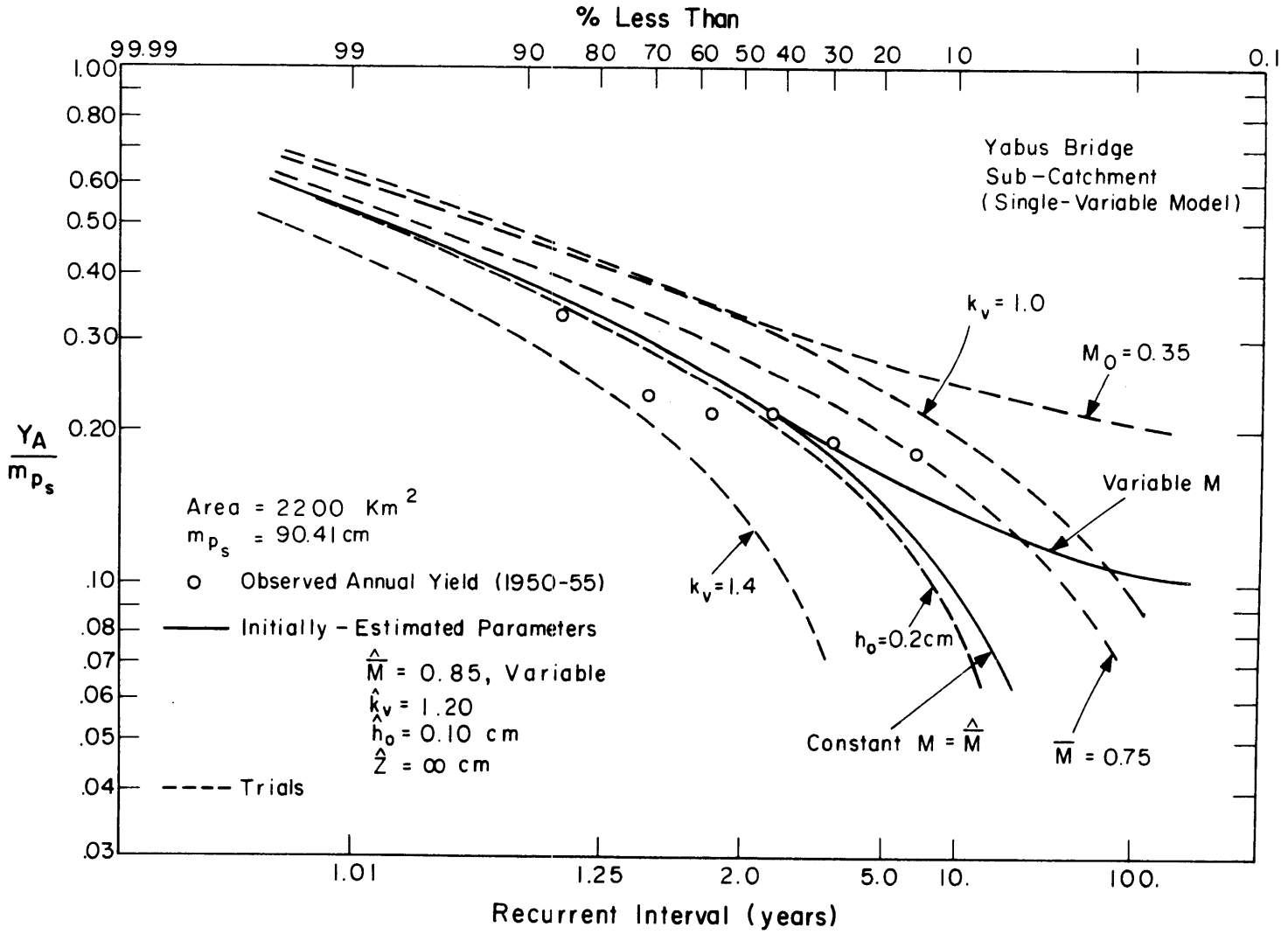

Figure 5.2

THE CUMULATIVE DISTRIBUTION FUNCTION OF ANNUAL YIELD AT YABUS BRIDGE COMPARED WITH OBSERVATIONS AND WITH SOME TRIAL PARAMETER SETS

comparison among these trials is that of the observed yield, as shown in Table 5.5.

Up to this point, the initially-estimated parameters give the best estimate of the cdf when compared with observations. However, the lower, dry, tail is in poor agreement with the observations. The number of data points controls the shape of the observed cdf in its tails and these points are only six. We therefore do not expect an exact fitting. The lower tail divergence is due either to a rough estimation of certain parameters or to the small number of data points. We will inspect the first case by some parameter sensitivity tests as follows:

1. The plant coefficient

This parameter has been estimated from the vegetation maps and from the literature to be about 1.2, as presented in Chapter 4. Changing this parameter to 1.4 yields underestimation of the yield while taking k_v equal to unity gives overestimation. Since a significant deviation results, we conclude that the plant coefficient is correctly estimated.

2. The surface retention capacity

We find that increasing this parameter, h_o, to 0.2 cm gives a slight underestimate of the annual (seasonal) yield. Therefore, fixing this parameter as 0.1 cm is the best estimation of the surface retention capacity.

3. The groundwater table depth

The groundwater table depth, Z, is used only in estimating the capillary rise from the water table. The hydrograph separation showed

the existence of inflow from groundwater through the presence of baseflow, but there are no available measurements of the groundwater table in the region.

Studying the effect of the groundwater table, we apply the single-variable (first order) model putting Z = 3m which keeps the groundwater table below the surface boundary layer and maintains $w/\bar{e}_p < 1$. As shown in Fig. 5.3, decreasing $\bar{M}$ with this Z improves the lower tail of the derived cdf. In this case, we allow the ratio $E[R_{g_A}]/E[R_{s_A}]$ to vary naturally. The derived cdf fits that of the observations when $\bar{M} = 0.70$.

Comparing the derived cdf's of Z = ∞ m and 3m, having the same canopy density, $\bar{M} = 0.85$, we find that the presence of a high water table (Z = 3m) gives:

1. Less yield in a wet year. This is because the capillary rise decreases the net percolation and adds dry season evaporation.
2. No change of yield in a drought year. This is because. with the low soil moisture of a dry year, the evaporation from this (constant) high groundwater table must be supplied from an outside source (i.e., negative groundwater flow). This causes no effect on the yield from local rainfall when compared to the Z = ∞ case.

In spite of the above fitting of the cdf, it is not possible to maintain the observed ratio, $E[R_{g_A}]/E[R_{s_A}]$, at this water table

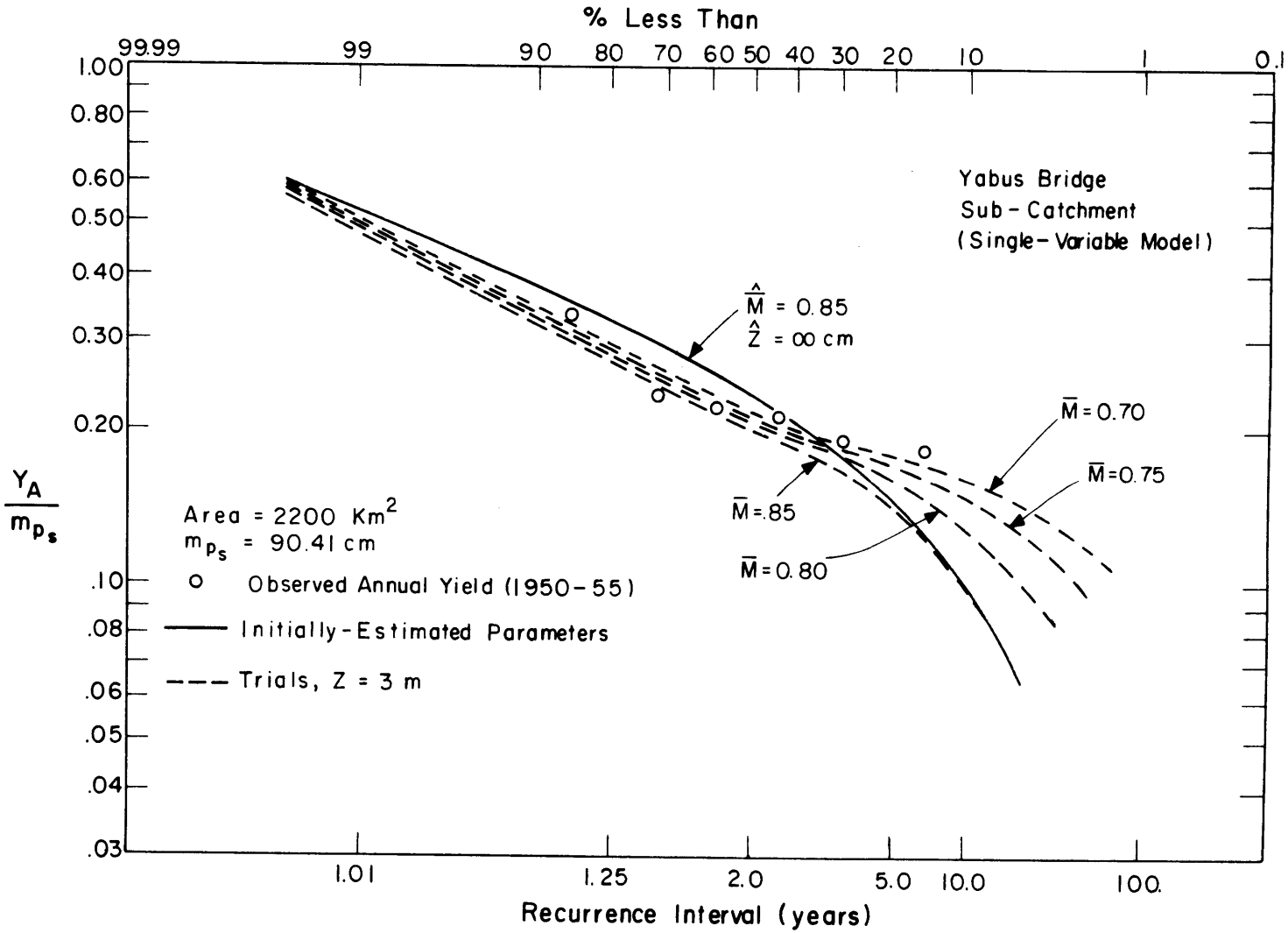

Figure 5.3

THE EFFECT OF VEGETATION CANOPY DENSITY ON THE CUMULATIVE DISTRIBUTION FUNCTION OF ANNUAL YIELD WITH THE WATER TABLE AT 3 m

elevation, Z = 3m, and still have a reasonable vegetation density. This is illustrated in Fig. 5.4. Raising Z decreases R_{g_A} and with R_{g_A}/R_{s_A} = constant, this requires a corresponding decrease in R_{s_A} which can occur only by lowering s_o. This causes the vegetation density to decrease. For each R_{g_A}/R_{s_A}, there is a minimum Z below which the water balance equation has no solution.

For large values of the groundwater depth (more than 15 m), the average canopy density takes on the constant value, 0.85, chosen earlier to give $R_{g_A}/R_{s_A} = 0.25$ at $Z = \infty$ m. Therefore, we conclude that taking any value for the groundwater depth greater than 15 m gives the same results, since the capillary rise is then negligible. This also is consistent with the observed existence of baseflow since putting $Z = \infty$ cm is only an artifice to cause the capillary rise, w, to vanish while the groundwater runoff still exists.

For these reasons, we will reject the high water table as a possible explanation for the shape of the cdf of yield and retain the initially-estimated parameters.

4. The vegetation canopy density

The model is very sensitive to this parameter because M and k_v control the evapotranspiration. Changing $\overline{M}$ from 0.85 to 0.75 gives more yield particularly in the drought years, as we see in Fig. 5.2. From a comparison of these derived cdf's with the observations, it appears that a significant part of the vegetation may die in the drought years giving a greater yield than that expected when the canopy density retains its average value. We should, therefore, take this aspect into

account by considering the vegetation density to vary with the seasonal soil moisture.

Eagleson (1978g) incorporated annual vegetation density change when studying a Santa Paula, California, catchment by assuming the system annually reaches the "equilibrium vegetation density," M_o[†], that would occur if that annual precipitation was the long-term mean value. This gave an increased yield in the dry years.

For these catchments, however, Eagleson's hypothesis of soil moisture maximization does not appear valid, since it leads to "equilibrium" vegetation densities, M_o, that are unrealistically small (i.e., $M_o \simeq 0.35$), as shown in Fig. 5.5. The reason for this is unclear, but the results, as shown in Fig. 5.2, cause us to abandon this hypothesis in this application.

Alternatively, we will allow for variable vegetation density by a linearized fitting of the observed yields. We see in Fig. 5.5 that, for the mean climatic conditions ($m_{p_s} = 90.41$ cm), the "observed vegetation density, $\bar{M} = 0.85$, gives a long-term average soil moisture, $\bar{s}_o = 0.55$. In Fig. 5.2, we saw that a vegetation density $M = 0.75$ fits the yield of the dry years. From the water balance equation, this occurs at an accompanying soil moisture $s_o = 0.20$ (and at a precipitation much lower than the long-term mean, of course). Assuming a linear variation of M with s_o, these two points give the empirical "vegetation growth function",

---

[†] M_o is the vegetation canopy density when the average soil moisture is maximum.

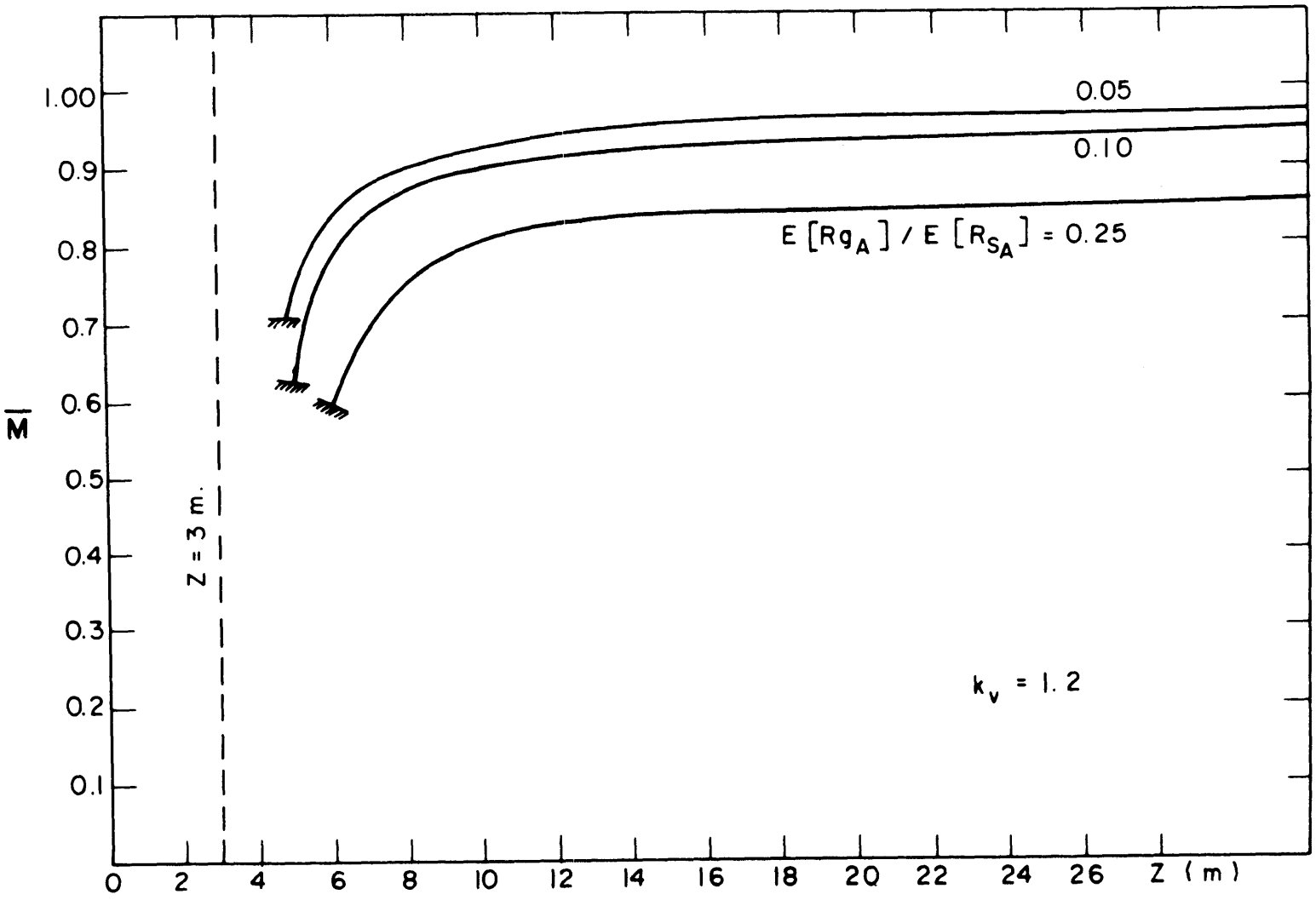

Figure 5.4

THE EFFECT OF THE GROUNDWATER DEPTH ON THE CANOPY DENSITY AT CONSTANT $E[R_{g_A}]/E[R_{s_A}]$

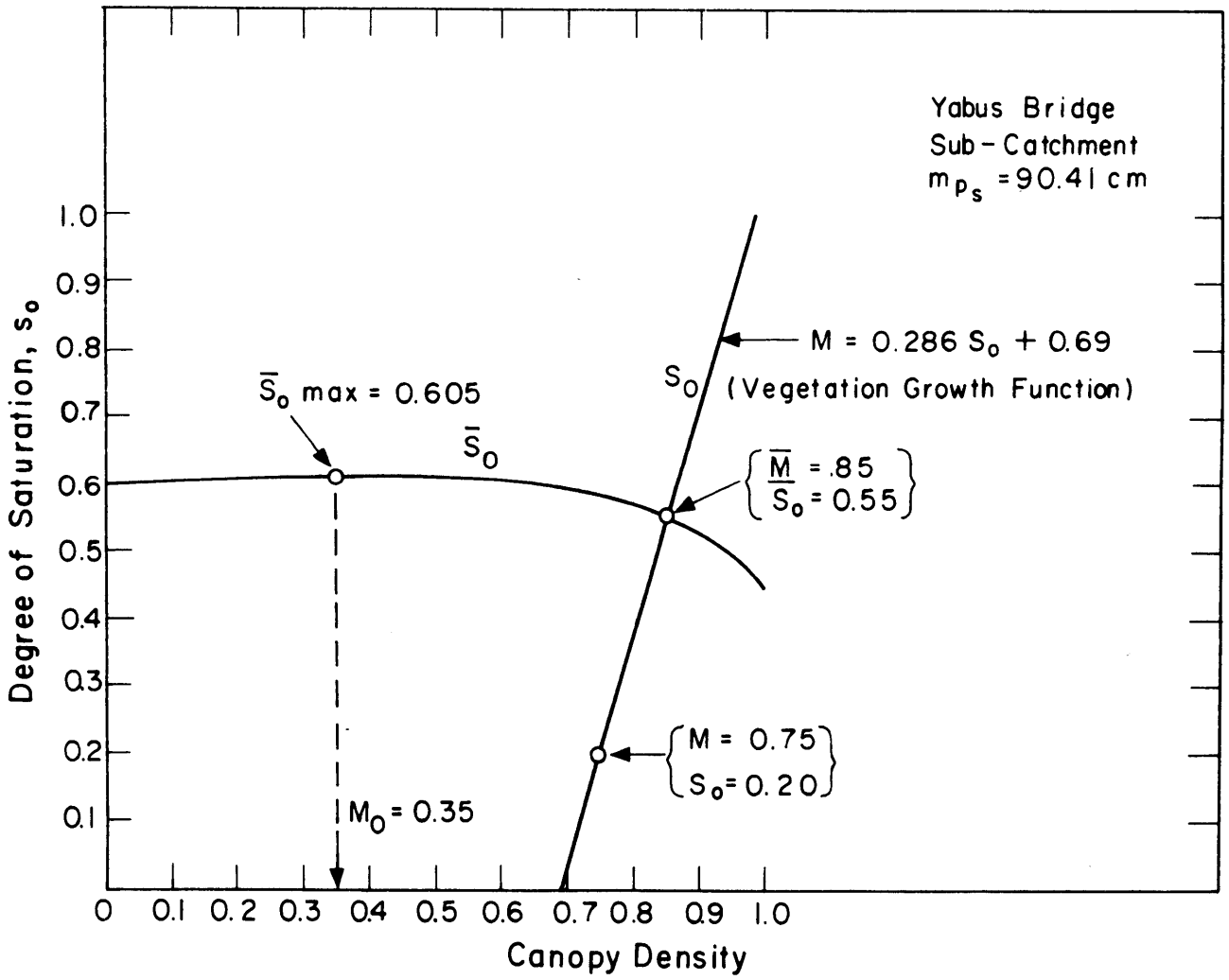

Figure 5.5

THE SOIL MOISTURE - CANOPY DENSITY FUNCTIONS FOR CONSTANT AND VARIABLE PRECIPITATION

$$M = 0.286\ s_o + 0.69 \qquad (5.9)$$

which is plotted also on Fig. 5.5. This function will be used for all the catchments.

From the vegetation map, Fig. 4.2, we find that the fraction of vegetation, which is forest and thus may be assumed to be perennial, is about 0.73, which agrees well with the constant 0.69 in Eq. 5.9. This indicates that the annual grasses are the species responsible for varying the composite vegetation density from year to year.

Applying the model again with the above relationship, Eq. (5.9), gives our final and best estimate of the derived cdf of the annual (seasonal) yield, as shown in Appendix I and Fig. 5.2.

As mentioned before, we chose Yabus Bridge for the parameter fitting because it appeared to have the least possibility of ungaged flow. Checking this, we see that the median of the derived cdf of the annual (seasonal) yield is about 21.52 cm while the observed average is about 20.70 cm. Since the derived cdf is skewed, the mean value is slightly different than the median. Application of the long-term average water balance, Eq. (3.48), gives the expected value of the annual (seasonal) yield as 21.72 cm. Therefore, the average ungaged flow is about 0.022 mld.

The model will now be applied on the Daga Post sub-catchment, using the climatic parameters of Daga Post meteorological station. The estimated parameters are shown in Appendix I. The derived cdf is plotted on Fig. 5.6 along with that of the observed yield shown in Table 5.5. According to the above comparison between the mean and the median

of the derived distribution of the annual (seasonal) yield, we will use the median directly as the approximate mean value for all catchments instead of applying Eq. (3.48).

The average ungaged flow from the Daga Post sub-catchment is about the same as at Yabus Bridge (0.022 mld), as shown in Fig. 5.6.

5.5 Sensitivity Analysis of the Two-Independent-Variable Model

Before applying the model which incorporates evapotranspiration as a second independent random variable, Eq. (3.73), to the Yabus Bridge sub-catchment, we will compare it with the analysis presented by Eagleson (1978g) for the south branch of the Nashua River at Clinton, Massachusetts, U.S.A.

Records of the potential evaporation at Clinton are not available. The average annual number of storms, m_ν, and shape parameter, κ, are 109 and 0.5, respectively (Eagleson, 1978g). The actual annual evapotranspiration is estimated as the difference between the annual precipitation and corresponding yield using the thirty years of data presented by Eagleson (1977). Plotting these estimated evapotranspiration values in Fig. 5.7, using Eq. (5.7) gives an essentially normal distribution, as we assumed in Chapter 3.

The statistics of E_{T_A} are presented in Table 5.6 along with those of the other independent variable, P_A. We notice that

1. The coefficient of variation of E_{T_A} is equal to that of P_A which emphasizes the importance of Eq. (3.73),
2. the two variables are highly correlated which violates the independence assumption used in deriving Eq. (3.73),

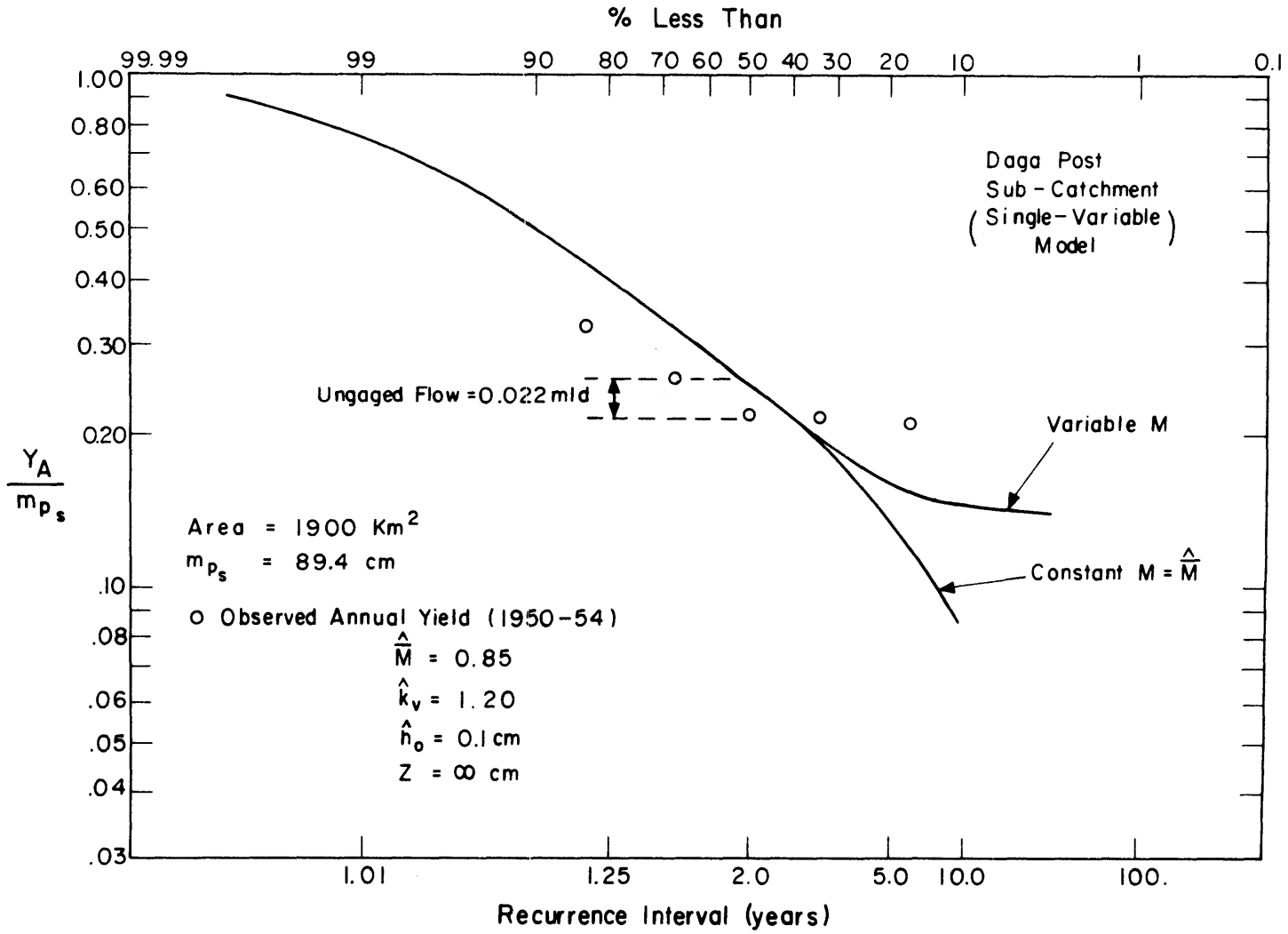

Figure 5.6

THE CUMULATIVE DISTRIBUTION FUNCTION OF THE ANNUAL YIELD AT DAGA POST

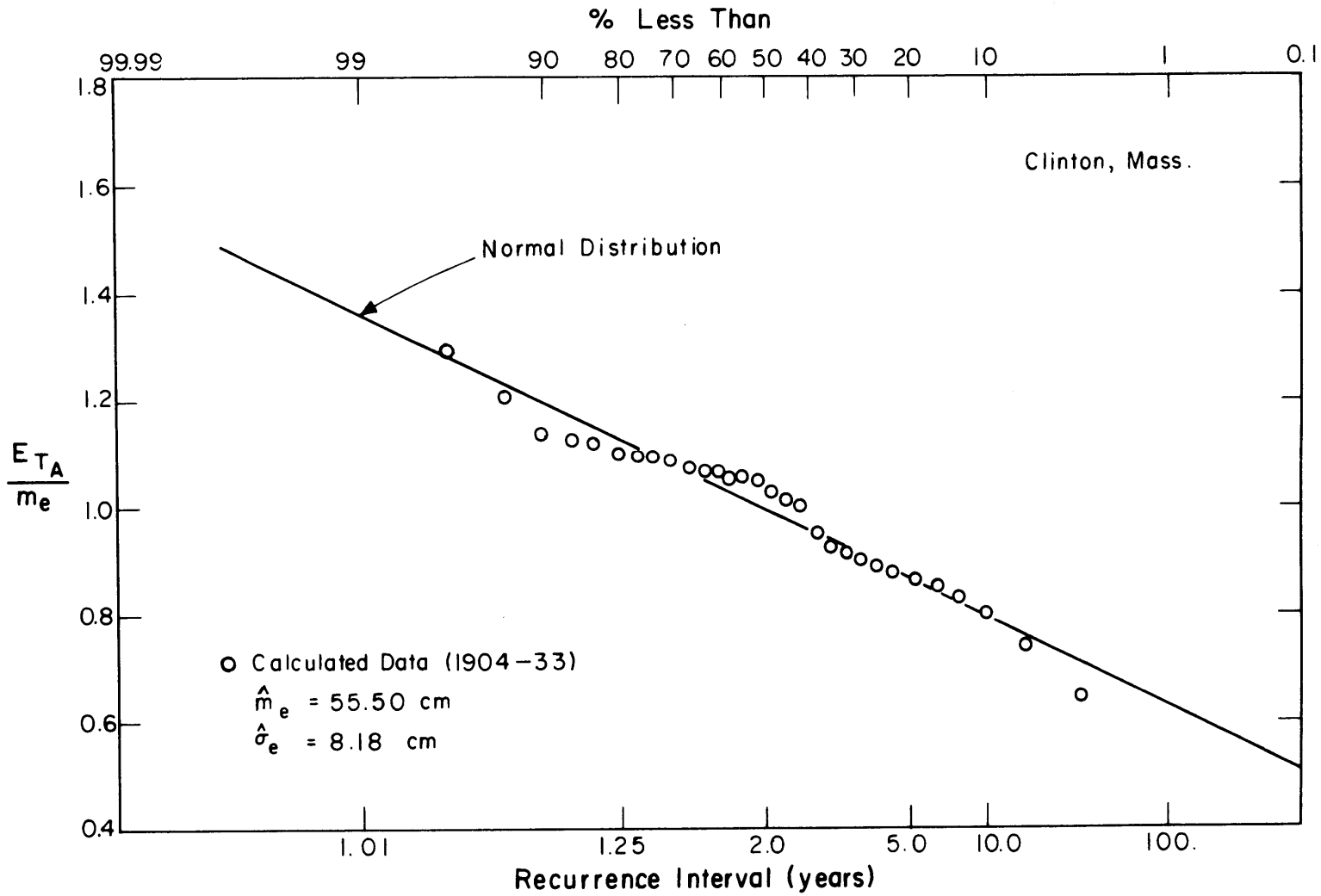

Figure 5.7

FITTED CUMULATIVE DISTRIBUTION FUNCTION OF THE ANNUAL EVAPOTRANSPIRATION AT CLINTON, MASSACHUSETTS

Table (5-6)

Climatic Data Analysis for Clinton, Massachusetts[†]

Parameter	P_A	E_{T_A}
Mean (Cm)	111.30	55.90
Standard Deviation (Cm)	16.38	8.18
Coefficient of Variation	0.15	0.15
Coefficient of Correlation	0.36	
m_v (storms)	109*	
K	0.50*	
B	1.00	

[†] Data are from Eagleson (1977)

* From Eagleson (1978g)

and

3. the parameter B in Eq. (3.56) takes on the value unity since we are dealing with actual rather than potential evapotranspiration.

We compare Eq. (3.73) with observations of annual yield at Clinton, Mass., in Fig. 5.8 for three values of the coefficient of variation of E_{T_A}; the observed value ($v_e = 0.15$), a value small enough to be negligible ($v_e = 10^{-2}$) and a value higher than the actual one ($v_e = 0.20$). From this figure, we see that

1. at $v_e = 0.0$, the cdf calculated by the two-variable model is closer to the observations than that from the single-variable model, particularly in the wet years. The approximations made in deriving the two-variable model cause it to differ from the single variable case in the limit as $v_e \to 0$.
2. increasing the variability (i.e., v_e) of E_{T_A} "tilts" the cdf increasing the yield in the wet years and decreasing the yield in the dry years.
3. neglecting the variability of E_{T_A} gives a better estimate of cdf of the annual yield than that estimated using the actual coefficient of variation, v_e.

Metzger and Eagleson (1980) find that taking the inter-annual changes of groundwater storage into account gives less yield in the wet years (water is being stored) while it gives more yield in the dry years (water is being withdrawn from storage). This means that we should study

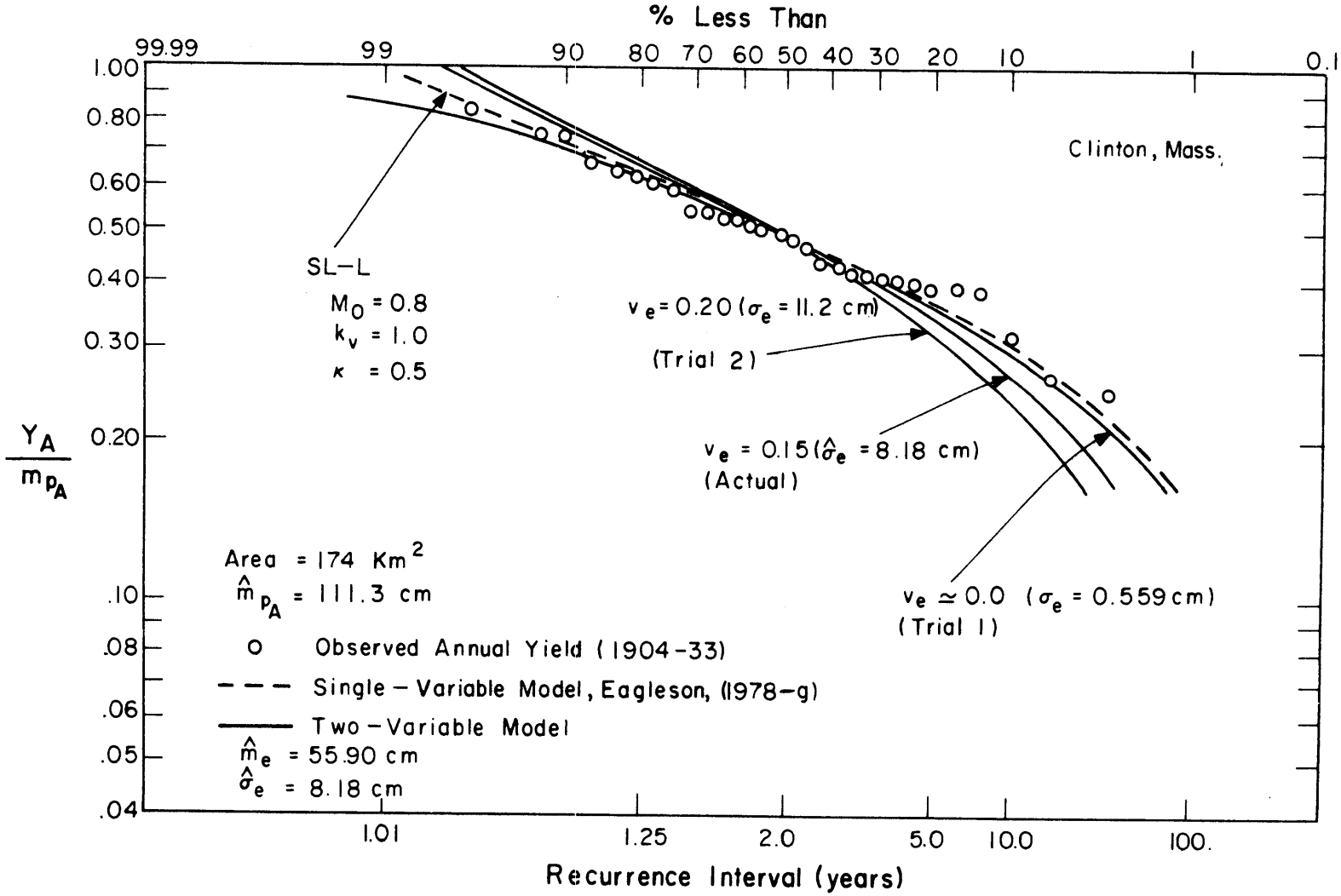

Figure 5.8

THE CUMULATIVE DISTRIBUTION FUNCTION OF THE ANNUAL YIELD AT CLINTON, MASSACHUSETTS

the change of groundwater storage together with the variability of the evapotranspiration in order to obtain the most accurate cdf of annual yield. However, neglecting both of them (as in the single-variable model) may give a better estimate than including either alone, because their effects are opposing.

We return now to the application of the two-variable model to the Yabus Bridge sub-catchment. We have assumed that the coefficient B in Eq. (3.65) is constant in order to simplify the analytical solution. For a first order approximation, we substitute this coefficient into both the numerical and the approximate analytical solutions of the two-variable model, Eqs. (3.73) and (3.91), respectively, as a function of the annual (seasonal) yield. This function can be obtained from the annual (seasonal) water balance equation (obtained by dropping the expected value symbol from Eq. (3.48)). The annual (seasonal) yield and corresponding evapotranspiration function, J, from this model are shown in Appendix I for the case of variable vegetation canopy density, M. These two variables are plotted together on Fig. 5.9 and a non-linear relationship is formulated by curve fitting. This is

$$J = 0.655\ (Y_A)^{0.1} \tag{5.10}$$

with Y_A in cm.

Substituting Eq. (5.10) in Eq. (3.56) gives B as a function of Y_A. Using the average canopy density, plant coefficient and $\overline{R}_2$, as estimated before, we get

$$B = c_1 + c_2(Y_A)^{c_3} \tag{5.11}$$

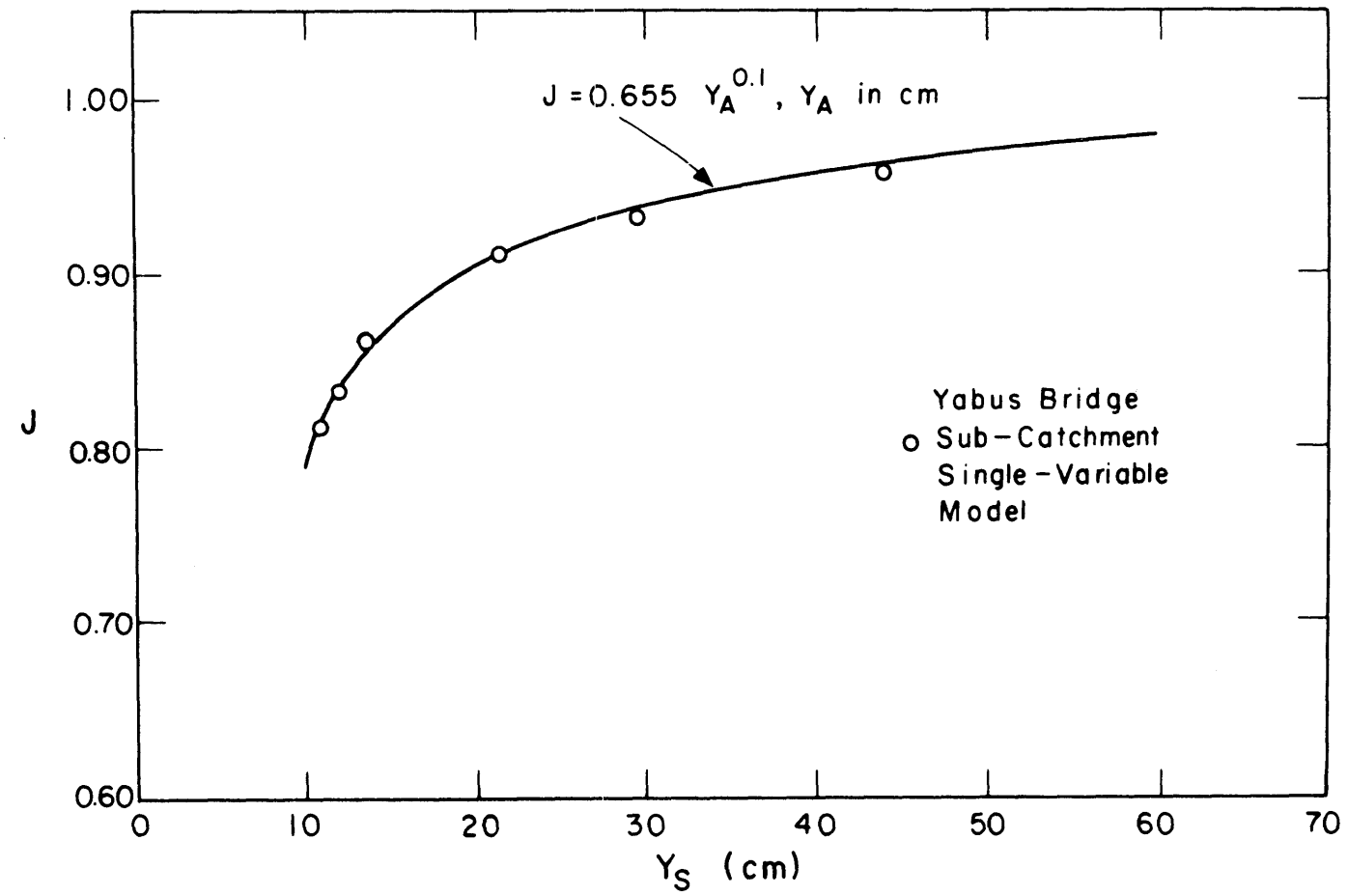

Figure 5.9

THE EVAPOTRANSPIRATION FUNCTION - ANNUAL YIELD RELATIONSHIP FOR VARIABLE CANOPY DENSITY IN YABUS BRIDGE SUB-CATCHMENTS

where

$$c_1 = 0.00$$

$$c_2 = 0.72$$

and

$$c_3 = 0.10$$

Equation (5.11) will be used (regionally) over all the eastern catchments along with the vegetation growth function, Eq. (5.9). It reduces the six parameters of the two-variable model to five: m_{P_A}, m_ν, κ, m_e and σ_e.

Applications of the numerical and approximate analytical versions of the two-variable model to the Yabus Bridge sub-catchment are shown in Fig. 5.10, along with the single-variable model of the annual (seasonal) yield, Eq. (3.52). These models are compared with the annual yield observed at Yabus Bridge gaging station, as given in Appendix A.

Comparing the two-variable model (numerical solution) and the single-variable one with the observations, we find that the latter still gives a better estimate of the derived cdf of the annual (seasonal) yield.

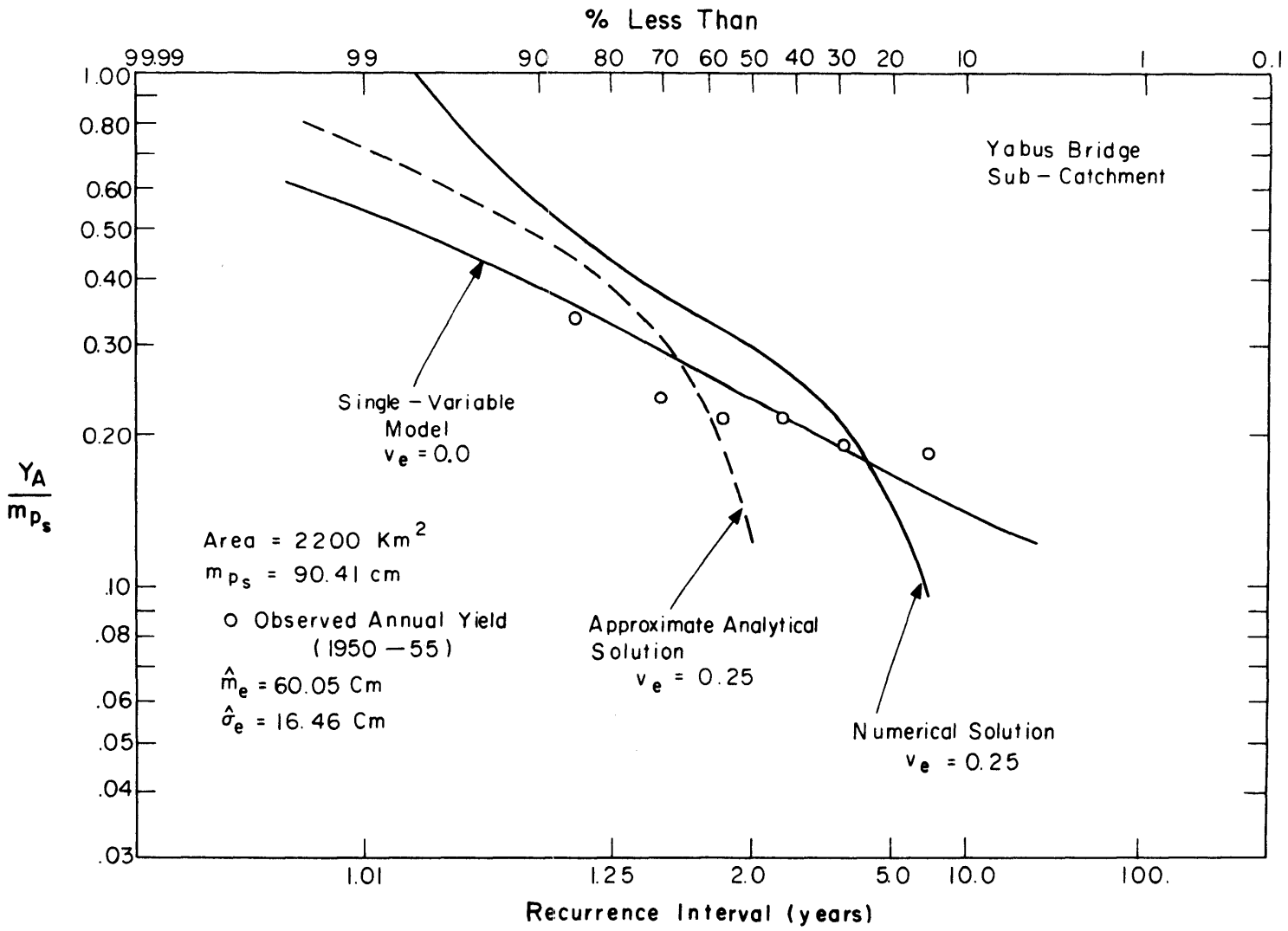

Figure 5.10

THE CUMULATIVE DISTRIBUTION FUNCTIONS OF THE ANNUAL YIELD CALCULATED BY THE SINGLE AND TWO-VARIABLE MODELS AT YABUS BRIDGE

Chapter 6

WATER BALANCE CALCULATIONS

6.1 Introduction

The model parameters have been estimated in Chapter 5 for all catchments of the Machar region, and the model has been verified and calibrated using the yield observations of the Yabus Bridge sub-catchment. Table 5.4 shows the estimated parameters for these catchments. We have estimated the soil parameters regionally where there are no soil data for the studied area.

The vegetation growth function, Eq. (5.9), will be used for all catchments in order to improve the derived cdf of the annual (seasonal) yield, particularly at the lower tail (in the drought years).

The Egyptian Ministry of Irrigation has proposed a channel from Machar (on the Baro River) to Adar (on the White Nile), passing through the plains and swamps. This channel will collect the water that is spilled from the Baro River and the Machar catchments.

From the preliminary water balance in the Machar region, we found that the average yield of the eastern catchments is of the same order as the Baro spillage. This yield flows to the swamps through the plains. The Ministry of Irrigation has proposed another channel passing by the ends of the eastern catchments (C-D) to intercept these flows, as shown in Fig. 6.1. Sizing this channel requires study of the statistics of the total flow downstream of each intercepted khor. These studies will be presented in this chapter using the single variable

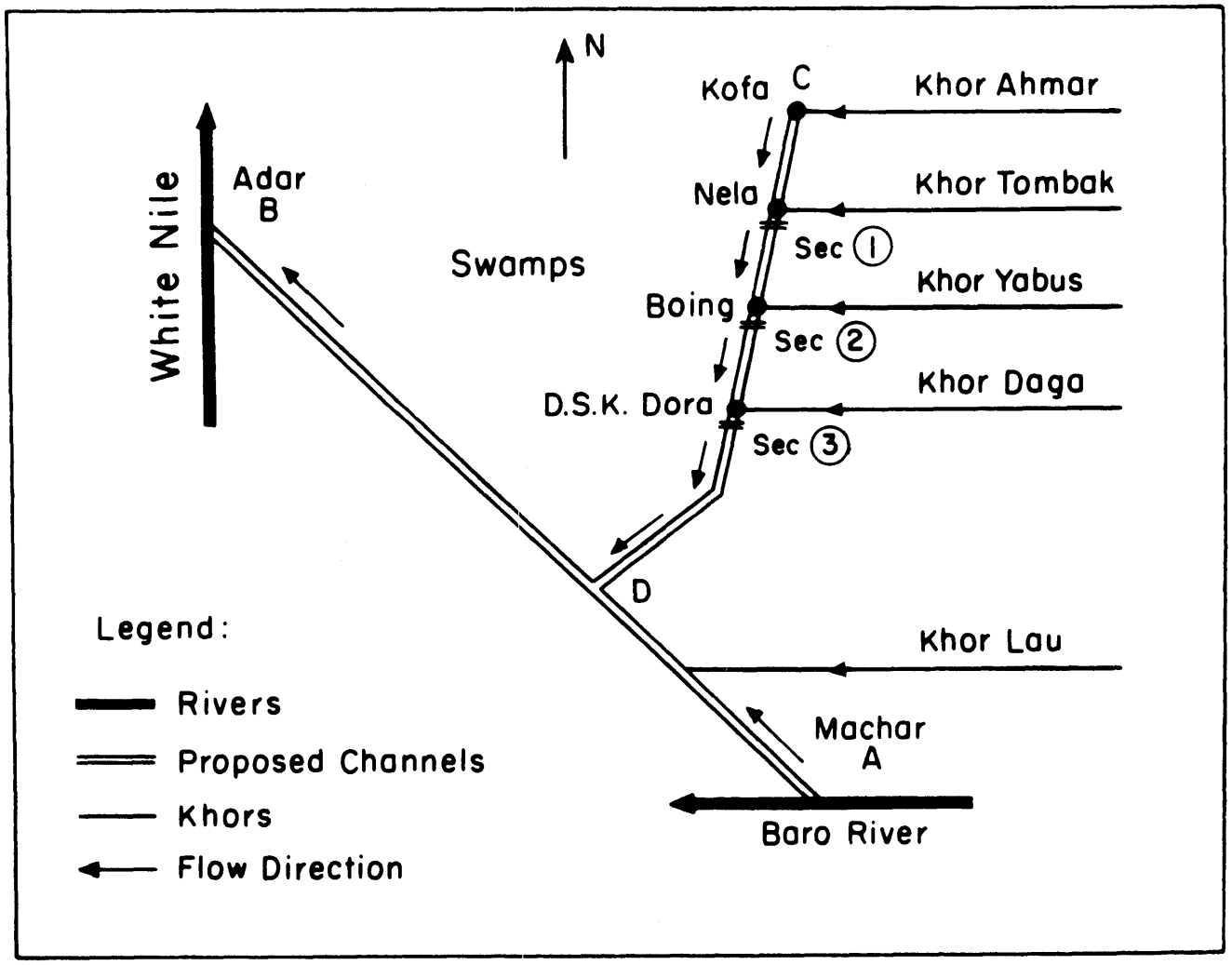

Figure 6.1

SCHEMATIC REPRESENTATION OF CHANNELIZATION SYSTEM IN MACHAR REGION

model.

6.2 Model Applications to the Eastern Catchments

The single-variable model has been applied on the five catchments, Ahmar, Tombak, Yabus, Daga and Lau, separately. The parameters of these catchments are shown in Table 5.3. The results of the applications are shown in Appendix I.

We analyze the cumulative distribution function of yield for each catchment as follows:

(a) Ahmar Catchment

The cdf of annual yield of Khor Ahmar at Kofa is shown in Fig. 6.2. The average annual yield is about 0.415 mld. The available yield observation (from July to October in 1974) is about 0.075mld. Therefore, the ungaged yield of this catchment is about 0.34 mld, assuming that this observation represents the average gaged flow from Khor Ahmar.

We can calculate from Fig. 6.2 that an annual yield less than 1.24 mlds occurs as often as once in 1.01 years. This means that a flow greater than or equal to this amount is found only about once in one hundred years. This frequency analysis can be used to design that portion of the proposed interceptor channel shown in Fig. 6.1, which runs from Kofa to Nela.

(b) Tombak Catchment

As shown in Fig. 6.3, the ungaged yield of Khor Tombak at Nela is about 0.044 mld. This is the lowest ungaged flow in the region.

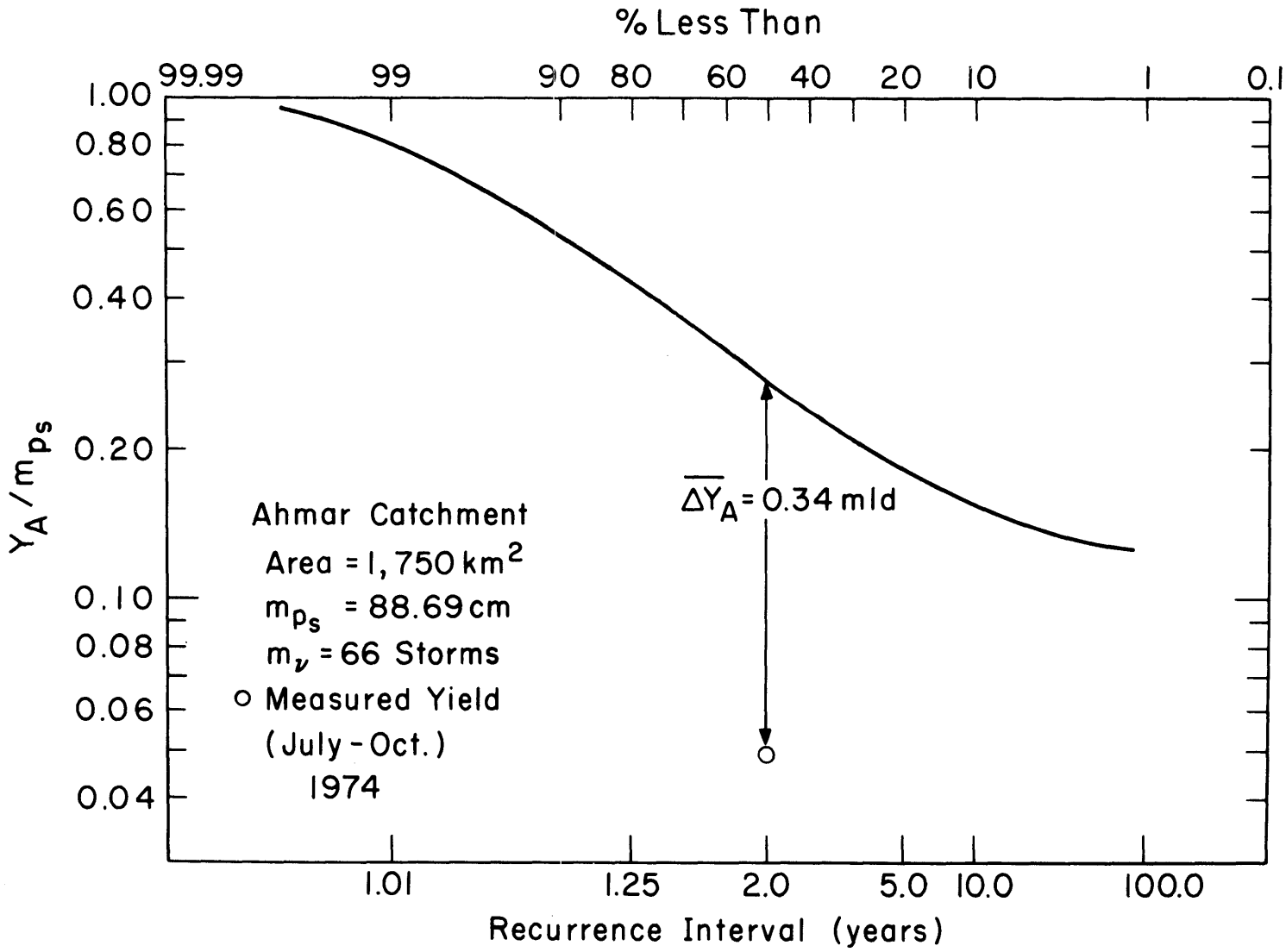

Figure 6.2

FREQUENCY OF ANNUAL YIELD OF KHOR AHMAR AT KOFA

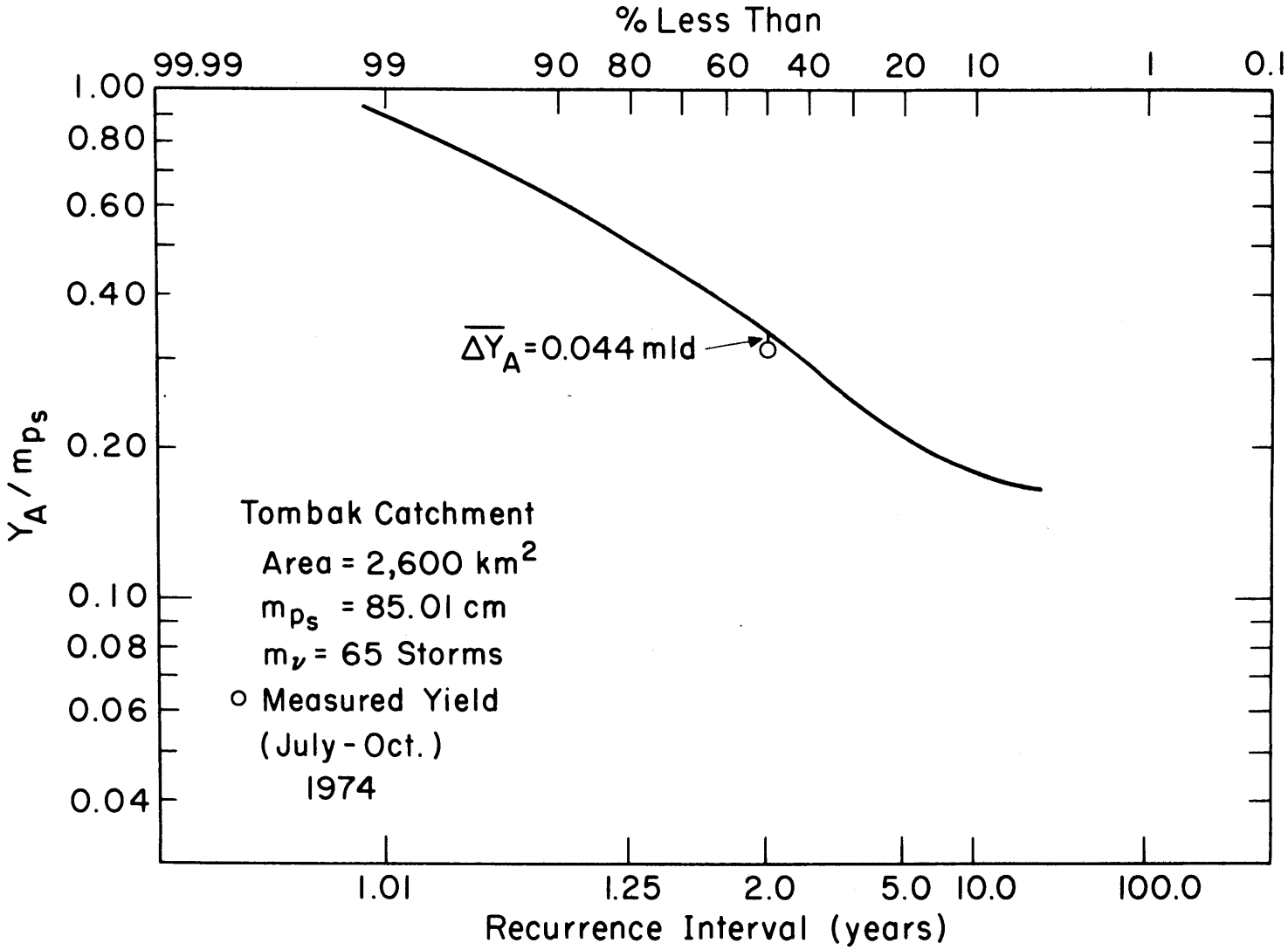

Figure 6.3

FREQUENCY OF ANNUAL YIELD OF KHOR TOMBAK AT NELA

The average annual yield of this khor is about 0.76 mld. The single observed flow is in the same period as that of Khor Ahmar. The derived probability distribution of the annual yield of Khor Tombak can be used along with that of the other khors for designing the cross-sections of the proposed channel. This will be presented in Section 6.3.

(c) Yabus Catchment

The model has been verified using the Yabus Bridge sub-catchment. Now we apply the model to the whole Yabus catchment. The probability distribution of the annual yield of Khor Yabus at Boing is shown on Fig. 6.4. The predicted average annual yield is about 1.35 mlds, but there are no available observations. This derived cdf differs from all others in that the low flow tail does not flatten. This may be due to the high value found for the shape parameter, κ, of the distribution of storm depth. This derived cdf will also be used for further studies.

(d) Daga Catchment

Only a few yield observations are available at Daga Post. These observations do not represent the yield of the whole catchment, however, since we have chosen the mouth of this catchment to be downstream of Khor Dora, as shown in Fig. 4.1. Since this will be the new position of the Daga outlet, a gaging station should be installed there to measure the yield of the whole catchment.

The annual average yield of Khor Daga downstream of Khor Dora is predicted to be about 0.83 mld while that of the Daga Post sub-catchment is predicted to be about 0.44 mld. The difference between

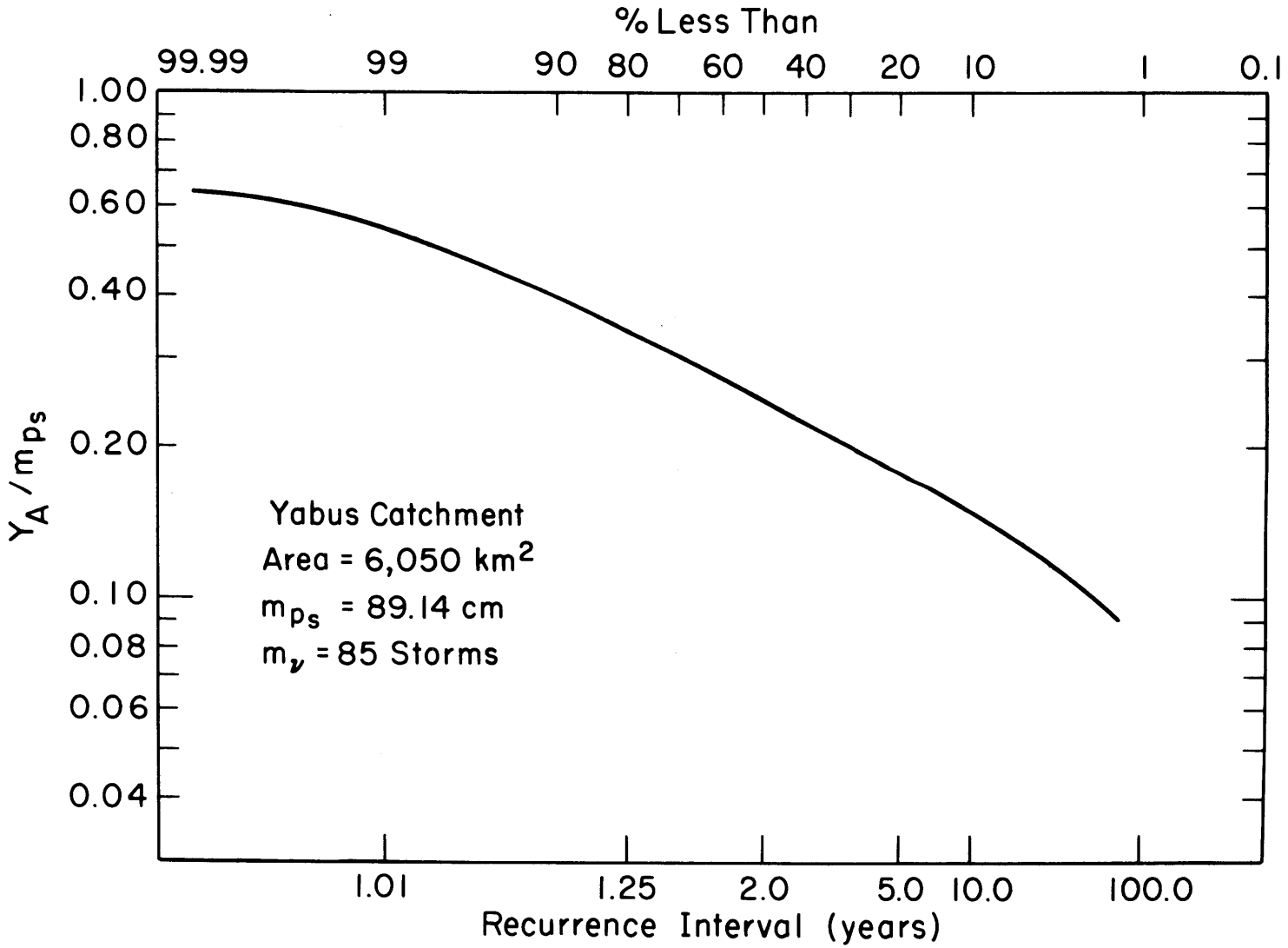

Figure 6.4

FREQUENCY OF ANNUAL YIELD OF KHOR YABUS AT BOING

these values is due to the effect of the area downstream of Daga Post.

As shown in Fig. 6.1, Khor Daga is the last stream crossed by the channel (C-D) before merging with the Machar-Adar channel proposed by the Egyptian Ministry of Irrigation. Figure 6.5 shows the cdf.

(e) Lau Catchment

In the present work, the Lau catchment has been identified as consisting of three sub-catchments, Lau (1), Lau (2), and Lau (3). The outlets of these sub-catchments drain directly to the plains, as shown in Fig. 4.1.

Treating the three sub-catchments as one, lumped catchment, the model gives a total average annual yield of about 0.84 mld. Only one observation at Kigille (one of the three sub-catchments) is available, however. It is about 0.30 mld. Hence, the total ungaged flow is estimated to be 0.54, as shown in Fig. 6.6.

Although the recurrence interval presented in Fig. 6.6 is not used to design the channel C-D, it assists in further studies of the main channel A-B.

According to the above model results, the total average annual yield of all the eastern catchments is about 4.2 mlds. From the preliminary annual water balance, however, we found that this yield was about 3.3 mlds. The difference between these values results from the different methods used to estimate the annual evapotranspiration. In the preliminary water balance, we used the <u>potential</u> evapotranspiration while the water balance model calculates the <u>actual</u> evapotranspiration from soil

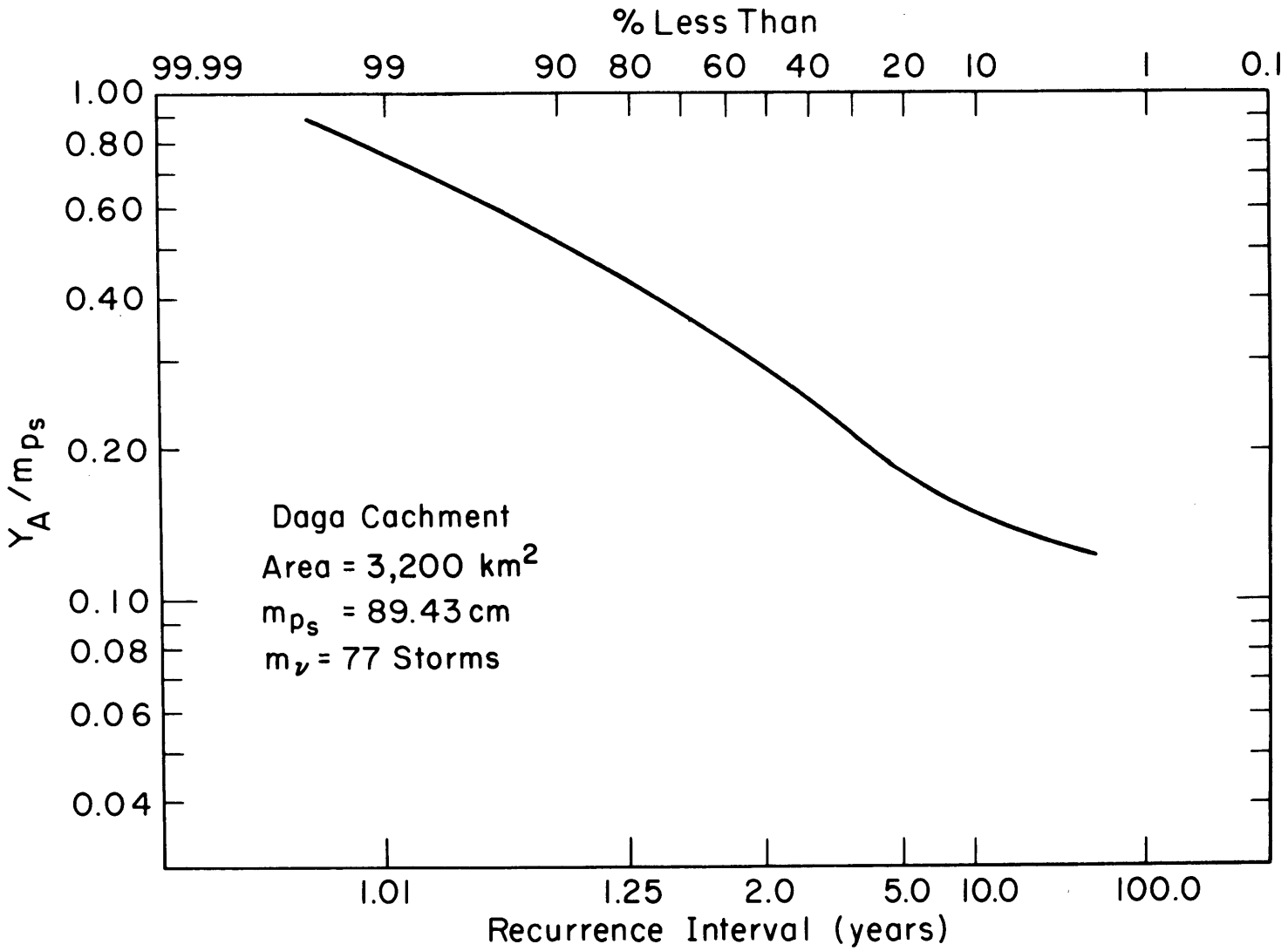

Figure 6.5

FREQUENCY OF ANNUAL YIELD OF KHOR DAGA

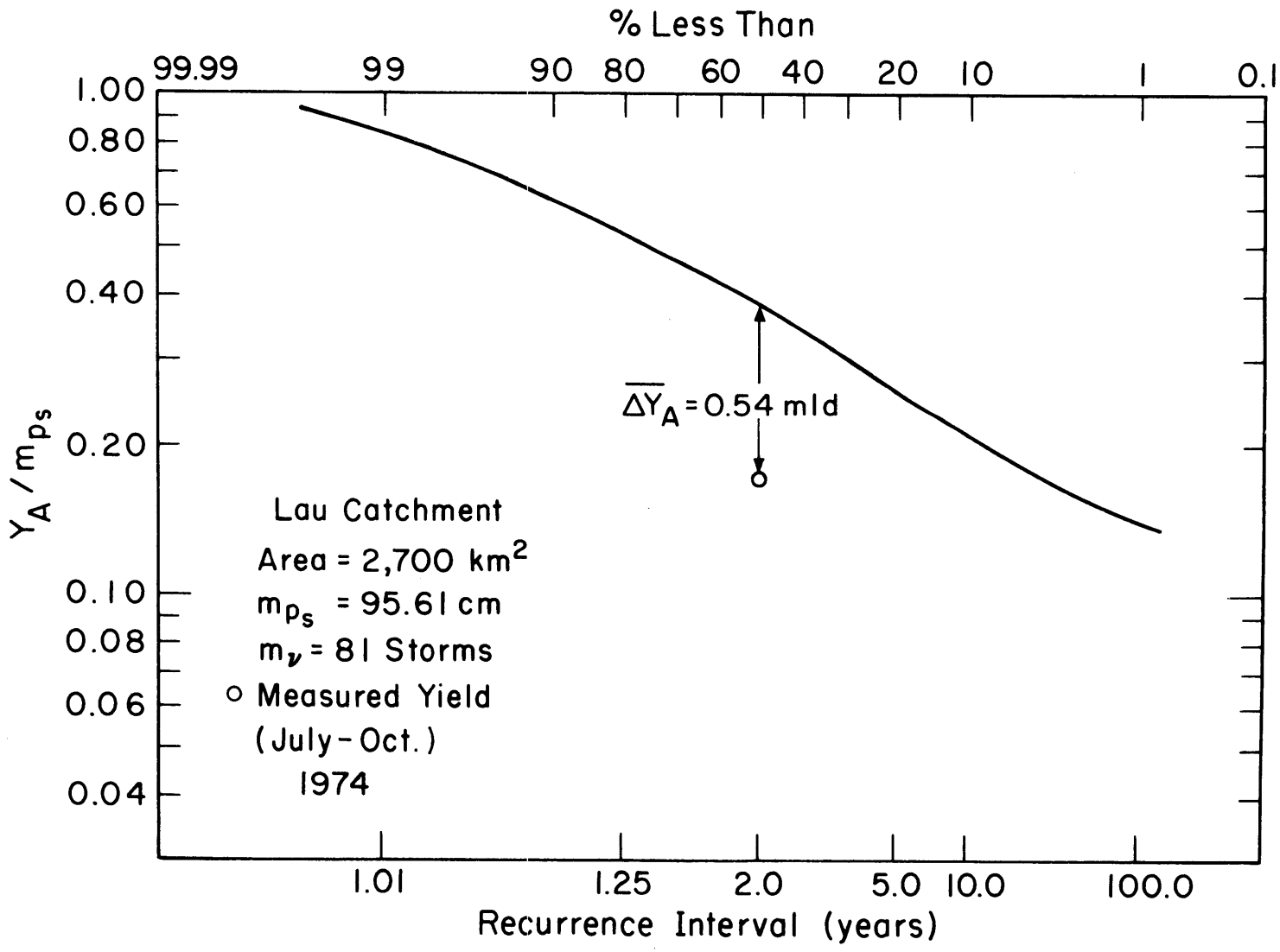

Figure 6.6

FREQUENCY OF ANNUAL YIELD OF KHOR LAU NEAR KHOR MACHAR

moisture considerations.

The total average annual flow at the outlet of the Machar-Adar channel will be about 9.03 mlds. This amount may be modified by further morphological studies in the swamps.

6.3 Frequency Analyses along the Proposed Channel

Designing the proposed channel (C-D) requires knowing the frequencies of the annual discharges at the cross-sections shown in Fig. 6.1.

Sufficient joint observations of yield are not available to estimate the correlations among the yields of these separate catchments. Consequently, two different approaches are proposed here to estimate the cdf of the combined annual flows at each design cross-section. The "true" cdf of the annual discharge may lie between these two estimates. These approaches will be presented in the next two sections.

6.3.1 Independent-Catchment Approach

In this approach, we assume that the annual yields of the catchments that lie above any cross-section are stochastically independent. The derived probability density function, pdf, of the annual yields of these catchments essentially fit Gamma distributions (Thom, 1968), as shown in Figs. 6.7 and 6.8. The cdf of the annual discharge of the cross-section i is then

$$P[Q_{A_i} < q] = \int_0^{b_i q} \frac{(b_i t)^{a_i - 1} \cdot e^{-b_i t}}{\Gamma(a_i)} d(b_i t) \qquad (6.1)$$

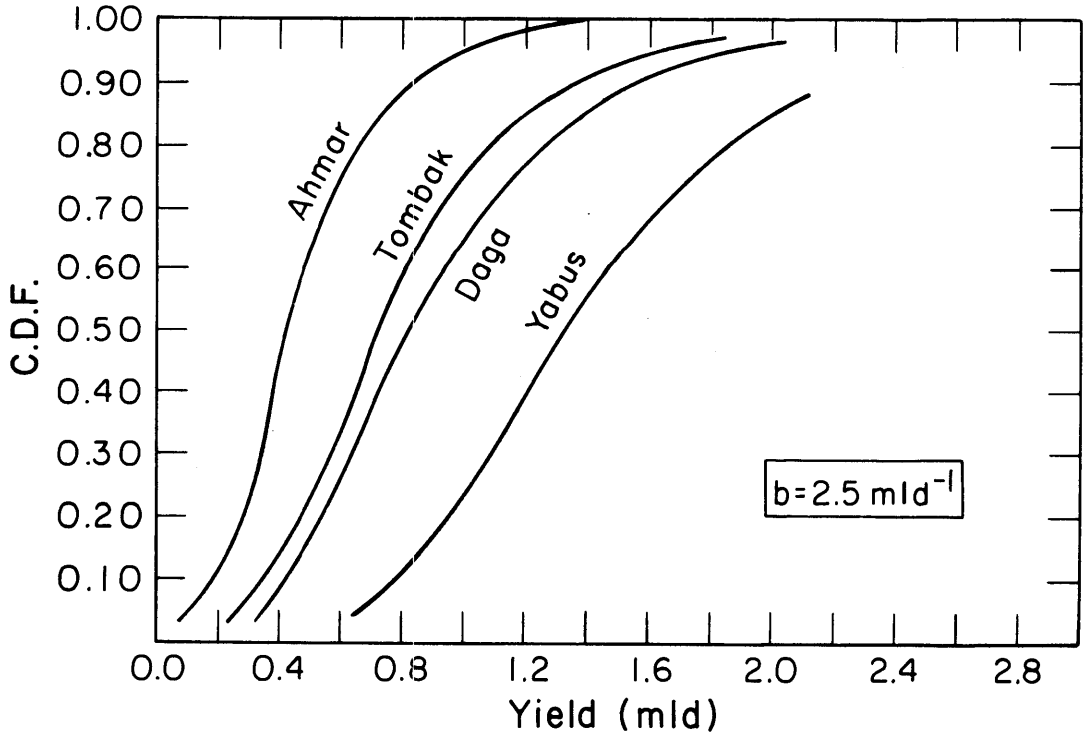

Figure 6.7

THE CUMULATIVE DISTRIBUTION FUNCTIONS OF MACHAR CATCHMENTS

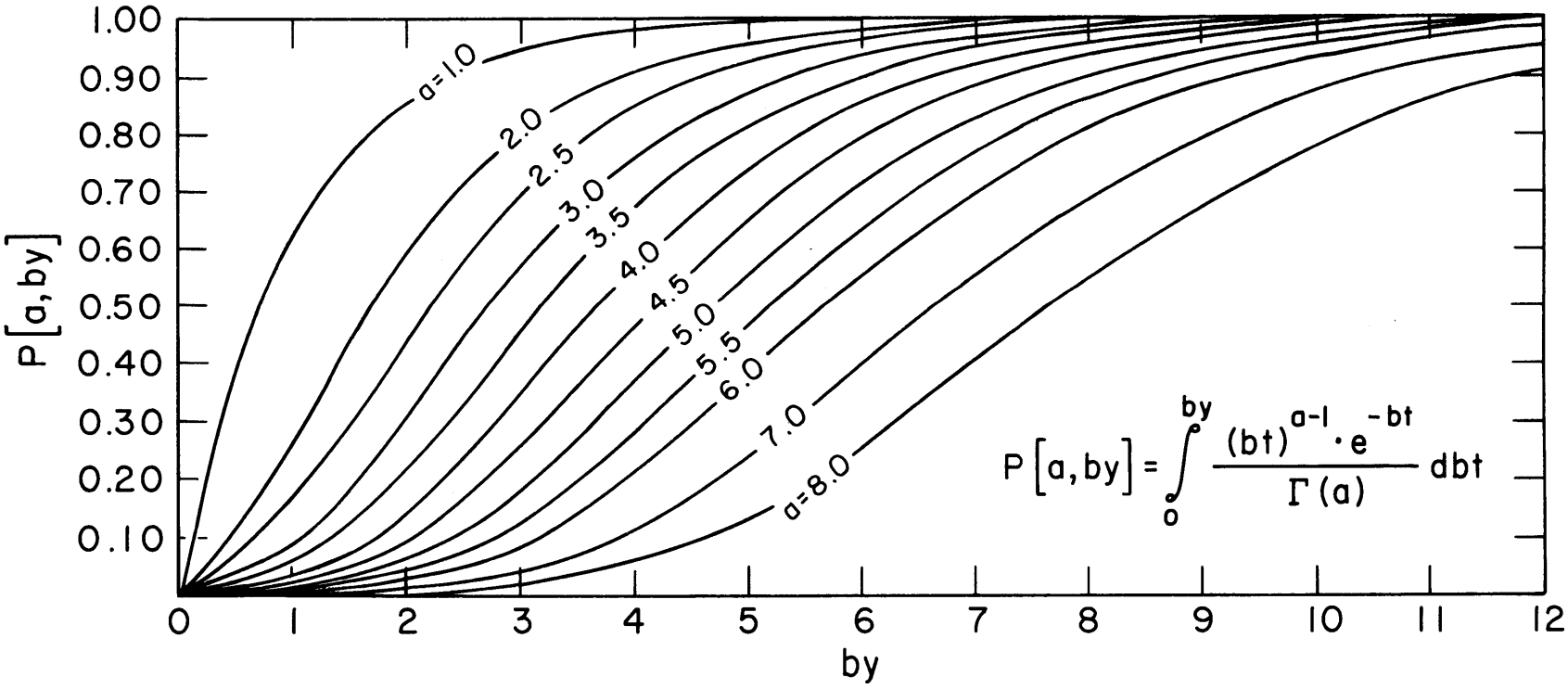

Figure 6.8

PEARSON'S INCOMPLETE GAMMA FUNCTION WITH DIFFERENT SHAPE PARAMETERS

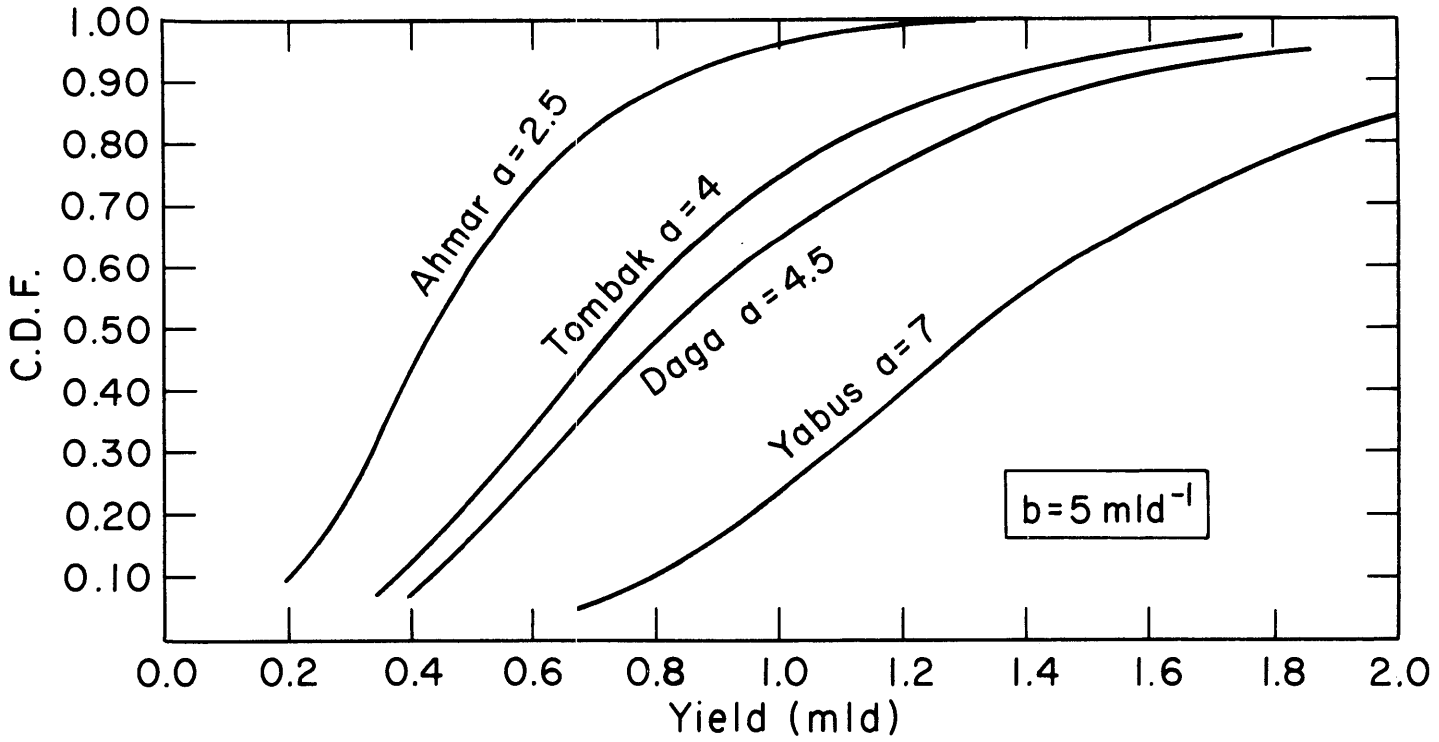

Figure 6.9

ESTIMATION OF SHAPE AND SCALE PARAMETERS OF MACHAR CATCHMENTS

where

a_i = the shape parameter of the Gamma distribution of the annual discharge at section i

and

b_i = the scale parameter of the Gamma distribution of the annual discharge at section i

In order that the regenerative property of Gamma distributions can be used in their summation, we assume the shape and scale parameters to be given by

$$a_i = \sum_{j=1}^{N_i} a_j \tag{6.2}$$

and

$$b_i = b_j \quad , \qquad j = 1, 2, 2 \ldots N_i \tag{6.3}$$

where

a_j = the shape parameter of catchment j

b_j = the scale parameter of any catchment

and

N_i = the number of catchments above section i

Plotting the cdf's of the annual yields with different values of the scale parameter, b_j, and matching them with the set of Pearson's incomplete Gamma functions, shown in Fig. 6.8, gives the best estimates of the shape and scale parameters of the studied catchments. When the scale parameter is about 5.0 mld^{-1}, the cdf of the annual yields of the

catchments, presented in Fig. 6.9 are almost coincident with those of Fig. 6.8. In this case, the shape parameters of these catchments can easily be estimated from the same figure. These parameters are indicated in Fig. 6.9.

Using Eqs. (6.2) and (6.3), the shape and scale parameters of the distribution of combined flows at the sections shown in Fig. 6.1 are calculated. These parameters and the average areal seasonal precipitation of the catchments upstream of the studied sections are presented in Table 6.1.

Section	a	b	m_{p_s}
		(mld^{-1})	(cm)
1	6.5	5.0	86.47
2	13.5	5.0	88.05
3	18.0	5.0	88.43

Table 6.1

ESTIMATED PARAMETERS OF DISTRIBUTION OF COMBINED FLOWS AT DESIGN CHANNEL SECTIONS

Now, applying Eq. (6.1) at the above sections yields the cumulative distribution functions and the frequency intervals of their discharges. Appendix J presents the FORTRAN program for Eq. (6.1) and the results of these applications. These results are plotted in dimensionless form on Figs. 6.10, 6.11 and 6.12 to be compared with the second approach.

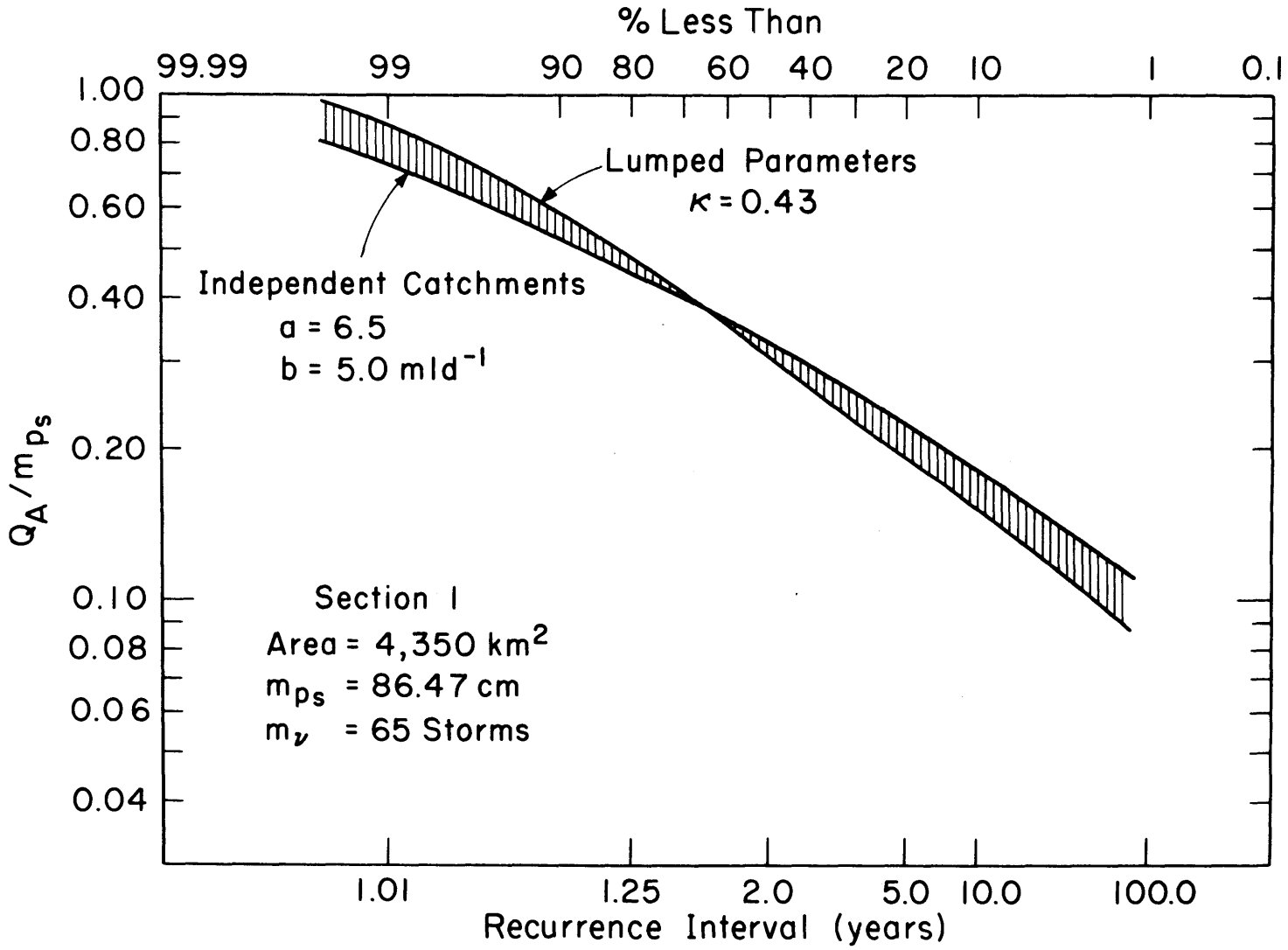

Figure 6.10

FREQUENCY OF ANNUAL DISCHARGE AT SECTION 1 ON THE INTERCEPTOR CHANNEL

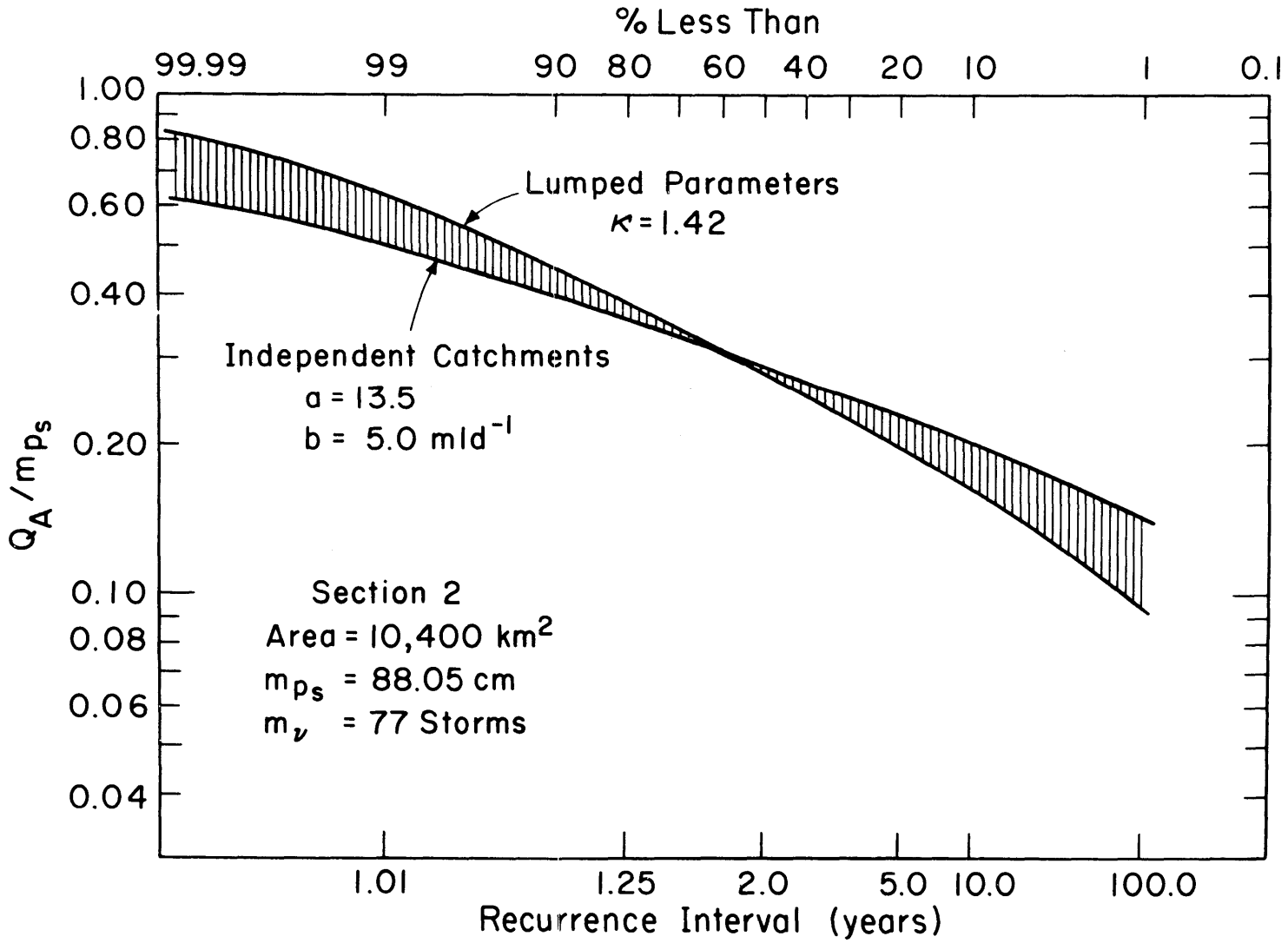

Figure 6.11

FREQUENCY OF ANNUAL DISCHARGE AT SECTION 2 ON THE INTERCEPTOR CHANNEL

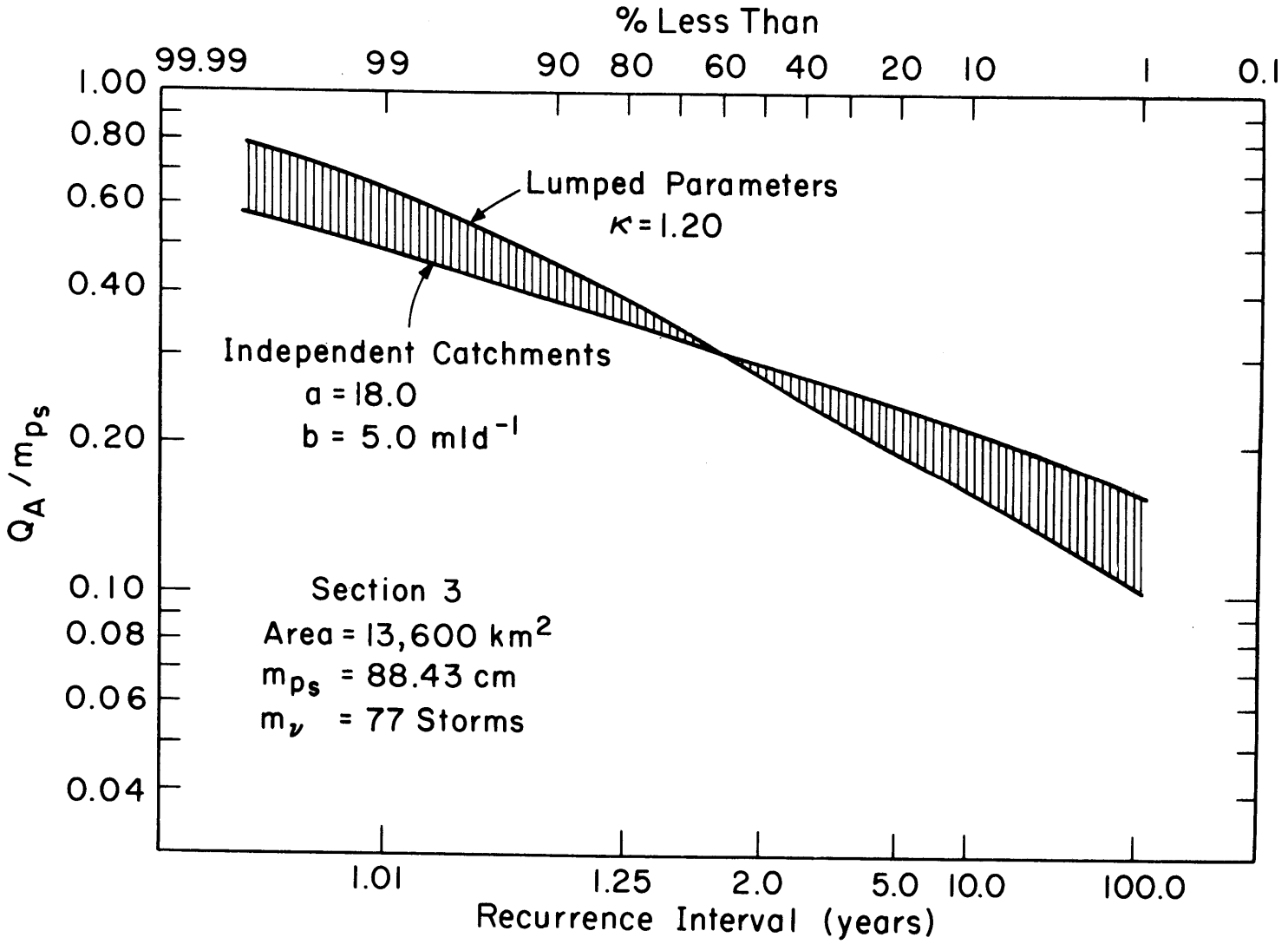

Figure 6.12

FREQUENCY OF ANNUAL DISCHARGE AT SECTION 3 ON THE INTERCEPTOR CHANNEL

6.3.2 Lumped-Parameter Approach

Here, we assume that the catchments upstream of any cross-section work as a single catchment. The transformation weights of the climatic parameters have been presented before in Table 4.4 along with the areas upstream of the cross-sections. The lumped parameters are presented in Appendix I. The FORTRAN program of the single-variable model, Eq. (3.52), has been used in this approach with the new lumped parameters at the three sections. The results of this program are presented in Appendix I. Plotting these results in comparison with the first approach, Figs. 6.10, 6.11 and 6.12, respectively, we find that:

1. The two approaches have the same expected value of annual discharge because this expected value is independent of the correlation coefficients. The expected value of the annual discharge of each cross-section can be determined from the corresponding graph where the two lines intersect.
2. A difference between the two approaches is expected because we assume that the catchments upstream of any cross-section are either independent (in the first approach) or lumped (in the second one). This difference increases gradually away from the expected value in both directions.
3. The two approaches are close at the first section while they have a big difference at the third one. This occurs because the more independent random variables that are added, the smaller will be the variance of their sum. This increases the gap between the two

estimates as the number of contributing catchments increases.

4. The lumped-parameter approach always gives the worst conditions for designing the cross-sections of the proposed channel. Therefore, we will use this approach and reject the other one for these studies.

Incorporation of the correlation between the yields of the separate catchments would reduce the variance of their sum even more than has been found by assuming independence. This has been done, however, in this investigation.

After this analysis, we are ready to estimate the worst flood at each cross-section using the lumped-parameter approach. Choosing a 100 year recurrence interval as the basis of design, we find that the biggest annual discharges at sections 1, 2 and 3 are 3.24, 5.86 and 7.70 mlds, respectively.

Chapter 7

SUMMARY AND CONCLUSIONS

7.1 Summary

This work has attempted to improve an existing water balance model and to apply this model to the eastern catchments of the Machar region in the Republic of the Sudan.

After brief introduction in Chapter 1 and a review of previous work in Chapter 2, Chapter 3 summarized the first order water balance (single-variable) model formulated by Eagleson (1978a, b, c, d, e, f, g), and presented the mathematical derivations of a new (two-variable) model in which the annual (seasonal) precipitation and potential evapotranspiration are both taken as independent random variables.

In Chapter 4, the available data from the Machar region were analyzed. The remote sensing drainage and vegetation maps of the Machar region have been used in this analysis to present a new identification of the region boundaries. This chapter also estimated a new preliminary water balance for all Machar zones, eastern catchments, plains and permanent swamps. For the first time, all the hydrologic components have been calculated separately, and then the closure error concept has been introduced.

The climate, vegetation and soil parameters of the water balance model have been initially estimated in Chapter 5. An approximate hydrograph separation was employed to estimate the soil properties of the eastern catchments where soil data are not available. In this

chapter, the first order model was verified and calibrated by a newly-introduced function (i.e., vegetation growth function). Some sensitivity analyses of the two-variable (new) model were also presented in this chapter.

Chapter 6 detailed the applications of the first order (one-variable) model to the eastern catchments and the estimation of design capacities for sections of the proposed channel.

7.2 Conclusions

From this work, we conclude:

1. The average annual net spilling from the Baro River to the Machar region is about 3.42 mlds (including the outflow of Khor Adar), while the total average annual yield from the eastern catchments is about 4.2 mlds.
2. More than 8 mlds can be contributed annually from the Machar region to the White Nile by executing the channel system proposed by the Ministry of Irrigation.
3. The soil of the eastern catchments is clay loam having a coefficient of permeability of about 1.0×10^{-4} cm/sec.
4. The variabilities of the potential evapotranspiration and groundwater storage should be studied together. However, neglecting both of them (as in the single-variable model) may give a better estimate than including either alone because their effects are opposing.
5. From the sensitivity analysis of the first order (one-variable) model at Yabus Bridge, we find that use of the vegetation growth function gives a better estimate of the cumulative distribution function of

the annual yield than does the assumption of constant vegetation density.

6. In the Machar region, the probability density function of the water surface potential evaporation fits essentially a normal distribution while that of the annual (seasonal) yield for each catchment fits a Gamma distribution.
7. Estimating the discharge-frequency of the proposed drainage channel by lumping all contributing areas gives a conservative estimate for designing the cross-sections of this channel.
8. Studying the Machar-Adar channel proposed by the Egyptian Ministry of Irrigation requires further research into the morphology of the Machar swamps.

References

1. Balek, J. and Perry, J.E., Hydrology of Seasonally Inundated African Headwater Swamps, Journal of Hydrology, 19 (1973), pp. 227-249.

2. Benjamin, J.R. and Cornell, C.A., Probability, Statistics and Decision for Civil Engineers, McGraw-Hill, New York, 1970.

3. Berry, L. and Whiteman, A.J., "The Nile in the Sudan," The Geographical Journal, Vol. 134, Part I, March 1968, p. 2.

4. Bhalotra, Y.P.R., Meteorology of Sudan, Sudan Meteorological Service, Memoir No. 6, Presented by P&T Department, September, 1963.

5. Chapas, L.C. and Rees, A.R., "Evaporation and Evapotranspiration in Southern Nigeria," Quarterly Journal, Royal Meteorology Society, Vol. 89, 1963, pp. 313-319.

6. Operation Navigation Chart, prepared and published by the Defence Mapping Agency Aerospace Center, St. Louis Air Force Station, Missouri 63118 (Series: ONC K-5)

7. Eagleson, P.S., and Chan, S.O., "Water Balance Estimates of a Sudd Tributary," Proceedings MIT/Cairo University Conference on Water Resources, Cairo, June 1979.

8. Eagleson, P.S., "Climate, Soil and the Water Balance," M.I.T. Department of Civil Engineering, 1977.

9. Eagleson, P.S., "Climate, Soil and Vegetation 1. Introduction to Water Balance Dynamics," Water Resources Research, Vol. 14(5), 1978a.

10. Eagleson, P.S., "Climate, Soil and Vegetation 2. The Distribution of Annual Precipitation Derived from Observed Storm Sequences," Water Resources Research, Vol. 14(5), 1978b.

11. Eagleson, P.S., "Climate, Soil and Vegetation 3. A Simplified Model of Soil Moisture Movement in the Liquid Phase," Water Resources Research, Vol. 14(5), 1978c.

12. Eagleson, P.S., "Climate, Soil and Vegetation 4. The Expected Value of Annual Evapotranspiration," Water Resources Research, Vol. 14(5), 1978d.

13. Eagleson, P.S., "Climate, Soil and Vegetation 5. A Derived Distribution of Storm Surface Runoff," Water Resources Research, Vol. 14(5), 1978e.

14. Eagleson, P.S., "Climate, Soil and Vegetation 6. Dynamics of the Annual Water Balance," Water Resources Research, Vol. 14(5), 1978f.

15. Eagleson, P.S. "Climate, Soil and Vegetation 7. A Derived Distribution of Annual Water Yield," Water Resources Research, Vol. 14(5), 1978g.

16. Eagleson, P.S., Dynamic Hydrology, McGraw-Hill, New York, 1970.

17. Hurst, H.E. and Phillips, P., The Nile Basin, Volume I, General Description of the Basin, Meteorology, Topography of the White Nile Basin; Ministry of Public Works, Egypt; Physical Department, Physical Department Paper No. 26, Government Press, Cairo, 1931, pp. 97-99.

18. Hurst, H.E., The Nile Basin, Volume VIII, The Hydrology of the Sobat and White Nile and the Topography of the B ue Nile and Atbara; Ministry of Public Works, Egypt; Physical Department, Physical Department Paper No. 55, Government Press, Cairo, 1950, pp. 1-27.

19. The Equatorial Nile Project (and Its Effects in the Anglo-Egyptian Sudan), a report by the Jonglei Investigation Team, Volume III, 1955, pp. 971-984.

20. Landsberg, H.E., Lippman, H., Paffen, K.H. and Troll, C., World Maps of Climatology (3rd edition). Publication of the Geomedical Research Unit of the Heidelberg Academy of Science, 1966.

21. Metzger, B.H. and Eagleson, P.S., The Effects of Annual Storage and Random Potential Evapotranspiration on the One-Dimensional Annual Water Balance, Technology Adaptation program, M.I.T., TAP Report 80-3, Spring 1980.

22. Machar Marshes Data, from the Egyptian General Inspectorate of Irrigation in Sudan, and Nile Control General Inspectorate, Ministry of Irrigation, Cairo.

23. The Nile Basin, Volume VI, up to 7th Supplement. Monthly and Annual Rainfall Totals and Number of Rainy Days at Stations in and near the Nile Basin by Nile Control Staff. Arab Republic of Egypt, Ministry of Irrigation, Nile Control Department, Paper No. 33.

24. The Nile Basin, Volume IV, up to the 8th supplement. Ten-Day Mean and Monthly Mean Discharges of the Nile and its Tributaries by Nile Control Staff. Ministry of Irrigation, Egypt, Nile Control Department, Paper No. 27, Cairo. General Organization for Government Printing Offices, 1971.

25. Oliver, J., "Problems of Determining Evapotranspiration in the Semi-Arid Tropics Illustrated with Reference to the Sudan," Journal of Tropical Geography, v(29) No. 1, June 1969, pp. 64-74.

26. General Drainage and Land Cover-Land Use Maps of River Sobat Area, Southeastern Sudan, Remote Sensing Center, Academy of Scientific Research and Technology, Cairo, 1979.

27. Soil Resources and Potential for Agriculture Development in Bahr el Jebel Area, Southern Sudan (Jonglei Canal Project Area). A report published by Remote Sensing Center, Academy of Scientific Research and Technology, Cairo, Egypt, for the permanent Joint Technical Commission for Nile Waters, April 1978.

28. Rzoska, J., The Nile, Biology of an Ancient River, the Hague, 1976.

29. Scheid, F., Theory and Problems of Numerical Analysis, Schaum's Outline Series in Mathematics, McGraw-Hill, New York, 1968.

30. Annual Meteorological Report, Council of Ministers Sudan Meteorological Department, up to Vol. 26, Khartoum, June 1978.

31. Tellers, T.E. and Eagleson, P.S., "Estimation of Effective Hydrologic Properties of Soils from Observations of Vegetation Density," M.I.T., Civil Eng. Dept., Tech. Rep. No. 254, R80-7, March 1980.

32. Tennessee Valley Authority, "Heat and Mass Transfer Between a Water Surface and Atmosphere," Water Resources Research, Laboratory Report No. 14, Norris, Tenn., 1972.

33. Thomas, H.A., "Frequency of Minor Floods," J. Boston Soc. Civil Eng., 35, 1948, pp. 425-442.

34. Thom, H.C.S., "Direct and Inverse Tables of the Gamma Distribution," Environmental Data Service, EDS-2, U.S. Dept. of Commerce, Washington, D.C., 1968, pp. 12-22.

Appendix A

Numerical Model

The derived probability distribution of the annual (seasonal) yield is expressed by Eq. (3.73). The integral in this equation is:

$$I_{\nu}(y) = \int_{o}^{\infty} e^{-\left(\frac{E-m_e}{\sqrt{2}\,\sigma_e}\right)^2} \cdot P\left[\nu\kappa,\ m_{\nu}\,\kappa\,\left(\frac{y + B\,E}{m_{p_A}}\right)\right] d\,E \qquad (A.1)$$

As mentioned in the text, this integral has no exact solution.

Using the characteristics of the two included functions we can easily solve the integral numerically as follows:

1. The exponential function decays rapidly around the mean, m_e. The relative area under this function is

$$A_{relative} > 0.95 \quad , \quad \text{for the range of } E = m_e \mp 2\,\sigma_e \qquad (A.2)$$

2. Pearson's incomplete Gamma function, P[ ], varies slowly as:

For E = 0

$$0 \leq P \leq 1 \quad , \quad \text{depending on } y \text{ and } \nu \qquad (A.3)$$

For E = ∞

$$P = 1 \qquad (A.4)$$

In the present work we choose the range of integration from $m_c - 2\sigma_e$ to me + 3 σ_e because the values of Pearson's incomplete Gamma function to the right of the mean, m_e, are always greater than that to the left of the same mean value.

Discretizing Eq. (A.1) using Simpson's rule (Scheid, 1968), gives

$$I_\nu(y) \simeq \frac{\Delta E}{3} [\ \zeta_o + 4\ \zeta_1 + 2\ \zeta_2 + 4\ \zeta_3 + ... + 2\ \zeta_{n-2} + 4\ \zeta_{n-1} + \zeta_n] \tag{A.5}$$

in which

$$\zeta_i = e^{-[\frac{E_i - m_e}{\sqrt{2}\ \sigma_e}]^2} \cdot P\ [\nu\ \kappa,\ m_\nu\ \kappa\ (\frac{y + B\ E_i}{m_{p_A}})] \quad , \ i = 0,1,2,..n \tag{A.6}$$

and

$$n = \frac{E_o - E_n}{\Delta\ E} = \text{number of segments} \tag{A.7}$$

where

$$E_i = E_o + \Delta\ E \tag{A.8}$$

$$E_o = m_e - 2\ \sigma_e \tag{A.9}$$

and

$$E_n = m_e + 3\ \sigma_e \tag{A.10}$$

The interval Δ E is chosen to be 1 Cm when m_e and σ_e are in Cms.

The coefficient B in Eq. (A.6) is a function of the annual (Seasonal) yield according to

$$B = C_1 + C_2\ Y_A^{C_3} \tag{A.11}$$

where

C_1, C_2 and C_3 are estimated as in Eq. (5.11).

A fortran program to compute the cumulative distribution function of the annual (seasonal) yield follows:

```
C                 NUMERICAL MODEL
C
C   THIS MODEL COMPUTES CDF OF THE YIELD
C  USING THE POTENTIAL EVAPOTRANSPIRATION
C  AS A RANDOM VARIABLE
C  THIS MODEL HAS BEEN DERIVED
C  AND PROGRAMMED BY EL-HEMRY
C
C*****************************************
C
C UNITS
C      ME=SE=MP=(SAME UNITES)  CM
C      MU=AK=B=DIM. LESS
C
C      NJ=NUMBER OF CDF POINTS   (YS)
C
C*****************************************
C
       REAL*8 NAME(20)
       REAL*8 FAC(500),Y(10),FN(200)
       REAL*8 SUM1,SUM2,T,DERF,DSQRT
       REAL*8 ABC,X,A,GAMLID,EPS,SSN,VNEW,SSS
       REAL*8 DLOG,DLGAMA,DXP
       REAL*8 MU,AK,YS,B,ME,SE,MP,YS1,EP,C1,C2,C3
       REAL*8 XOLD,XSUM,SUM,SUF,SUFT,GAML,TOT,VTOT,VOLD,DLH
       INTEGER V,VM,VMAX
       DO 123 J=1,500
       VTOT=0.0D0
       DO 700 IV=1,J
  700   VTOT=VTOT+DLOG(DFLOAT(IV))
       FAC(J)=VTOT
  123  CONTINUE
       READ(8,1)NAME
    1  FORMAT(20A4)
       READ(8,*)C1,C2,C3
       READ(8,*)ME,SE,MU,AK,MP
       READ(8,*)EPS,DLH
       READ(8,*)NJ,(Y(J),J=1,NJ)
       WRITE(6,19)NAME
   19  FORMAT(20A4)
       WRITE(6,31)C1,C2,C3
   31  FORMAT(' C1= ',F7.4,/,' C2= ',F7.4,/,' C3= ',F7.4,/)
       WRITE(6,2)ME,SE,MU,AK,MP
    2  FORMAT(' ME = ',F9.4,/,' SE = ',F9.4,/,' MU = ',F9
      *.4,/,' AK = ',F9.4,/,' MP = ',F9.4,//)
       WRITE(6,8)
    8  FORMAT(9X,'YS',6X,'PROB',6X,'YS1',//)
       VM=IFIX(SNGL(MU))
       VMAX=IFIX(SNGL(3.0D0*MU))
       T=1.0D0+DERF(ME/(DSQRT(2.0D0)*SE))
       DO 444 KK=1,NJ
       YS=Y(KK)
       B=C1+C2*YS**C3
       YS1=YS/MP
       II=0

       JJ=1
       SUM1=0.0D0
       SUM2=0.0D0
   13  V=VM-II
       IF(V.EQ.0)GO TO 500
   23  IF(V.EQ.VMAX)GO TO 600
       A=DFLOAT(V)*AK
       CALL ABC(MP,ME,SE,EPS,DLH,MU,AK,B,A,YS,SUFT)
       GAMLID=DLOG(SUFT)
C
C      COMPUTE THE SUMMATION OF ALL V TERMS
```

```
      VOLD=DFLOAT(V)*DLOG(MU)-FAC(V)+GAMLID-MU
      IF(VOLD.LE.-170.)VOLD=-170.
      VNEW=DEXP(VOLD)
      IF(V.GT.VM)GO TO 800
      SUM1=SUM1+VNEW
      IF((VNEW/SUM1).LE.EPS)GO TO 500
      II=II+1
      GO TO 13
  500 V=VM+JJ
      GO TO 23
  800 SUM2=SUM2+VNEW
      IF((VNEW/SUM2).LE.EPS)GO TO 600
      JJ =JJ+1
      GO TO 500
C
C
  600 CONTINUE
      IF(MU.GT.170.0)MU=170.0D0
      PROB=DEXP(-MU)+(SUM1+SUM2)/(1.25331413D0*SE*T)
      IF(PROB.GT.1.0)PROB=0.99999
      IF(PROB.LE.0.0)PROB=0.00
      WRITE(6,88)YS,PROB,YS1
   88 FORMAT(' ',D10.3,2F10.5,/)
  444 CONTINUE
      STOP
      END
C
C
      SUBROUTINE ABC(MP,ME,SE,EPS,DLH,MU,AK,B,A,YS,SUFT)
C ***********************************************************
C
      REAL*8 FN(200)
      REAL*8 MP,ME,SE,EPS,DLH,MU,AK,YS,SUFT,SUF,EP
      REAL*8 X,XOLD,XSUM,GAML,SSN
      REAL*8 A,DLOG,DLGAMA,DEXP,ABC,SSS
      EP=ME-2.0D0*SE
      PQ=5.0D0*SE/DLH
      NN=IFIX(PQ)+1
      DO 99 JK=1,NN
      X=MU*AK*(B*EP+YS)/MP
      XOLD=1.0D0/A
      XSUM=1.0D0/A
      I=1

  100 XOLD=(XOLD/(A+I))*X
      XSUM=XSUM+XOLD
      IF((XOLD/XSUM).LE.EPS) GO TO 200
      I=I+1
      GO TO 100
  200 CONTINUE
      GAML=A*DLOG(X)-X+DLOG(XSUM)-DLGAMA(A)
      SSN=0.5D0*((EP-ME)/SE)*((EP-ME)/SE)
      SSS=GAML-SSN
      IF(SSS.LE.-170.0) SSS=-170.0
      FN(JK)=DEXP(SSS)
      EP=EP+DLH
   99 CONTINUE
      SUF=0.0D0
      NR=(NN-1)/2
      DO 7 JX=1,NR
      SUF=SUF+4.0D0*FN(2*JX)+2.0D0*FN(2*JX+1)
    7 CONTINUE
      SUFT=(DLH/3.0D0)*(SUF+FN(1)-FN(NN))
      RETURN
      END
```

Appendix B

Table (B-1)

The Annual and Seasonal Precipitation (mm),

Rainy Season Length (months) and

Number of Rainy Days $\geq$ 1.0 mm (days).

Year	Station Notations*	Kurmuk	Gambela	Chali	Daga P.	Doro	Yabus Br.
1950	P_A†	912.0	1241.0	702.0	---	949.0	---
	P_s	861.0	1189.0	682.0	---	906.0	---
	τ	6.0	7.0	7.0	---	7.0	---
	ν`	67.0	118.0	51.0	---	96.0	---
1951	P_A†	853.0	1447.0	693.0	---	761.0	817.0
	P_s	851.0	1375.0	660.0	---	761.0	817.0
	τ	7.0	7.0	6.0	---	6.0	7.0
	ν`	84.0	102.0	62.0	---	69.0	99.0
1952	P_A†	946.0	1170.0	941.0	931.0	629.0	885.0
	P_s	884.0	1136.0	917.0	894.0	616.0	866.0
	τ	5.0	8.0	6.0	7.0	6.0	7.0
	ν`	53.0	104.0	69.0	78.0	51.0	91.0

Table (B-1) Continued

Year	Station Notations*	Kurmuk	Gambela	Chali	Daga P.	Doro	Yabus Br.
1953	P_A†	1083.0	1249.0	902.0	1053.0	995.0	931.0
	P_s	1078.0	1228.0	895.0	1041.0	964.0	931.0
	τ	8.0	10.0	7.0	8.0	6.0	8.0
	ν`	78.0	98.0	69.0	85.0	54.0	114.0
1954	P_A†	1224.0	1757.0	1119.0	1160.0	906.0	1048.0
	P_s	1198.0	1696.0	1117.0	1112.0	885.0	1040.0
	τ	6.0	8.0	7.0	7.0	6.0	7.0
	ν`	61.0	106.0	73.0	85.0	55.0	100.0
1955	P_A†	1065.0	1431.0	927.0	---	795.0	1152.0
	P_s	974.0	1372.0	870.0	---	713.0	1134.0
	τ	7.0	8.0	6.0	---	7.0	8.0
	ν`	67.0	122.0	76.0	---	85.0	117.0
1956	P_A†	1197.0	1427.0	871.0	1215.0	1192.0	1076.0
	P_s	1098.0	1385.0	785.0	1114.0	1161.0	1038.0
	τ	6.0	8.0	6.0	6.0	6.0	7.0
	ν`	71.0	92.0	63.0	89.0	80.0	79.0

Table (B-1) Continued

Year	Station Notations*	Kurmuk	Gambela	Chali	Daga P.	Doro	Yabus Br.
1957	P_A†	809.0	916.0	763.0	---	592.0	797.0
	P_s	692.0	774.0	747.0	---	568.0	731.0
	τ	6.0	7.0	6.0	---	6.0	7.0
	ν`	52.0	80.0	56.0	---	52.0	76.0
1958	P_A†	1043.0	1214.0	816.0	937.0	746.0	915.0
	P_s	1010.0	1127.0	814.0	863.0	663.0	891.0
	τ	7.0	7.0	7.0	6.0	6.0	7.0
	ν`	101.0	93.0	62.0	82.0	65.0	87.0
1959	P_A†	875.0	1374.0	832.0	834.0	804.0	953.0
	P_s	861.0	1292.0	788.0	826.0	721.0	877.0
	τ	7.0	8.0	6.0	8.0	5.0	7.0
	ν`	94.0	120.0	70.0	81.0	49.0	82.0
1960	P_A†	945.0	1179.0	875.0	597.0	720.0	816.0
	P_s	940.0	1129.0	875.0	554.0	720.0	813.0
	τ	7.0	8.0	7.0	5.0	7.0	7.0
	ν`	100.0	132.0	95.0	44.0	66.0	75.0

Table (B-1) Continued

Year	Station / Notations*	Kurmuk	Gambela	Chali	Daga P.	Doro	Yabus Br.
1961	P_A †	968.0	1785.0	933.0	938.0	612.0	1091.0
	P_s	853.0	1726.0	867.0	910.0	586.0	1026.0
	τ	5.0	8.0	5.0	7.0	5.0	5.0
	ν`	42.0	136.0	74.0	90.0	57.0	78.0
1962	P_A †	1136.0	1460.0	1248.0	---	879.0	821.0
	P_s	1105.0	1377.0	1222.0	---	758.0	758.0
	τ	7.0	7.0	7.0	---	5.0	6.0
	ν`	59.0	93.0	73.0	---	56.0	71.0
1963	P_A †	1075.0	1581.0	1034.0	---	836.0	968.0
	P_s	1007.0	1540.0	970.0	---	803.0	831.0
	τ	6.0	9.0	6.0	---	6.0	6.0
	ν`	66.0	108.0	89.0	---	61.0	72.0
1964	P_A †	1089.0	1790.0	1437.0	790.0	---	---
	P_s	1071.0	1628.0	1424.0	735.0	---	---
	τ	7.0	7.0	7.0	6.0	---	---
	ν`	70.0	90.0	70.0	59.0	---	---

Table (B-1) Continued

Year	Station Notations*	Kurmuk	Gambela	Chali	Daga P.	Doro	Yabus Br.
1965	P_A†	627.0	1092.0	1052.0	---	---	---
	P_s	566.0	1027.0	988.0	---	---	---
	τ	5.0	9.0	5.0	---	---	---
	ν`	54.0	106.0	30.0	---	---	---
1966	P_A†	1295.0	1494.0	633.0	---	---	---
	P_s	1288.0	1462.0	510.0	---	---	---
	τ	7.0	8.0	6.0	---	---	---
	ν`	84.0	100.0	55.0	---	---	---
1967	P_A†	1077.0	1339.0	482.0	---	---	---
	P_s	1000.0	1336.0	388.0	---	---	---
	τ	6.0	9.0	5.0	---	---	---
	ν`	65.0	105.0	32.0	---	---	---
1973	P_A†	741.0	1101.0	450.0	---	---	---
	P_s	709.0	1060.0	410.0	---	---	---
	τ	6.0	7.0	5.0	---	---	---
	ν`	64.0	80.0	25.0	---	---	---

Table (B-1) Continued

Year	Station / Notations*	Kurmuk	Gambela	Chali	Daga P.	Doro	Yabus Br.
1974	P_A†	1291.0	1318.0	500.0	---	---	---
	P_s	1203.0	1268.0	414.0	---	---	---
	τ	6.0	7.0	6.0	---	---	---
	$\nu`$	79.0	101.0	35.0	---	---	---

* Notations:

P_A = Annual precipitation (mm)

P_s = Seasonal precipitation (mm)

τ = Rainy season length (months)

$\nu`$ = Number of days $\geq$ 1.0 mm rain

† From Sudan Meteorological Department

Appendix C

Table (C-1)

Monthly Discharge at Yabus Bridge

(in million cubic meter)

Year	Jan.	Feb.	Mar.	April	May	June	July	Aug.	Sept.	Oct.	Nov.	Dec.	Total
1950	10.68	4.78	4.93	4.10	7.71	19.30	28.87	65.20	105.20	109.19	50,90	21.80	432.66
1951	10.58	5.48	3.51	1.80	7.79	18.30	25.96	84.21	74.30	90.01	39.20	18.22	379.36
1952	8.93	2.94	2.67	3.10	4.62	12.10	21.57	81.47	82.50	103.90	29.50	15.68	368.98
1953	8.41	4.60	2.86	2.50	18.46	25.00	26.24	87.19	142.00	92.78	35.60	18.59	464.23
1954	11.38	5.68	3.27	4.30	5.09	16.20	31.77	95.30	102.80	106.84	29.30	15.58	427.51
1955	9.28	4.74	3.11	3.10	7.85	15.20	46.26	118.88	204.20	146.65	72.20	27.96	659.43
Average	9.88	4.70	3.39	3.15	8.59	17.68	30.11	88.70	118.5	108.23	42.78	19.64	455.35
Average* (Cm)	0.449	0.214	0.154	0.143	0.390	0.804	1.369	4.032	5.386	4.920	1.945	0.893	20.70

* Area of Yabus Sub-Catchment = 2,200 Km^2

Table (C-2)

Monthly Discharge at Daga Post

(in million cubic meter)

Year	Jan.	Feb.	Mar.	April	May	June	July	Aug.	Sept.	Oct.	Nov.	Dec.	Total
1950	0.00	0.00	0.00	0.00	5.91	21.90	103.65	135.10	118.10	110.50	46.20	13.50	554.86
1951	4.20	1.70	1.55	0.00	7.99	15.40	26.53	95.77	59.10	90.60	54.80	13.40	371.04
1952	0.00	1.5	0.00	2.20	9.01	9.60	22.05	96.32	104.60	96.12	22.70	7.05	369.15
1953	2.15	1.40	0.00	3.00	4.18	16.50	33.09	107.40	71.10	82.00	29.10	9.47	359.39
1954	2.55	1.48	0.00	0.00	2.18	18.50	55.40	128.88	116.10	80.27	28.80	11.18	445.34
Average	1.78	1.24	0.31	1.04	5.85	16.38	48.14	112.70	93.8	91.5	36.32	10.92	420
Average* (Cm)	0.094	0.065	0.016	0.055	0.308	0.862	2.534	5.932	4.937	4.816	1.912	0.575	22.10

* Area od Daga Sub-Catchment = 1,900 Km^2

Appendix D

Table (D-1)

The Seasonal Meteorological Data of Kurmuk

Year	Mean Air Temperature °C 0600	1200	Mean Relative Humitidy % 0600	1200	Mean Cloud Amount (0 - 8) 0600	1200	Mean daily piche Evap. mm/day	Period of Rainy Season 1st of	End of
1950									
1951	25.60	30.10	66.90	54.10	5.43	6.14	4.84	May -	Nov.
1952	23.50	29.10	78.80	56.80	6.60	5.80	3.38	June -	Oct.
1953	25.30	30.55	69.00	60.30	4.00	5.50	5.01	Apr. -	Nov.
1954	24.20	29.60	78.20	58.30	0.30	0.00	3.23	May -	Oct.
1955	24.80	30.40	74.00	53.40	6.70	7.60	5.49	Apr. -	Oct.
1956	25.50	31.06	80.80	73.80	5.83	6.50	4.03	May -	Oct.
1957	25.90	31.00	72.50	51.30	5.33	6.00	3.67	May -	Oct.
1958	24.90	31.16	75.40	53.60	6.29	5.71	3.73	Apr. -	Oct.
1959	25.30	31.60	71.71	50.90	6.00	5.57	4.30	Apr. -	Oct.
1960	25.18	31.40	72.70	51.60	5.86	5.14	4.40	Apr. -	Oct.
1961	24.10	28.20	76.80	59.80	5.40	5.20	3.10	June -	Oct.
1962	24.50	30.10	74.10	52.30	5.00	6.14	4.26	May -	Nov.
1963	24.60	30.03	74.16	53.83	4.80	6.83	4.93	May -	Oct.
1964	24.19	29.90	72.60	51.71	4.57	6.28	5.01	Apr. -	Oct.
1965	24.18	29.80	74.40	53.60	5.60	6.00	4.86	July -	Oct.
1966	24.20	30.03	72.71	52.10	4.71	5.14	4.40	May -	Nov.
1967	24.00	29.18	76.17	55.83	4.83	6.17	4.28	May -	Oct.
Mean	27.47		64.83		5.38		4.29		
St. dev.	2.87		10.52		1.51		0.69		

Table (D-2)

The Seasonal Meteorological Data of Gambela

Year	Mean Air Temperature °C 0600	1200	Mean Relative Humidity % 0600	1200	Mean Cloud Amount (0 - 8) 0600	1200	Mean daily piche Evap. mm/day	Period of Rainy Season 1st of	End of
1950									
1951	24.20	31.50	83.60	55.60	6.00	5.60	3.04	May -	Nov.
1952	23.90	31.50	84.40	55.30	6.30	6.30	2.94	Apr. -	Nov.
1953									
1954	24.50	31.80	80.40	52.40	6.25	6.13	3.91	Mar. -	Oct.
1955	23.70	32.30	85.40	53.50	5.60	6.00	2.93	Apr. -	Nov.
1956	23.60	31.60	87.10	56.10	6.00	6.00	3.36	Mar. -	Oct.
1957	25.02	33.70	83.10	53.40	4.30	4.30	3.46	May -	Nov.
1958	25.00	32.00	82.40	54.30	5.00	4.85	3.61	Apr. -	Oct.
1959	24.70	31.80	80.50	53.30	4.60	4.30	3.45	Apr. -	Nov.
1960	25.00	32.00	78.50	52.12	4.50	4.40	3.43	Apr. -	Nov.
1961									
1962	24.64	31.60	88.00	58.60	7.47	8.00	3.67	Apr. -	Oct.
1963	24.80	34.73	83.60	43.40	7.77	7.77	2.16	Mar. -	Nov.
1964	24.76	32.20	81.40	50.60	7.50	8.00	2.76	Apr. -	Oct.
1965	26.10	35.10	65.33	35.88	7.50	7.50	2.94	Mar. -	Nov.
1966	25.83	33.50	66.00	42.75	7.38	7.50	2.60	Mar. -	Oct.
1967	25.15	32.40	78.50	53.20	5.33	5.11	3.86	Mar. -	Nov.
Mean	28.62		65.96		6.11		3.208		
St. Dev.	4.07		16.10		1.27		0.493		

Table (D-3)

The Annual Meteorological Data of Nasir

Year	Air Temperature °C 0600	1200	Mean Relative Humidity % 0600	1200	Mean Cloud Amount (0 - 8) 0600	1200	Mean daily piche Evap. mm/day
1950	24.5	31.4	70	50	5	5	6.7
1951	25.0	32.2			5	5	9.5
1952	25.8	32.8	66	44			9.2
1953	25.7	32.4					8.5
1954	25.3	32.3	68	47	3	3	7.9
1955							
1956	24.8	31.4	73	50	3	3	6.5
1957	25.1	31.9	71	49	4	4	5.9
1958	26.0	32.8	69	47	5	5	7.3
1959	25.3	32.3	68	48	4	3	6.9
1960	25.2	32.6	73	49	5	5	6.2
1961	25.5	31.8	69	49	5	5	7.7
1962							
1963	25.1	32.1	74	49	4	3	6.2
1964	25.2	31.7	69	50	5	5	6.6
1965	25.2	32.8	67	45	5	5	8.1
1966							
1967	25.8	31.9	65	47	4	5	7.6
1973	25.9	33.0	63	45	4	3	9.5
1974	25.4	31.1	65	49	4	4	7.4
1975	25.5	31.7	65	50	4	3	
Mean	28.80		58.20		4.22		7.51
St. Dev.	3.50		10.50		0.85		1.16

Table (D-4)

Total Seasonal Precipitation and Water Surface

Potential Evaporation at Kurmuk and Gambela

Station	Kurmuk		Gambela	
Variable	P_s (cm)	E_{p_w}† (cm)	P_s (Cm)	E_{p_w}† (Cm)
1950	86.10	---	118.90	---
1951	85.10	79.28	137.50	54.26
1952	88.40	39.55	113.60	59.98
1953	107.80	93.79	122.80	---
1954	119.80	45.35	169.60	79.76
1955	97.40	89.93	137.20	59.77
1956	109.80	56.58	138.50	68.55
1957	69.20	51.53	77.40	61.76
1958	101.00	61.11	112.70	64.44
1959	86.10	70.43	129.20	70.38
1960	94.00	72.07	112.90	69.97
1961	85.30	36.27	127.60	---
1962	110.50	69.78	137.70	65.51
1963	100.70	69.22	154.00	49.57
1964	107.10	82.07	162.80	49.27
1965	56.60	56.86	102.70	67.48
1966	128.80	72.07	146.20	53.04
1967	100.00	60.09	133.60	88.59
1973	70.90	---	106.00	---
1974	120.30	---	126.80	---

† $E_{p_w} = \tau x R_1 x e_{piche}$

Appendix E

Estimation of the Initial Soil Parameters

The clay soil sections are selected from the Jonglei Project Report (Remo Sensing Center, 1978). These experimental data are shown in Table (E.1).

$\bar{\Theta}_{a_1}$ ≡ The average soil moisture at 1/3 atm (3.45×10^2 Cm section) = 0.43

$\bar{\Theta}_{a_2}$ ≡ The average soil moisture at 15 atm (1.55×10^4 Cm section) = 0.26

Assuming that the sample of maximum soil moisture at 1/3 atm ($\Theta_{a\ max} = 0.545$) is saturated ($s_a = 1$), then

$$n_a \equiv \frac{\Theta_{a\ max}}{s_a} = \frac{0.545}{1.00} = 0.545 \quad , \quad \text{(Eagleson 1977)}$$

Residual degree of saturation (s_r) ≈ 0.21, (Eagleson 1970)

Thus $n \equiv n_a (1 - s_r) = 0.43$, (Eq.3.16)

$\bar{s}_{a_1}$ ≡ The average degree of saturation at 1/3 atm $= \frac{\bar{\Theta}_{a1}}{n_a} = 0.785$

$\bar{s}_{a_2}$ ≡ The average degree of saturation at 15 atm $= \frac{\bar{\Theta}_{a_2}}{n_a} = 0.478$

$\bar{s}_1$ = The average effective degree of saturation at 1/3 atm

$$= \frac{\bar{s}_{a_1} - s_r}{1 - s_r} = 0.73 \quad , \quad \text{Eq. (3.15)}$$

$\bar{s}_2$ = The average effective degree of saturation at 15 atm

$$= \frac{\bar{s}_{a_2} - s_r}{1 - s_r} = 0.33 \quad , \qquad \text{Eq. (3.15)}$$

Plotting these values vs. the corresponding soil matrix potential, $\Psi(s)$, on logarithmic paper gives the pore size-distribution index, m, and the saturated soil matrix potential, $\psi(1)$, as shown in Fig. (E.1). These parameters are 0.23 and 85 cm (suction), respectively.

According to Eq. (3.20), the saturated effective hydraulic conductivity (coefficient of permeability), K(1) is about 6×10^{-5} cm/sec.

Matching this soil (having about 60% clay) with the soils presented in (Remote Sensing Center, 1978), we find that the range of the coefficient of permeability is from 4.23×10^{-5} Cm/sec to 14.1×10^{-5} Cm/sec.

Table (E-1)

The Soil Moistures at Different Soil Matrix Potentials[†]

Section	Moisture Percent at 1/3 atm	Moisture Percent at 15 atm
1	37.40	22.59
	40.57	27.98
	54.50	29.86
2	37.70	24.31
	38.93	25.07
5	45.73	25.06
	46.31	25.38
6	39.05	25.19
	39.19	26.35
	44.69	29.64
	46.35	25.33
Mean ($\bar{\Theta}$)	42.77	26.07

[†]Remote Sensing Center, 1978

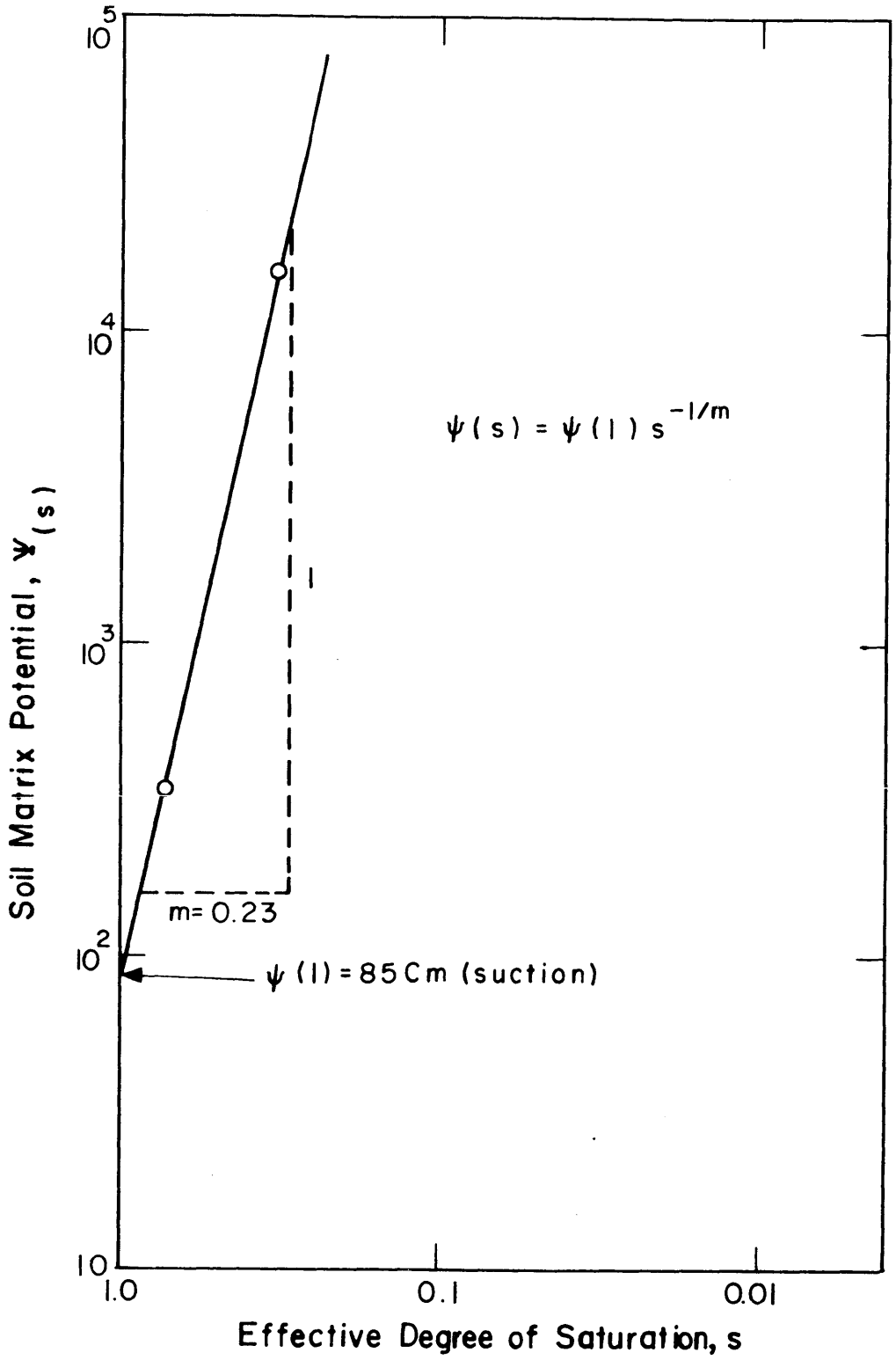

Figure E.1

SOIL MOISTURE - MATRIX POTENTIAL RELATIONSHIP

Appendix F

PRELIMINARY WATER BALANCE OF MACHAR REGION

A. The Eastern Catchments

1. The total seasonal average evapotranspiration, $E_{T_{ca}}$,

$\bar{m}_\tau$ = 200 days, lumped from the stations

A_T = 16,300 km^2 Table 4.1

$\bar{e}_p$ = 3.11 mm/day, Kurmuk station Table 4.10

$$\bar{M} = \sum_{i=1}^{5} \bar{M}_i A_i / \sum_{i=1}^{5} A_i = 0.77 \quad \text{(F.1)}$$

$$\bar{k}_v = \sum_{i=1}^{5} \bar{M}_i A_i \bar{k}_{v_i} / \sum_{i=1}^{5} M_i A_i = 1.13 \quad \text{(F.2)}$$

where

$\bar{M}_i$ = average canopy density of catchment i Table 4.11

A_i = area of catchment i Table 4.1

and

$\bar{k}_{v_i}$ = average plant coefficient of catchment i Table 4.11

$$E_{T_{ca}} = \bar{m}_\tau \cdot \bar{e}_p [1 - \bar{M}(1 - \bar{k}_v)] \cdot A_T \quad \text{(F.3)}$$

2. The total seasonal average rainfall, P_{ca}

P_{ca} = 15.21 x 0.95 mlds Table 4.11

= 14.25 mlds

3. The total seasonal (annual) average yield, Y_{ca}

$$Y_{ca} = P_{ca} - E_{T_{ca}}$$

or

Y_{ca} = 14.45 - 11.15 = 3.30 mlds

4. The total average ungaged flow, U_{ca},

U_{ca} = 3.30 - 1.97 = 1.33 mlds Table 4.9

B. The Plains

1. The total seasonal average evapotranspiration, $E_{T_{p\ell}}$

$\bar{m}_{\tau}$ = 200 days, lumped from the stations

A_T(area) = 14,100 Km^2 Table 4.1

$\bar{e}_p$ = 3.43 mm/day, Nasir Station Table 4-10

From vegetation map, Fig. 4.2:

Forests = 20%

Grasses = 70%

Wet soil = 10%

$\bar{M}$ = 0.71, using Table 4.2 and Eq. 4.9

$\bar{k}_v$ = 0.97, using Table 4.2 and Eq. 4.10

$E_{T_{p\ell}}$ = 9.47 mlds, using Eq. (F-3)

2. The total seasonal average rainfall, $P_{p\ell}$,

$P_{p\ell}$ = 11.45 × 0.95 mlds, Table 4.11

= 10.88 mlds

3. The total seasonal (annual) average yield $Y_{p\ell}$,

$$Y_{p\ell} = P_{p\ell} + Y_{ca} - E_{T_{p\ell}}$$

or

$$Y_{p\ell} = 10.88 + 3.30 - 9.47 = 4.71 \text{ mlds}$$

A part of $Y_{p\ell}$ comes from the plains that lie at the west of permanent swamps

C. The Swamps

1. The total annual average evapotranspiration, E_{T_o},

$\bar{m}_\tau = 365$ days

A_T(area) = 8,700 Km^2 Table 4.1

From vegetation map, Fig. 4.2

Forests = 25%

Grasses = 35%

Wet Soil and water bodies = 40%

The swamps area is divided into:

I. Vegetated land covered by forests and grasses

II. Wet soils and water bodies covered by papyrus

I. Vegetated land, $\bar{e}_p$ = 3.43 mm/day, Nasir station, Table 4.10

$\bar{M}$ = 0.81, using Table 4.2 and Eq. 4.9

$\bar{k}_v$ = 1.05, using Table 4.2 and Eq. 4.10

E_{T_I} = 5.80 mlds, using Eq. F.3

II. Papyrus, [$\bar{e}_p$ = 2200 mm/year, Section 4.4]

$E_{T_{II}}$ = 2.200 × 0.4 × 8.700 = 7.66 mlds

E_{T_o} = E_{T_I} + $E_{T_{II}}$ = 13.46 mdls

2. The total annual average rainfall, P_o

P_o = 7.28 mlds Table 4.11

3. The total annual average net spilling, S_p,

S_p = 3.42 mlds Section 4.3.1

4. The total average ungaged flow from swamps (annual)

$L_o = P_o + Y_{p\ell} + S_p - E_{T_o}$

or

L_o = 7.28 + 4.71 + 3.42 - 13.46 = 1.95

% error = 1.95 × 100/37.36 = 5%

In case of 50% vegetated land and 50% papyrus

E_{T_I} = 4.83 mlds

and

$E_{T_{II}}$ = 9.58 mlds

Then

E_{To} = 14.41 mlds

and

L_o = 7.28 + 4.71 + 3.42 - 14.41 = 1.00 mld

$$\% \text{ error} = \frac{1.0 \times 100}{37.36} = 2.7\%$$

where 37.36 mlds. are the total annual rainfall and spilling all over the region.

Appendix G

THE cdf OF THE SEASONAL PRECIPITATIONS

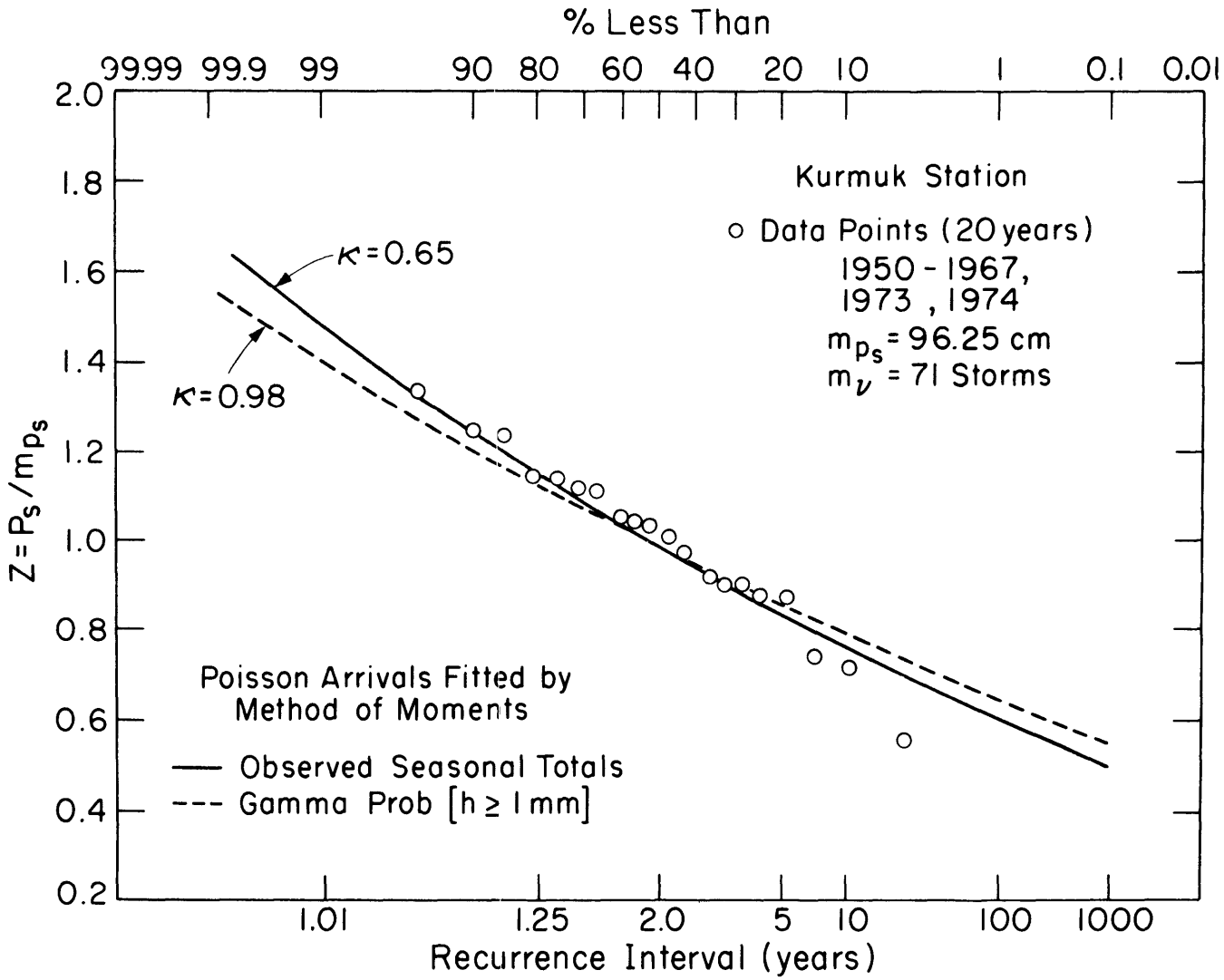

Figure G.1

SEASONAL POINT PRECIPITATION AT KURMUK

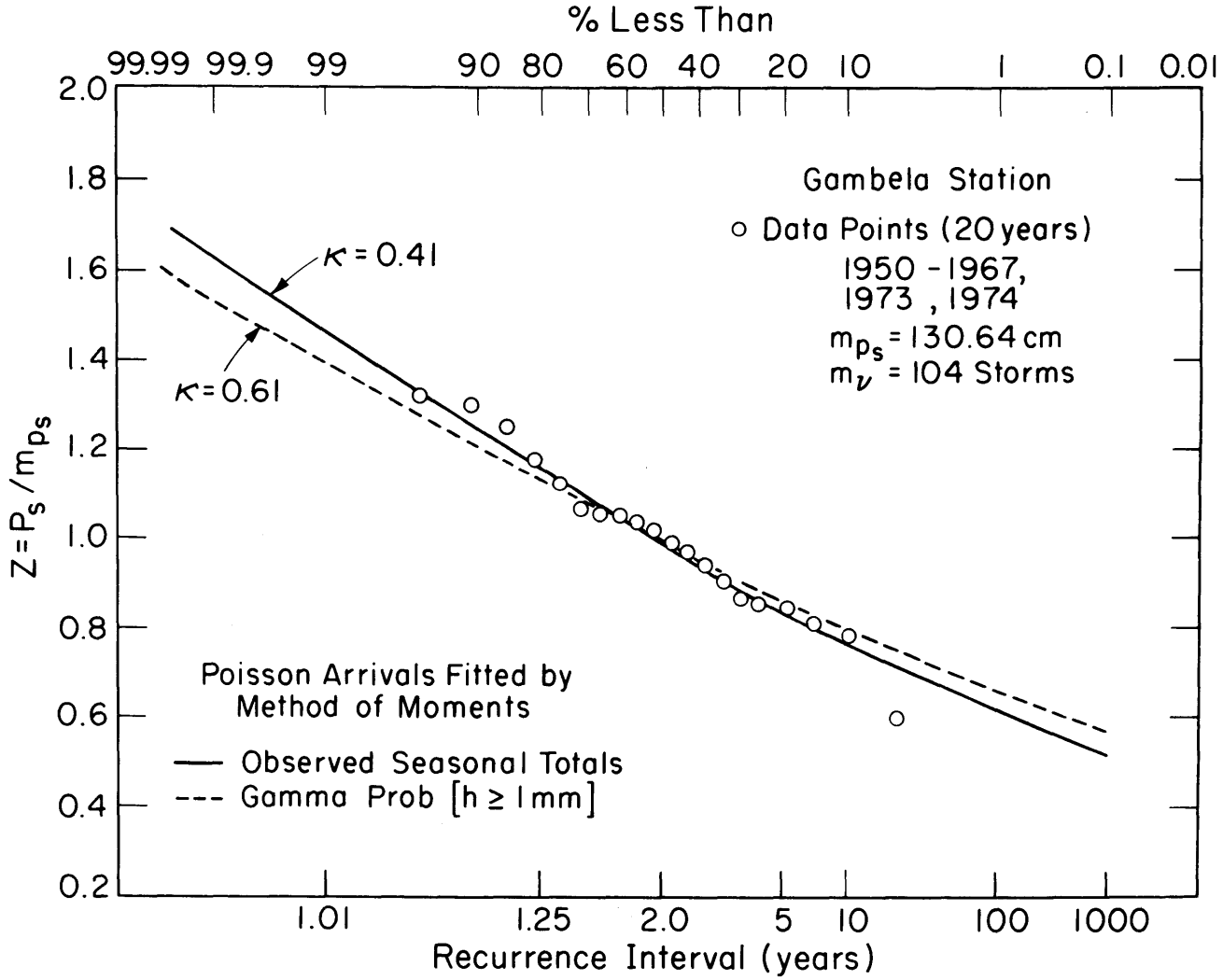

Figure G.2

SEASONAL POINT PRECIPITATION AT GAMBELA

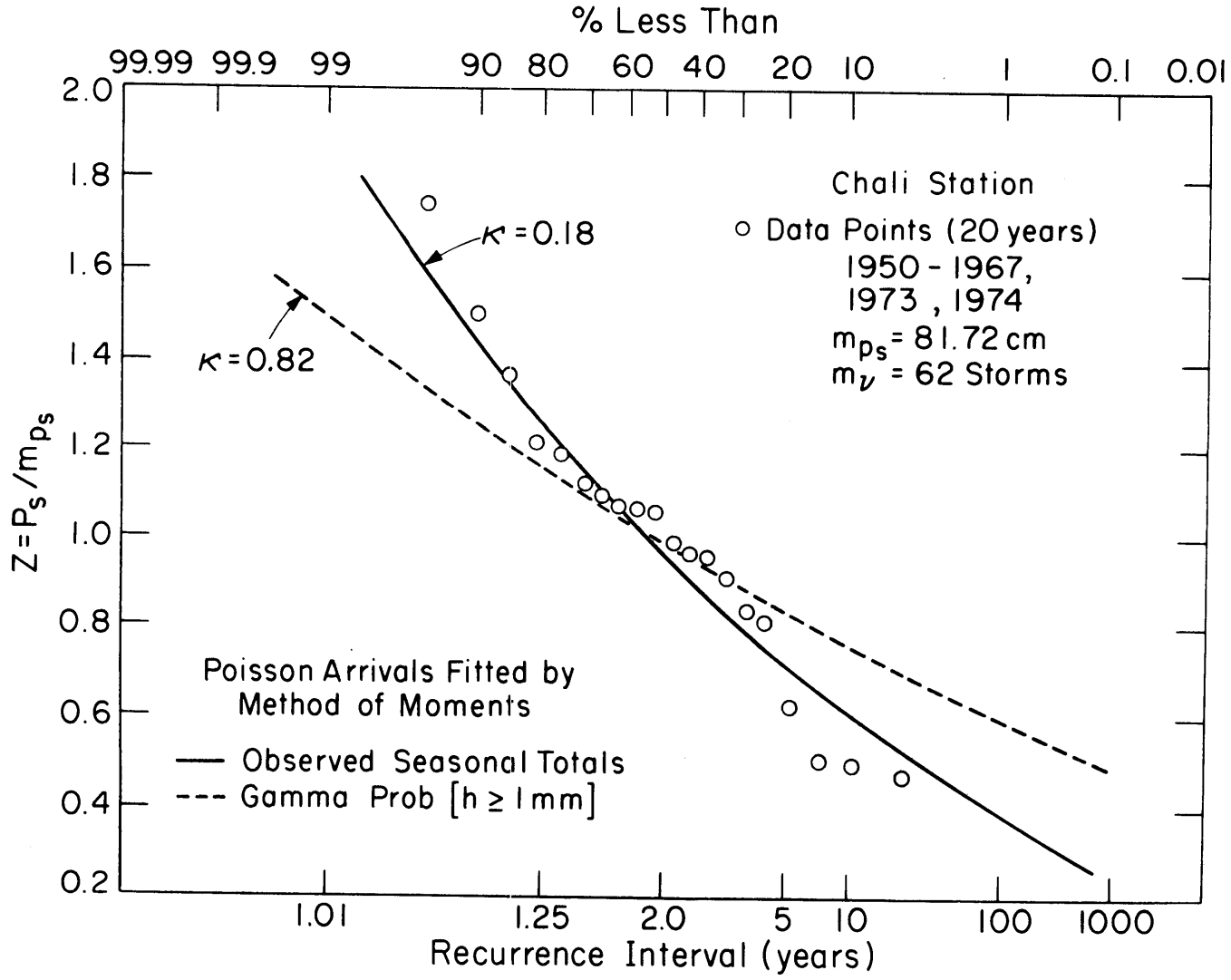

Figure G.3

SEASONAL POINT PRECIPITATION AT CHALI

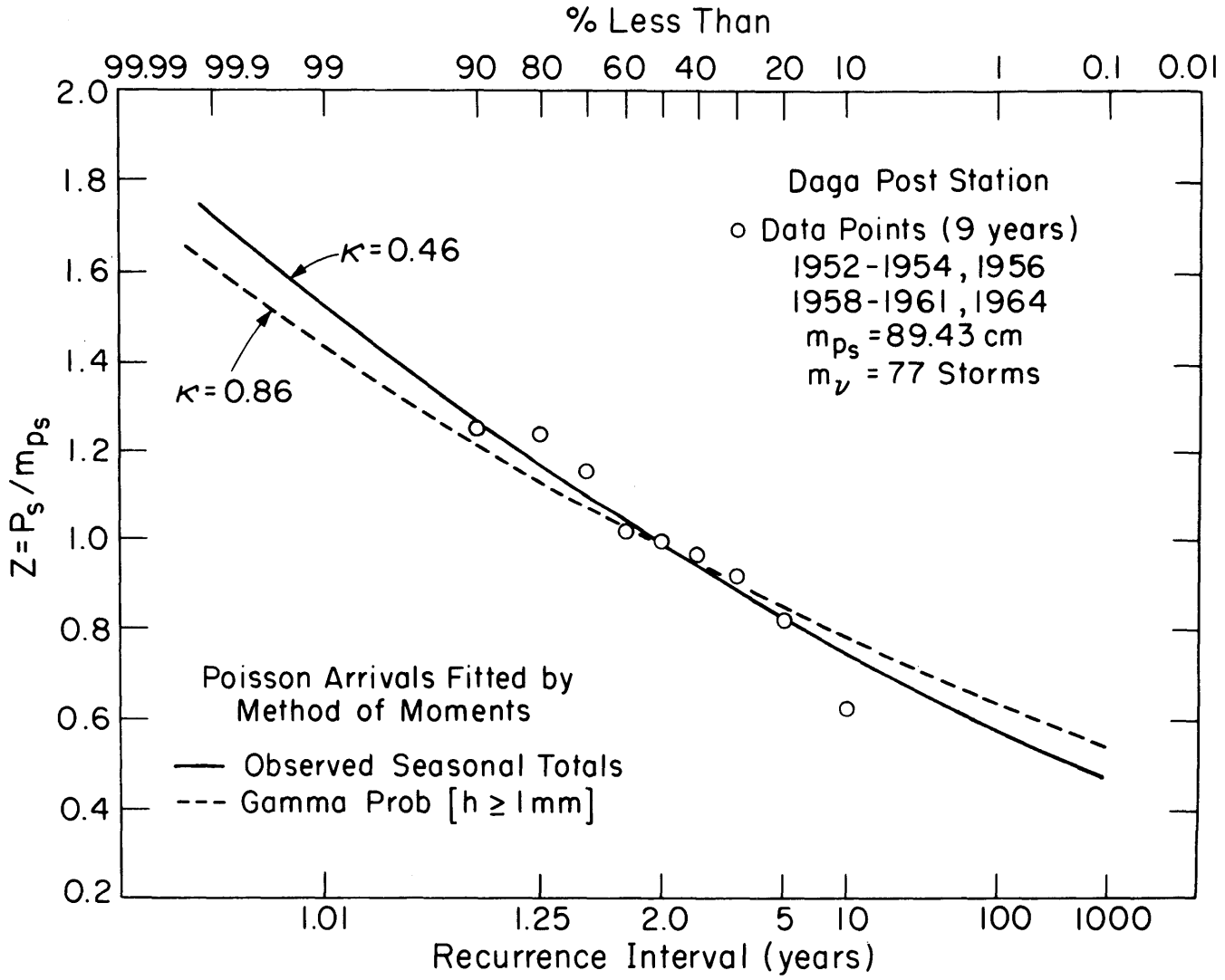

Figure G.4

SEASONAL POINT PRECIPITATION AT DAGA POST

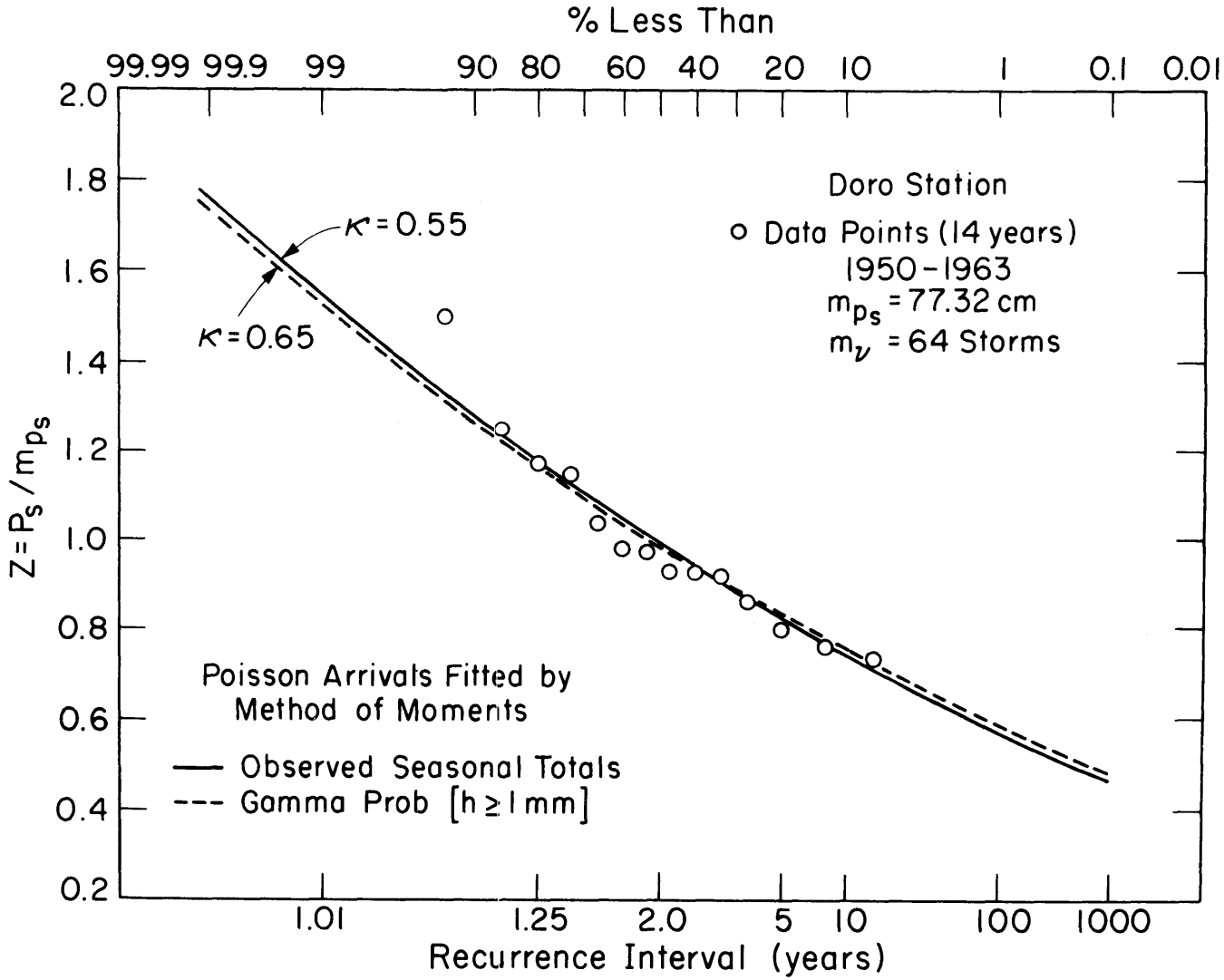

Figure G.5

SEASONAL POINT PRECIPITATION AT DORO

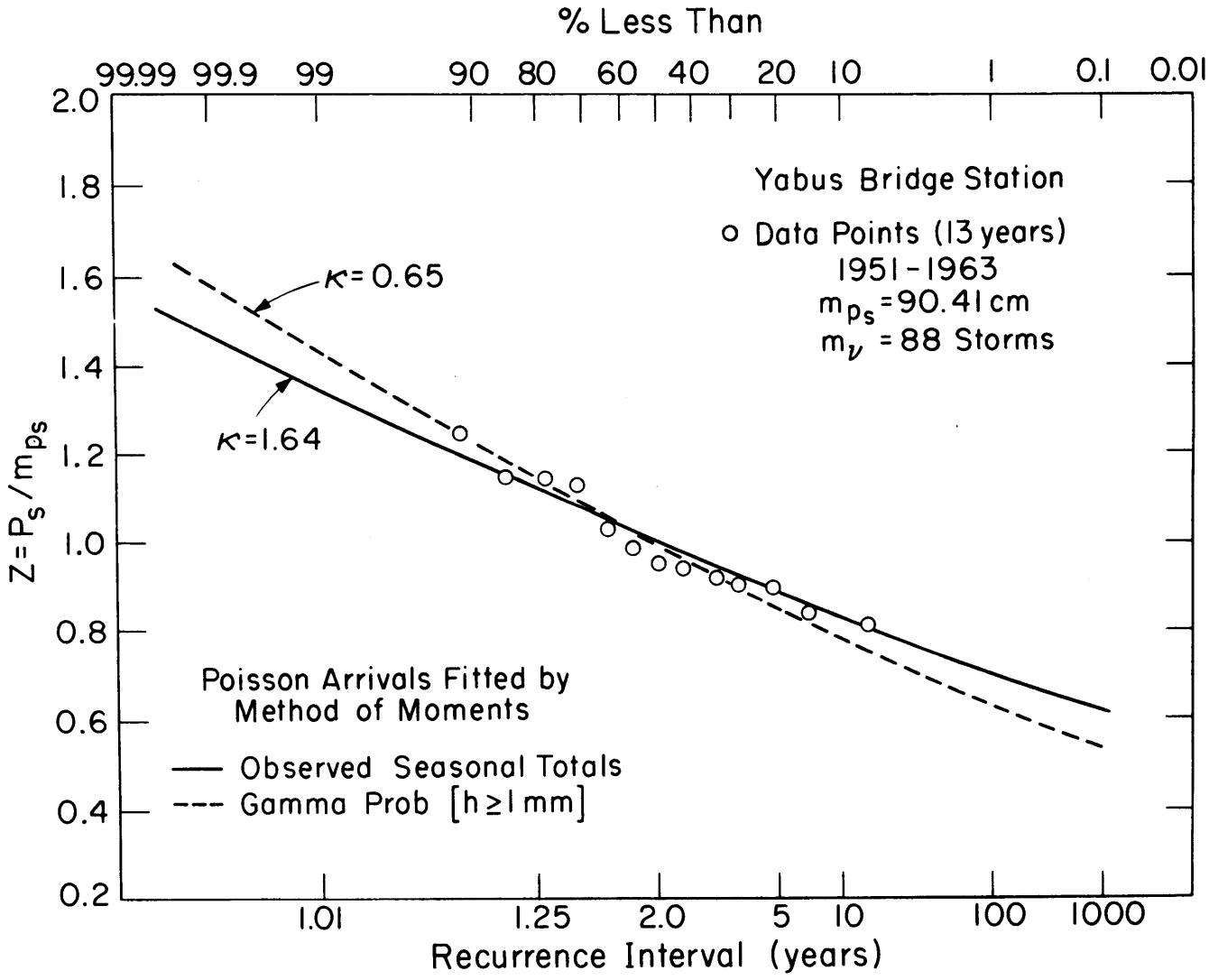

Figure G.6

SEASONAL POINT PRECIPITATION AT YABUS BRIDGE

Appendix H
LONG-TERM AVERAGE WATER BALANCE
(Yabus Bridge Sub-Catchment)

YABUS BR

EPR=	0.0130	MTB=	2.3400
MTR=	0.0500	TAU=	210.0000
TA =	27.5000	K1 =	0.3000E-04
MS =	0.1800	N =	0.4600
MH =	1.0300	MI =	0.8580
PA =	90.4100	W =	0.0001
H0 =	0.1000	AK =	1.6430
WT =	0.2500E+04	BM =	0.0
SI1=	100.0000	MU =	87.7700
AKV=	1.20		

M	SO	RSA	RGA	EVAPO	YIEP
0.95	0.1725	16.9418	0.0	73.46	0.1874E+00
0.90	0.3975	20.3016	0.0	70.03	0.2246E+00
0.85	0.5225	23.6784	0.0	66.85	0.2619E+00
0.80	0.5912	26.1448	0.0	64.37	0.2892E+00
0.75	0.6256	27.6517	0.20	62.47	0.3081E+00
0.70	0.6475	28.7527	0.66	61.09	0.3253E+00
0.65	0.6600	29.4472	1.02	59.93	0.3370E+00
0.60	0.6694	30.0010	1.36	59.14	0.3469E+00
0.55	0.6756	30.3867	1.63	58.57	0.3541E+00
0.50	0.6788	30.5845	1.77	58.05	0.3579E+00
0.45	0.6811	30.7352	1.89	57.77	0.3608E+00
0.40	0.6819	30.7859	1.93	57.55	0.3618E+00
0.35	0.6834	30.8878	2.01	57.68	0.3638E+00
0.30	0.6827	30.8367	1.96	57.61	0.3628E+00
0.25	0.6819	30.7859	1.93	57.67	0.3618E+00
0.20	0.6803	30.6848	1.85	57.72	0.3598E+00

YABUS BR

EPR=	0.0130	MTB=	2.3400
MTR=	0.0500	TAU=	210.0000
TA =	27.5000	K1 =	0.5000E-04
MS =	0.2150	N =	0.4400
MH =	1.0300	MI =	0.8580
PA =	90.4100	W =	0.0001
H0 =	0.1000	AK =	1.6430
WT =	0.2500E+04	BM =	0.0
SI1=	90.0000	MU =	87.7700
AKV=	1.20		

M	SO	RSA	RGA	EVAPO	YIEP
0.95	0.4600	16.7640	0.0	73.51	0.1854E+00
0.90	0.5537	19.5246	0.17	70.62	0.2179E+00
0.85	0.5944	21.0903	1.05	68.31	0.2449E+00
0.80	0.6162	22.0082	1.89	66.43	0.2644E+00
0.75	0.6319	22.7184	2.74	64.99	0.2816E+00
0.70	0.6412	23.1754	3.38	63.80	0.2937E+00
0.65	0.6491	23.5749	3.99	62.98	0.3049E+00
0.60	0.6538	23.8230	4.40	62.31	0.3122E+00
0.55	0.6569	23.9919	4.70	61.82	0.3173E+00
0.50	0.6584	24.0775	4.85	61.43	0.3200E+00
0.45	0.6600	24.1638	5.01	61.27	0.3227E+00
0.40	0.6600	24.1638	5.01	61.09	0.3227E+00
0.35	0.6608	24.2073	5.09	61.14	0.3240E+00
0.30	0.6600	24.1638	5.01	61.09	0.3227E+00
0.25	0.6600	24.1638	5.01	61.21	0.3227E+00
0.20	0.6600	24.1638	5.01	61.37	0.3227E+00

YABUS BR

EPR=	0.0130	MTB=	2.3400
MTR=	0.0500	TAU=	210.0000
TA =	27.5000	K1 =	0.6000E-04
MS =	0.2300	N =	0.4300
MH =	1.0300	MI =	0.8580
PA =	90.4100	W =	0.0000
H0 =	0.1000	AK =	1.6430
WT =	0.2500E+04	BM =	0.0
SI1=	85.0000	MU =	87.7700
AKV=	1.20		

M	SO	RSA	RGA	EVAPO	YIEP
0.95	0.5100	16.8637	0.01	73.65	0.1867E+00
0.90	0.5631	18.5175	0.92	70.92	0.2150E+00
0.85	0.5944	19.7275	2.08	68.76	0.2412E+00
0.80	0.6100	20.3666	2.96	66.92	0.2580E+00
0.75	0.6225	20.8999	3.86	65.52	0.2738E+00
0.70	0.6319	21.3250	4.67	64.47	0.2875E+00
0.65	0.6381	21.6209	5.29	63.66	0.2977E+00
0.60	0.6412	21.7727	5.62	62.93	0.3030E+00
0.55	0.6444	21.9272	5.98	62.50	0.3086E+00
0.50	0.6459	22.0053	6.16	62.16	0.3115E+00
0.45	0.6475	22.0843	6.35	62.03	0.3145E+00
0.40	0.6475	22.0843	6.35	61.86	0.3145E+00
0.35	0.6475	22.0843	6.35	61.81	0.3145E+00
0.30	0.6475	22.0843	6.35	61.85	0.3145E+00
0.25	0.6475	22.0843	6.35	61.94	0.3145E+00
0.20	0.6475	22.0843	6.35	62.05	0.3145E+00

YABUS BR

EPR=	0.0130	MTB=	2.3400
MTR=	0.0500	TAU=	210.0000
TA =	27.5000	K1 =	0.8000E-04
MS =	0.2600	N =	0.3900
MH =	1.0300	MI =	0.8580
PA =	90.4100	W =	0.0000
H0 =	0.1000	AK =	1.6430
WT =	0.2500E+04	BM =	0.0
SI1=	75.0000	MU =	87.7700
AKV=	1.20		

M	SO	RSA	RGA	EVAPO	YIEP
0.95	0.5100	16.0269	0.81	73.74	0.1863E+00
0.90	0.5506	17.2447	2.19	71.08	0.2149E+00
0.85	0.5725	18.0106	3.46	68.83	0.2375E+00
0.80	0.5881	18.6102	4.70	67.01	0.2579E+00
0.75	0.5991	19.0578	5.79	65.53	0.2748E+00
0.70	0.6069	19.3658	6.69	64.37	0.2882E+00
0.65	0.6123	19.5866	7.39	63.45	0.2984E+00
0.60	0.6162	19.7484	7.93	62.76	0.3061E+00
0.55	0.6194	19.8803	8.38	62.31	0.3126E+00
0.50	0.6209	19.9471	8.62	61.95	0.3160E+00
0.45	0.6217	19.9807	8.74	61.70	0.3177E+00
0.40	0.6225	20.0144	8.86	61.63	0.3194E+00
0.35	0.6225	20.0144	8.86	61.58	0.3194E+00
0.30	0.6225	20.0144	8.86	61.62	0.3194E+00
0.25	0.6217	19.9807	8.74	61.63	0.3177E+00
0.20	0.6209	19.9471	8.62	61.68	0.3160E+00

YABUS BR

EPR=	0.0130	MTB=	2.3400
MTR=	0.0500	TAU=	210.0000
TA =	27.5000	K1 =	0.1000E-03
MS =	0.2800	N =	0.3500
MH =	1.0300	MI =	0.8580
PA =	90.4100	W =	0.0000
H0 =	0.1000	AK =	1.6430
WT =	0.2500E+04	BM =	0.0
SI1=	65.0000	MU =	87.7700
AKV=	1.20		

M	SO	RSA	RGA	EVAPO	YIEP
0.95	0.4912	15.5587	1.16	73.70	0.1849E+00
0.90	0.5319	16.6941	2.82	70.95	0.2159E+00
0.85	0.5537	17.3872	4.34	68.58	0.2403E+00
0.80	0.5694	17.9286	5.81	66.61	0.2626E+00
0.75	0.5803	18.3320	7.09	64.97	0.2812E+00
0.70	0.5881	18.6330	8.15	63.63	0.2962E+00
0.65	0.5944	18.8818	9.09	62.61	0.3094E+00
0.60	0.5975	19.0090	9.60	61.70	0.3164E+00
0.55	0.6006	19.1357	10.13	61.12	0.3237E+00
0.50	0.6022	19.1951	10.40	60.66	0.3274E+00
0.45	0.6037	19.2551	10.68	60.44	0.3311E+00
0.40	0.6045	19.2852	10.83	60.33	0.3331E+00
0.35	0.6045	19.2852	10.83	60.28	0.3331E+00
0.30	0.6045	19.2852	10.83	60.34	0.3331E+00
0.25	0.6037	19.2551	10.68	60.39	0.3311E+00
0.20	0.6037	19.2551	10.68	60.58	0.3311E+00

YABUS BR

EPR=	0.0130	MTB=	2.3400
MTR=	0.0500	TAU=	210.0000
TA =	27.5000	K1 =	0.1000E-03
MS =	0.2800	N =	0.3500
MH =	1.0300	MI =	0.8580
PA =	90.4100	W =	0.0038
H0 =	0.1000	AK =	1.6430
WT =	0.4000E+03	BM =	0.0
SI1=	65.0000	MU =	87.7700
AKV=	1.20		

M	SO	RSA	RGA	EVAPO	YIEP
0.95	0.5225	16.4904	0.0	74.01	0.1824E+00
0.90	0.5725	18.1203	0.0	72.15	0.2004E+00
0.85	0.6037	19.3390	0.0	71.13	0.2139E+00
0.80	0.6194	19.9684	0.0	70.36	0.2209E+00
0.75	0.6319	20.5097	0.0	69.94	0.2269E+00
0.70	0.6381	20.7935	0.0	69.50	0.2300E+00
0.65	0.6444	21.0864	0.0	69.26	0.2332E+00
0.60	0.6506	21.3887	0.0	69.15	0.2366E+00
0.55	0.6538	21.5434	0.0	68.93	0.2383E+00
0.50	0.6569	21.7005	0.0	68.73	0.2400E+00
0.45	0.6600	21.8601	0.0	68.52	0.2418E+00
0.40	0.6662	22.1868	0.0	68.36	0.2454E+00
0.35	0.6694	22.3539	0.0	68.01	0.2473E+00
0.30	0.6741	22.6096	0.36	67.62	0.2540E+00
0.25	0.6748	22.6528	0.75	67.10	0.2589E+00
0.20	0.6756	22.6961	1.15	66.54	0.2637E+00

YABUS BR

EPR=	0.0130	MTB=	2.3400
MTR=	0.0500	TAU=	210.0000
TA =	27.5000	K1 =	0.1000E-03
MS =	0.2800	N =	0.3500
MH =	1.0300	MI =	0.8580
PA =	90.4100	W =	0.0012
H0 =	0.1000	AK =	1.6430
WT =	0.6000E+03	BM =	0.0
SI1=	65.0000	MU =	87.7700
AKV=	1.20		

M	SO	RSA	RGA	EVAPO	YIEP
0.95	0.5225	16.4412	0.0	73.88	0.1819E+00
0.90	0.5850	18.5364	0.0	71.94	0.2050E+00
0.85	0.6053	19.3418	0.77	70.35	0.2224E+00
0.80	0.6116	19.5887	1.99	68.83	0.2387E+00
0.75	0.6162	19.7792	2.99	67.59	0.2518E+00
0.70	0.6202	19.9416	3.87	66.64	0.2634E+00
0.65	0.6225	20.0406	4.43	65.86	0.2707E+00
0.60	0.6248	20.1407	5.00	65.34	0.2781E+00
0.55	0.6256	20.1744	5.20	64.89	0.2807E+00
0.50	0.6272	20.2421	5.60	64.68	0.2858E+00
0.45	0.6272	20.2421	5.60	64.45	0.2858E+00
0.40	0.6280	20.2762	5.80	64.38	0.2885E+00
0.35	0.6280	20.2762	5.80	64.30	0.2885E+00
0.30	0.6280	20.2762	5.80	64.25	0.2885E+00
0.25	0.6288	20.3104	6.01	64.27	0.2911E+00
0.20	0.6288	20.3104	6.01	64.20	0.2911E+00

YABUS BR

EPR=	0.0130	MTB=	2.3400
MTR=	0.0500	TAU=	210.0000
TA =	27.5000	K1 =	0.1000E-03
MS =	0.2800	N =	0.3500
MH =	1.0300	MI =	0.8580
PA =	90.4100	W =	0.0005
H0 =	0.1000	AK =	1.6430
WT =	0.8000E+03	BM =	0.0
SI1=	65.0000	MU =	87.7700
AKV=	1.20		

M	SO	RSA	RGA	EVAPO	YIEP
0.95	0.5225	16.4285	0.0	73.85	0.1817E+00
0.90	0.5662	17.8275	1.08	71.50	0.2091E+00
0.85	0.5803	18.3427	2.68	69.39	0.2326E+00
0.80	0.5897	18.7055	3.97	67.59	0.2508E+00
0.75	0.5975	19.0202	5.19	66.15	0.2678E+00
0.70	0.6037	19.2664	6.28	65.03	0.2825E+00
0.65	0.6069	19.3878	6.86	64.04	0.2903E+00
0.60	0.6100	19.5112	7.47	63.37	0.2985E+00
0.55	0.6123	19.6050	7.95	62.90	0.3048E+00
0.50	0.6131	19.6366	8.11	62.51	0.3069E+00
0.45	0.6147	19.7000	8.45	62.39	0.3113E+00
0.40	0.6147	19.7000	8.45	62.24	0.3113E+00
0.35	0.6147	19.7000	8.45	62.20	0.3113E+00
0.30	0.6147	19.7000	8.45	62.23	0.3113E+00
0.25	0.6147	19.7000	8.45	62.31	0.3113E+00
0.20	0.6147	19.7000	8.45	62.41	0.3113E+00

YABUS BR

EPR=	0.0130	MTB=	2.3400
MTR=	0.0500	TAU=	210.0000
TA =	27.5000	K1 =	0.1000E-03
MS =	0.2800	N =	0.3500
MH =	1.0300	MI =	0.8580
PA =	90.4100	W =	0.0001
H0 =	0.1000	AK =	1.6430
WT =	0.1500E+04	BM =	0.0
SI1=	65.0000	MU =	87.7700
AKV=	1.20		

M	SO	RSA	RGA	EVAPO	YIEP
0.95	0.5006	15.8256	0.86	73.74	0.1845E+00
0.90	0.5381	16.8861	2.61	71.04	0.2157E+00
0.85	0.5584	17.5468	4.15	68.71	0.2400E+00
0.80	0.5725	18.0431	5.57	66.75	0.2611E+00
0.75	0.5834	18.4525	6.91	65.16	0.2805E+00
0.70	0.5897	18.6960	7.78	63.77	0.2929E+00
0.65	0.5959	18.9467	8.75	62.79	0.3063E+00
0.60	0.5991	19.0748	9.27	61.91	0.3135E+00
0.55	0.6022	19.1967	9.81	61.36	0.3209E+00
0.50	0.6037	19.2566	10.09	60.92	0.3246E+00
0.45	0.6053	19.3170	10.38	60.72	0.3285E+00
0.40	0.6061	19.3474	10.53	60.63	0.3305E+00
0.35	0.6061	19.3474	10.53	60.58	0.3305E+00
0.30	0.6053	19.3170	10.38	60.54	0.3285E+00
0.25	0.6053	19.3170	10.38	60.68	0.3285E+00
0.20	0.6053	19.3170	10.38	60.86	0.3285E+00

Appendix I
THE cdf OF THE ANNUAL (SEASONAL) YIELDS

YABUS BR

EPR=	0.0130	MTB=	2.3400
MTR=	0.0500	TAU=	210.0000
TA =	27.5000	K1 =	0.1000E-03
MS =	0.2800	N =	0.3500
MH =	1.0300	MI =	0.8580
PA =	90.4100	W =	0.0000
HO =	0.1000	AK =	1.6430
WT =	0.2500E+06	BM =	0.8500
SI1=	65.0000	MU =	87.7700
AKV =	1.20		

Z	PROB	YIE1	RS1	ET1
0.839	0.11351	0.102	0.102	0.736
0.850	0.13125	0.113	0.113	0.736
0.859	0.14844	0.123	0.123	0.736
0.869	0.16783	0.133	0.133	0.737
0.884	0.19717	0.146	0.145	0.738
0.908	0.25397	0.167	0.160	0.742
0.958	0.38954	0.207	0.181	0.751
1.071	0.70835	0.302	0.207	0.769
1.332	0.98981	0.537	0.241	0.795
1.928	0.99990	1.111	0.286	0.817

YABUS BR

EPR=	0.0130	MTB=	2.3400
MTR=	0.0500	TAU=	210.0000
TA =	27.5000	K1 =	0.1000E-03
MS =	0.2800	N =	0.3500
MH =	1.0300	MI =	0.8580
PA =	90.4100	W =	0.0000
HO =	0.1000	AK =	1.6430
WT =	0.2500E+05	BM =	0.8500
SI1=	65.0000	MU =	87.7700
AKV =	1.40		

Z	PROB	YIE1	RS1	ET1
0.959	0.39199	0.102	0.102	0.857
0.970	0.42395	0.113	0.113	0.857
0.980	0.45262	0.123	0.123	0.857
0.990	0.48258	0.133	0.133	0.857
1.004	0.52375	0.146	0.145	0.858
1.028	0.59263	0.167	0.160	0.861
1.076	0.72091	0.207	0.181	0.869
1.188	0.91306	0.302	0.207	0.885
1.447	0.99885	0.537	0.241	0.910
2.045	0.99990	1.111	0.286	0.934

YABUS BR

EPR=	0.0130	MTB=	2.3400
MTR=	0.0500	TAU=	210.0000
TA =	27.5000	K1 =	0.1000E-03
MS =	0.2800	N =	0.3500
MH =	1.0300	MI =	0.8580
PA =	90.4100	W =	0.0000
HO =	0.2000	AK =	1.6430
WT =	0.2500E+05	BM =	0.8500
SI1=	65.0000	MU =	87.7700
AKV =	1.20		

Z	PROB	YIE1	RS1	ET1
0.850	0.13163	0.102	0.102	0.748
0.861	0.15110	0.113	0.113	0.748
0.870	0.16983	0.123	0.123	0.748
0.881	0.19073	0.133	0.133	0.748
0.895	0.22186	0.146	0.145	0.749
0.919	0.28072	0.167	0.160	0.752
0.968	0.41699	0.207	0.181	0.760
1.079	0.72582	0.302	0.207	0.776
1.336	0.99051	0.537	0.241	0.799
1.929	0.99990	1.111	0.286	0.818

YABUS BR

EPR=	0.0130	MTB=	2.3400
MTR=	0.0500	TAU=	210.0000
TA =	27.5000	K1 =	0.1000E-03
MS =	0.2800	N =	0.3500
MH =	1.0300	MI =	0.8580
PA =	90.4100	W =	0.0000
HO =	0.1000	AK =	1.6430
WT =	0.2500E+05	BM =	0.8500
SI1=	65.0000	MU =	87.7700
AKV =	1.00		

Z	PROB	YIE1	RS1	ET1
0.718	0.01371	0.102	0.102	0.616
0.729	0.01736	0.113	0.113	0.616
0.739	0.02125	0.123	0.123	0.616
0.749	0.02607	0.133	0.133	0.616
0.764	0.03433	0.146	0.145	0.618
0.789	0.05366	0.167	0.160	0.622
0.841	0.11740	0.207	0.181	0.634
0.957	0.38518	0.302	0.207	0.655
1.218	0.94121	0.537	0.241	0.680
1.810	0.99990	1.111	0.286	0.700

YABUS BR

EPR=	0.0130	MTB=	2.3400
MTR=	0.0500	TAU=	210.0000
TA =	27.5000	K1 =	0.1000E-03
MS =	0.2800	N =	0.3500
MH =	1.0300	MI =	0.8580
PA =	90.4100	W =	0.0000
H0 =	0.1000	AK =	1.6430
WT =	0.2500E+05	BM =	0.3500
SI1=	65.0000	MU =	87.7700
AKV =	1.20		

Z	PROB	YIE1	RS1	ET1
0.458	0.00000	0.102	0.102	0.356
0.469	0.00000	0.113	0.113	0.356
0.480	0.00000	0.123	0.123	0.357
0.494	0.00001	0.133	0.133	0.361
0.524	0.00003	0.146	0.145	0.378
0.594	0.00046	0.167	0.160	0.427
0.732	0.01858	0.207	0.181	0.525
0.946	0.35610	0.302	0.207	0.644
1.266	0.97029	0.537	0.241	0.728
1.866	0.99990	1.111	0.286	0.756

YABUS BR

EPR=	0.0130	MTB=	2.3400
MTR=	0.0500	TAU=	210.0000
TA =	27.5000	K1 =	0.1000E-03
MS =	0.2800	N =	0.3500
MH =	1.0300	MI =	0.8580
PA =	90.4100	W =	0.0000
H0 =	0.1000	AK =	1.6430
WT =	0.2500E+05	BM =	0.7500
SI1=	65.0000	MU =	87.7700
AKV =	1.20		

Z	PROB	YIE1	RS1	ET1
0.762	0.03365	0.102	0.102	0.660
0.773	0.04109	0.113	0.113	0.660
0.783	0.04875	0.123	0.123	0.660
0.794	0.05809	0.133	0.133	0.661
0.809	0.07416	0.146	0.145	0.663
0.837	0.11170	0.167	0.160	0.671
0.897	0.22663	0.207	0.181	0.689
1.026	0.58842	0.302	0.207	0.724
1.306	0.98414	0.537	0.241	0.768
1.912	0.99990	1.111	0.286	0.801

YABUS BR

EPR=	0.0130	MTB=	2.3400
MTR=	0.0500	TAU=	210.0000
TA =	27.5000	K1 =	0.1000E-03
MS =	0.2800	N =	0.3500
MH =	1.0300	MI =	0.8580
PA =	90.4100	W =	0.0000
H0 =	0.1000	AK =	1.6430
WT =	0.2500E+05	BM =	
SI1=	65.0000	MU =	87.7700
AKV =	1.20		

Z	PROB	YIE1	RS1	ET1
0.741	0.02215	0.102	0.102	0.639
0.767	0.03663	0.113	0.113	0.654
0.792	0.05656	0.123	0.123	0.669
0.818	0.08445	0.133	0.133	0.685
0.848	0.12793	0.146	0.145	0.702
0.888	0.20649	0.167	0.160	0.721
0.953	0.37441	0.207	0.181	0.746
1.077	0.72242	0.302	0.207	0.775
1.342	0.99146	0.537	0.241	0.805
1.938	0.99990	1.111	0.286	0.827

YABUS BR

EPR=	0.0130	MTB=	2.3400
MTR=	0.0500	TAU=	210.0000
TA =	27.5000	K1 =	0.1000E-03
MS =	0.2800	N =	0.3500
MH =	1.0300	MI =	0.8580
PA =	90.4100	W =	0.0085
H0 =	0.1000	AK =	1.6430
WT =	0.3000E+03	BM =	0.8500
SI1=	65.0000	MU =	87.7700
AKV =	1.20		

Z	PROB	YIE1	RS1	ET1
0.840	0.11508	0.103	0.103	0.736
0.851	0.13318	0.114	0.114	0.736
0.861	0.15092	0.124	0.124	0.737
0.872	0.17203	0.134	0.134	0.738
0.888	0.20700	0.146	0.146	0.742
0.916	0.27449	0.162	0.162	0.754
0.959	0.39277	0.183	0.183	0.777
1.011	0.54522	0.209	0.209	0.802
1.064	0.68969	0.243	0.243	0.821
1.119	0.81238	0.291	0.289	0.828

YABUS BR

EPR=	0.0130	MTB=	2.3400
MTR=	0.0500	TAU=	210.0000
TA =	27.5000	K1 =	0.1000E-03
MS =	0.2800	N =	0.3500
MH =	1.0300	MI =	0.8580
PA =	90.4100	W =	0.0085
H0 =	0.1000	AK =	1.6430
WT =	0.3000E+03	BM =	0.8000
SI1=	65.0000	MU =	87.7700
AKV =	1.20		

Z	PROB	YIE1	RS1	ET1
0.802	0.06588	0.103	0.103	0.698
0.813	0.07827	0.114	0.114	0.698
0.823	0.09090	0.124	0.124	0.699
0.834	0.10721	0.134	0.134	0.700
0.854	0.13834	0.146	0.146	0.708
0.888	0.20780	0.162	0.162	0.726
0.941	0.33978	0.183	0.183	0.758
1.000	0.51220	0.209	0.209	0.791
1.056	0.67051	0.243	0.243	0.813
1.112	0.79906	0.291	0.289	0.821

YABUS BR

EPR=	0.0130	MTB=	2.3400
MTR=	0.0500	TAU=	210.0000
TA =	27.5000	K1 =	0.1000E-03
MS =	0.2800	N =	0.3500
MH =	1.0300	MI =	0.8580
PA =	90.4100	W =	0.0085
H0 =	0.1000	AK =	1.6430
WT =	0.3000E+03	BM =	0.7500
SI1=	65.0000	MU =	87.7700
AKV =	1.20		

Z	PROB	YIE1	RS1	ET1
0.763	0.03429	0.103	0.103	0.660
0.775	0.04194	0.114	0.114	0.660
0.785	0.05011	0.124	0.124	0.661
0.798	0.06188	0.134	0.134	0.664
0.821	0.08853	0.146	0.146	0.675
0.864	0.15743	0.162	0.162	0.702
0.925	0.29775	0.183	0.183	0.743
0.991	0.48511	0.209	0.209	0.782
1.050	0.65302	0.243	0.243	0.807
1.105	0.78527	0.291	0.289	0.814

YABUS BR

EPR=	0.0130	MTB=	2.3400
MTR=	0.0500	TAU=	210.0000
TA =	27.5000	K1 =	0.1000E-03
MS =	0.2800	N =	0.3500
MH =	1.0300	MI =	0.8580
PA =	90.4100	W =	0.0085
H0 =	0.1000	AK =	1.6430
WT =	0.3000E+03	BM =	0.7000
SI1=	65.0000	MU =	87.7700
AKV =	1.20		

Z	PROB	YIE1	RS1	ET1
0.725	0.01608	0.103	0.103	0.622
0.737	0.02031	0.114	0.114	0.622
0.747	0.02510	0.124	0.124	0.623
0.762	0.03318	0.134	0.134	0.628
0.791	0.05558	0.146	0.146	0.645
0.844	0.12184	0.162	0.162	0.682
0.913	0.26546	0.183	0.183	0.730
0.983	0.46341	0.209	0.209	0.774
1.044	0.63666	0.243	0.243	0.800
1.098	0.77095	0.291	0.289	0.807

DAGA POST

EPR=	0.0130	MTB=	2.5500
MTR=	0.0500	TAU=	200.0000
TA =	27.5000	K1 =	0.1000E-03
MS =	0.2800	N =	0.3500
MH =	1.1610	MI =	0.9680
PA =	89.4300	W =	0.0000
HO =	0.1000	AK =	0.4580
WT =	0.2500E+05	BM =	0.8500
SI1=	65.0000	MU =	77.0000
AKV =	1.20		

Z	PROB	YIE1	RS1	ET1
0.837	0.21669	0.128	0.128	0.709
0.849	0.23705	0.141	0.141	0.709
0.860	0.25567	0.152	0.152	0.709
0.872	0.27548	0.163	0.163	0.709
0.887	0.30326	0.177	0.176	0.710
0.913	0.35134	0.199	0.193	0.714
0.963	0.45041	0.241	0.216	0.722
1.075	0.66175	0.335	0.244	0.739
1.330	0.93910	0.565	0.280	0.764
1.909	0.99990	1.121	0.328	0.787

DAGA POST

EPR=	0.0130	MTB=	2.5500
MTR=	0.0500	TAU=	200.0000
TA =	27.5000	K1 =	0.1000E-03
MS =	0.2800	N =	0.3500
MH =	1.1610	MI =	0.9680
PA =	89.4300	W =	0.0000
HO =	0.1000	AK =	0.4580
WT =	0.2500E+05	BM =	
SI1=	65.0000	MU =	77.0000
AKV =	1.20		

Z	PROB	YIE1	RS1	ET1
0.740	0.09215	0.128	0.128	0.612
0.768	0.12128	0.141	0.141	0.627
0.794	0.15364	0.152	0.152	0.642
0.820	0.19120	0.163	0.163	0.658
0.851	0.24025	0.177	0.176	0.674
0.893	0.31333	0.199	0.193	0.693
0.958	0.43991	0.241	0.216	0.717
1.081	0.67192	0.335	0.244	0.745
1.340	0.94427	0.565	0.280	0.775
1.919	0.99990	1.121	0.328	0.797

AHMAR

EPR=	0.0130	MTB=	2.8100
MTR=	0.0500	TAU=	187.8800
TA =	27.5000	K1 =	0.1000E-03
MS =	0.2800	N =	0.3500
MH =	1.3480	MI =	1.1230
PA =	88.6900	W =	0.0000
H0 =	0.1000	AK =	0.4320
WT =	0.2500E+05	BM =	
SI1=	65.0000	MU =	65.8200
AKV =	1.28		

Z	PROB	YIE1	RS1	ET1
0.782	0.16561	0.165	0.165	0.617
0.812	0.20585	0.179	0.179	0.633
0.840	0.24756	0.192	0.192	0.648
0.868	0.29300	0.204	0.204	0.664
0.901	0.34840	0.220	0.219	0.681
0.943	0.42391	0.244	0.238	0.699
1.009	0.54069	0.287	0.263	0.722
1.128	0.73083	0.380	0.293	0.749
1.379	0.94492	0.602	0.331	0.778
1.934	0.99973	1.133	0.381	0.801

TOMBAK

EPR=	0.0130	MTB=	2.8200
MTR=	0.0500	TAU=	187.0800
TA =	27.5000	K1 =	0.1000E-03
MS =	0.2800	N =	0.3500
MH =	1.3050	MI =	1.0880
PA =	85.0100	W =	0.0000
H0 =	0.1000	AK =	0.4130
WT =	0.2500E+05	BM =	
SI1=	65.0000	MU =	65.1400
AKV =	1.07		

Z	PROB	YIE1	RS1	ET1
0.694	0.07961	0.157	0.157	0.537
0.721	0.10323	0.171	0.171	0.550
0.746	0.12902	0.183	0.183	0.564
0.772	0.15884	0.195	0.195	0.577
0.803	0.19827	0.211	0.210	0.592
0.844	0.25832	0.234	0.228	0.609
0.909	0.36580	0.277	0.252	0.631
1.030	0.57802	0.372	0.282	0.658
1.287	0.88955	0.601	0.320	0.686
1.856	0.99920	1.150	0.369	0.706

YABUS

EPR=	0.0130	MTB=	2.3900
MTR=	0.0500	TAU=	206.4000
TA =	27.5000	K1 =	0.1000E-03
MS =	0.2800	N =	0.3500
MH =	1.0530	MI =	0.8780
PA =	89.1400	W =	0.0000
H0 =	0.1000	AK =	1.6770
WT =	0.2500E+05	BM =	
SI1=	65.0000	MU =	84.6600
AKV =	1.18		

Z	PROB	YIE1	RS1	ET1
0.734	0.02083	0.107	0.107	0.628
0.760	0.03445	0.118	0.118	0.642
0.785	0.05320	0.128	0.128	0.658
0.811	0.07948	0.138	0.138	0.673
0.841	0.12068	0.151	0.150	0.690
0.881	0.19569	0.172	0.166	0.709
0.946	0.35801	0.213	0.187	0.733
1.070	0.70399	0.308	0.214	0.762
1.335	0.98949	0.544	0.248	0.792
1.929	0.99990	1.116	0.294	0.813

DAGA

EPR=	0.0130	MTB=	2.5500
MTR=	0.0500	TAU=	200.0000
TA =	27.5000	K1 =	0.1000E-03
MS =	0.2800	N =	0.3500
MH =	1.1610	MI =	0.9680
PA =	89.4300	W =	0.0000
H0 =	0.1000	AK =	0.4580
WT =	0.2500E+05	BM =	
SI1=	65.0000	MU =	77.0000
AKV =	1.14		

Z	PROB	YIE1	RS1	ET1
0.710	0.06653	0.128	0.128	0.582
0.737	0.08944	0.141	0.141	0.596
0.762	0.11548	0.152	0.152	0.611
0.788	0.14651	0.163	0.163	0.626
0.818	0.18841	0.177	0.176	0.641
0.859	0.25367	0.199	0.193	0.660
0.924	0.37353	0.241	0.216	0.683
1.047	0.61176	0.335	0.244	0.711
1.306	0.92587	0.565	0.280	0.740
1.883	0.99986	1.121	0.328	0.761

LAU

EPR=	0.0130	MTB=	2.4800
MTR=	0.0500	TAU=	205.4000
TA =	27.5000	K1 =	0.1000E-03
MS =	0.2800	N =	0.3500
MH =	1.1790	MI =	0.9830
PA =	95.6100	W =	0.0000
HO =	0.1000	AK =	0.5820
WT =	0.2500E+05	BM =	
SI1=	65.0000	MU =	81.1000
AKV =	0.98		

Z	PROB	YIE1	RS1	ET1
0.615	0.01003	0.132	0.132	0.484
0.640	0.01557	0.144	0.144	0.495
0.662	0.02282	0.156	0.156	0.507
0.685	0.03277	0.167	0.167	0.519
0.713	0.04873	0.181	0.180	0.532
0.752	0.07965	0.203	0.198	0.548
0.815	0.15495	0.245	0.220	0.570
0.933	0.37414	0.337	0.249	0.596
1.181	0.83940	0.559	0.285	0.622
1.733	0.99973	1.096	0.333	0.637

SECTION 1

EPR=	0.0130	MTB=	2.8140
MTR=	0.0500	TAU=	187.3800
TA =	27.5000	K1 =	0.1000E-03
MS =	0.2800	N =	0.3500
MH =	1.3220	MI =	1.1020
PA =	86.4700	W =	0.0000
HO =	0.1000	AK =	0.4280
WT =	0.2500E+05	BM =	
SI1=	65.0000	MU =	65.4200
AKV =	1.16		

Z	PROB	YIE1	RS1	ET1
0.732	0.11077	0.160	0.160	0.572
0.761	0.14126	0.174	0.174	0.587
0.787	0.17389	0.186	0.186	0.601
0.814	0.21069	0.199	0.199	0.616
0.846	0.25771	0.214	0.213	0.631
0.887	0.32594	0.238	0.232	0.649
0.952	0.44054	0.281	0.256	0.671
1.073	0.64840	0.375	0.286	0.698
1.327	0.91844	0.601	0.324	0.726
1.891	0.99953	1.143	0.374	0.748

SECTION 2

EPR=	0.0130	MTB=	2.5400
MTR=	0.0500	TAU=	198.4400
TA =	27.5000	K1 =	0.1000E-03
MS =	0.2800	N =	0.3500
MH =	1.1500	MI =	0.9580
PA =	88.0500	W =	0.0000
H0 =	0.1000	AK =	1.4220
WT =	0.2500E+05	BM =	
SI1=	65.0000	MU =	76.6000
AKV =	1.17		

EPR= 0.0 MTB=

Z	PROB	YIE1	RS1	ET1
0.730	0.02854	0.126	0.126	0.604
0.757	0.04499	0.138	0.138	0.619
0.783	0.06648	0.149	0.149	0.634
0.809	0.09528	0.160	0.160	0.649
0.839	0.13857	0.174	0.173	0.665
0.880	0.21364	0.197	0.191	0.683
0.945	0.36704	0.238	0.213	0.706
1.067	0.68427	0.333	0.241	0.734
1.328	0.98133	0.564	0.277	0.763
1.909	0.99990	1.124	0.324	0.785

SECTION 3

EPR=	0.0130	MTB=	2.5400
MTR=	0.0500	TAU=	198.8100
TA =	27.5000	K1 =	0.1000E-03
MS =	0.2800	N =	0.3500
MH =	1.1530	MI =	0.9610
PA =	88.4300	W =	0.0000
H0 =	0.1000	AK =	1.2000
WT =	0.2500E+05	BM =	
SI1=	65.0000	MU =	76.7000
AKV =	1.17		

Z	PROB	YIE1	RS1	ET1
0.729	0.03243	0.127	0.127	0.602
0.756	0.04995	0.139	0.139	0.617
0.781	0.07238	0.150	0.150	0.632
0.807	0.10189	0.161	0.161	0.646
0.838	0.14553	0.175	0.174	0.662
0.878	0.21989	0.197	0.191	0.681
0.943	0.36919	0.239	0.214	0.704
1.066	0.67569	0.334	0.242	0.732
1.325	0.97702	0.565	0.278	0.761
1.906	0.99990	1.123	0.325	0.782

Appendix J

THE cdf OF THE ANNUAL (SEASONAL) DISCHARGES
FITTED BY GAMMA DISTRIBUTION

```
C THIS PROGRAM COMPUTES CDF OF THE SECTIONS ALONG THE CHANNEL
C ASSUMING THAT YIELDS OF BRANCHS ARE INDEPENDENT AND HAVE GAMMA
C DISTRIBUTIONS
C IT HAS BEEN FORMULATED BY EL-HEMRY
C*************************************************************
C
C   A     =SHAPE PARAMETER OF CDF OF COMBINED YIELDS
C   B     =SCALE PARAMETER OF CDF OF COMBINED YIELDS  (1/MLD)
C   Y     =YIELD  (MLD)
C   AREA =AREA ABOVE THE SECTION  (SQ. KM.)
C   PM    =AREAL PRECIPITION ABOVE THE SECTION  (CM)
C
C ********************************************
      DIMENSION NAME(20)
      REAL*8 X,Y,A,DLOG,DLGAMA,GAMLID,EPS,B,PM
      REAL*8 DLY,YMIN,YMAX,XOLD,XSUM
C**********
      READ(8,4)NAME
    4 FORMAT(20A4)
      READ(8,*)A,B,AREA,PM,YMIN,YMAX,DLY
      WRITE(6,18)NAME
   18 FORMAT(20A4)
      WRITE(6,19)A,B,AREA,PM
   19 FORMAT('  A =',F10.5/,'  B=',F10.5/,'  AREA=',F13.2,/
     *'  PM=',F10.5//)
      WRITE(6,21)
   21 FORMAT(5X,'Y MLD',6X,'PROB',7X,'Y1')
      Y=YMIN
    6 Y=Y+DLY
      Y1=(Y*1.0D5)/(AREA*PM)
      X=B*Y
      EPS=0.0001
      XOLD=1.0D0/A
      XSUM=1.0D0/A
      I=1
  100 XOLD=(XOLD/(A+I))*X
      XSUM=XSUM+XOLD
      IF((XOLD/XSUM).LE.EPS)GO TO 200
      I=I+1
      GO TO 100
  200 GAMLID=A*DLOG(X)-X+DLOG(XSUM)-DLGAMA(A)
      PROB=DEXP(GAMLID)
      WRITE(6,23)Y,PROB,Y1
   23 FORMAT(3F10.5)
      IF(Y.GE.YMAX)GO TO 7
      IF(PROB.GE.0.9999)GO TO 7
      GO TO 6
    7 STOP
      END
```

SECTION 1
A = 6.50000
B= 5.00000
AREA= 4350.00
PM= 86.47000

Y MLD	PROB
0.60000	0.05385
0.80000	0.15640
1.00000	0.30606
1.20000	0.47235
1.40000	0.62613
1.60000	0.75085
1.80000	0.84244
2.00000	0.90476
2.20000	0.94459
2.40000	0.96883
2.60000	0.98294
2.80000	0.99091
3.00000	0.99523

SECTION 2
A = 13.50000
B= 5.00000
AREA= 10400.00
PM= 88.05000

Y MLD	PROB
1.50000	0.03057
2.00000	0.16924
2.50000	0.42551
3.00000	0.68582
3.50000	0.86109
4.00000	0.94869
4.50000	0.98368
5.00000	0.99537
5.50000	0.99875
6.00000	0.99961
6.50000	0.99986
7.00000	0.99989

SECTION 3
A = 18.00000
B= 5.00000
AREA= 13600.00
PM= 88.43000

Y MLD	PROB
1.50000	0.00079
2.00000	0.01428
2.50000	0.08416
3.00000	0.25112
3.50000	0.48397
4.00000	0.70292
4.50000	0.85545
5.00000	0.93942
5.50000	0.97773
6.00000	0.99264
6.50000	0.99773
7.00000	0.99928
7.50000	0.99976
8.00000	0.99986
8.50000	0.99988